

American University in Cairo

## AUC Knowledge Fountain

---

Theses and Dissertations

Student Research


---

Winter 1-31-2022

# Repurposing Metformin and Antifolates for the Treatment of Hepatocellular Carcinoma

Sherouk Mohamed Tawfik  
sherouk.tawfik@aucegypt.edu

Follow this and additional works at: <https://fount.aucegypt.edu/etds>

 Part of the [Cancer Biology Commons](#), [Molecular Biology Commons](#), [Neoplasms Commons](#), and the [Pharmacology Commons](#)

---

### Recommended Citation

#### APA Citation

Mohamed Tawfik, S. (2022). *Repurposing Metformin and Antifolates for the Treatment of Hepatocellular Carcinoma* [Master's Thesis, the American University in Cairo]. AUC Knowledge Fountain.

<https://fount.aucegypt.edu/etds/1836>

#### MLA Citation

Mohamed Tawfik, Sherouk. *Repurposing Metformin and Antifolates for the Treatment of Hepatocellular Carcinoma*. 2022. American University in Cairo, Master's Thesis. *AUC Knowledge Fountain*.

<https://fount.aucegypt.edu/etds/1836>

This Master's Thesis is brought to you for free and open access by the Student Research at AUC Knowledge Fountain. It has been accepted for inclusion in Theses and Dissertations by an authorized administrator of AUC Knowledge Fountain. For more information, please contact [thesisadmin@aucegypt.edu](mailto:thesisadmin@aucegypt.edu).



THE AMERICAN UNIVERSITY IN CAIRO  
الجامعة الأمريكية بالقاهرة

School of Sciences and Engineering

**Repurposing Metformin and Antifolates for the Treatment of  
Hepatocellular Carcinoma**

A Thesis Submitted to  
The Chemistry Master's Program  
In partial fulfillment of the requirements for  
The degree of Master of Science

By:

**Sherouk Mohamed Tawfik**

Under the supervision of:

**Dr. Anwar Abd Elnaser (Advisor)**

Assistant Professor, Institute of Global Health and Human Ecology (IGHHE), The American  
University of Cairo

**Prof. Dr. Hassan Elfawal (Co-advisor)**

Professor and Dean, School of Sciences and Engineering, The American University in Cairo

**Dr. Maha Abdollah (Co-advisor)**

Assistant Professor, Department of Pharmacology, Faculty of Pharmacy,  
The British University in Egypt

**Prof. Dr. Mohey Elmazar (Co-advisor)**

Professor and Dean, Department of Pharmacology, Faculty of Pharmacy, The British University  
in Egypt

**June 2021**

The American University in Cairo

**Repurposing Metformin and Antifolates for the Treatment of  
Hepatocellular Carcinoma**

Thesis Submitted by

**Sherouk Mohamed Tawfik**

To the Chemistry Graduate Program

In partial fulfillment of the requirements for  
The degree of Master of Science in Chemistry

Has been approved by

---

Dept. Chair/ Director

Date

Dean Date

## ACKNOWLEDGEMENT

Verily, with every hardship comes ease. [Quran 94.6]

First and foremost, I would like to thank Allah, whose many blessings have made me who I am today.

I would also like to thank everyone who made this work possible. Firstly, I would like to express my gratitude to my advisor, Dr. Anwar Abdelnaser, for introducing me to the world of research. I benefited greatly from his keen scientific insight, his impeccable ability in tackling research debacles and his unwavering support and guidance. Since day one, his skillful planning and persistence positively impacted my research journey. He taught me how to solve any issues at hand and analyze results obtained meticulously. I am deeply indebted to his impactful contributions and abiding commitment. It was truly an utmost privilege to have been one of his students.

I would also like to express my sincere appreciation to my co-advisor, Dr. Maha Abdallah, who has been an unimpeachable source of positivity. I was extremely fortunate to have met her, let alone work under her supervision. She so patiently taught me key cell culture techniques, mentored me throughout my thesis and believed in me every step of the way. I am truly indebted for her contribution to my research work.

They say a good support system is all you need. I would like to extend my deepest gratitude to Prof. Mohey Elmazar. He went beyond the definition of a dean, advisor or mentor and took on the role of a father, relentlessly listening and acting upon my concerns and aspirations. He has always been a massive support system and I am grateful for his contribution to my thesis.

I would also like to thank Prof. Hassan Elfawal for teaching me the conception of writing a thesis through an extensive research seminar course at AUC and granting me access to work in his laboratory under his kind supervision. I immensely appreciate his insights and suggestions on my research work.

I would also like to express my gratitude towards my friends and fellow colleagues for making this such an enjoyable journey. Your words kept me going when the effect of my morning coffee gradually wore off each day. To you, I am eternally grateful.

I would like to thank my father, Essam Tawfik, and my sisters, Kheloud and Nora, for

supporting me throughout my sleepless nights and bearing with my sometimes-irrational requests. Words will never suffice how grateful I am to have been blessed with you in my life. Last but not least, I would like to express my appreciation to my mother, Elham Ghali. Her prayers for me are what sustained me thus far. Without her, I would not have become the person writing this acknowledge this very minute. Thank you for believing in me, and for that, I dedicate every milestone I reach in life to you.

## **ABSTRACT**

Hepatocellular carcinoma (HCC), one of the most prevalent types of cancers worldwide, continues to maintain high levels of resistance to standard therapy. As clinical data revealed poor response rates, the need for developing new methods has increased to improve the overall wellbeing of patients with HCC. Due to its safety, wide availability and previously reported anti-cancer effects, metformin (MET) serves to be a possible therapeutic agent when combined with other well-known anti-cancer agents. The aim of this study was to investigate the potential anti-cancer effects of MET, an anti-diabetic agent, when combined with two antifolate drugs: trimethoprim (TMP) or methotrexate (MTX), and the underlying mechanisms involved. In this study, single drugs and combinations were investigated using *in vitro* assays, cytotoxicity assay (MTT), RT-PCR, flow cytometry, scratch wound assay and Seahorse XF analysis, to reveal their potential anti-cancer effects on a human HCC cell line, HepG2. The cytotoxicity assay was performed to determine the  $IC_{50}$  concentration of MET alone and in combination with antifolates. The co-treatment of both drugs increased Bax and p53 apoptotic markers, while decreased the anti-apoptotic marker; Bcl-2. Both combinations increased the percentage of apoptotic cells and halted cancer cell migration, when compared to MET alone. Furthermore, both combinations decreased the MET-induced increase in glycolysis, while also induced mitochondrial damage, altering cancer cell bioenergetics. This study introduces two novel therapeutic combinations, which enhance the anti-proliferative and apoptotic effects of MET on HepG2 cells, and hence, potentially combat the aggressiveness of HCC.

# Table of Contents

<b>ACKNOWLEDGEMENT</b> .....	<b>i</b>
<b>ABSTRACT</b> .....	<b>iii</b>
<b>Table of Contents</b> .....	<b>iv</b>
<b>LIST OF TABLES</b> .....	<b>vii</b>
<b>LIST OF FIGURES</b> .....	<b>viii</b>
<b>LIST OF ABBREVIATIONS</b> .....	<b>x</b>
<b>CHAPTER 1: INTRODUCTION AND LITERATURE REVIEW</b> .....	<b>1</b>
<b>1.1 Hepatocellular carcinoma (HCC)</b> .....	<b>1</b>
<b>1.1.1 Risk factors</b> .....	<b>2</b>
<b>1.2 Hallmarks of cancer</b> .....	<b>4</b>
<b>1.3 Metabolic pathway in cancer</b> .....	<b>8</b>
<b>1.3.1 Glycolysis</b> .....	<b>11</b>
<b>1.3.2 Oxidative phosphorylation</b> .....	<b>11</b>
<b>1.4 The need for drug repurposing</b> .....	<b>16</b>
<b>1.5 Metformin as an anti-diabetic agent</b> .....	<b>16</b>
<b>1.5.1 The discovery of metformin as an anti-diabetic agent</b> .....	<b>18</b>
<b>1.5.2 Safety profile</b> .....	<b>18</b>
<b>1.5.3 Metformin as an anti-cancer agent</b> .....	<b>18</b>
<b>1.6 Antifolates</b> .....	<b>21</b>
<b>1.6.1 Trimethoprim (TMP)</b> .....	<b>21</b>
<b>1.6.2 Methotrexate (MTX)</b> .....	<b>22</b>
<b>1.6.3 Metformin as an anti-folate agent</b> .....	<b>23</b>
<b>1.7 Rationale</b> .....	<b>24</b>
<b>1.8 Hypothesis</b> .....	<b>24</b>
<b>1.9 Aims and Objectives</b> .....	<b>24</b>

<b>CHAPTER 2: MATERIALS AND METHODS.....</b>	<b>26</b>
<b>2.1 Materials.....</b>	<b>26</b>
<b>2.2 Cell culture.....</b>	<b>27</b>
<b>2.3 Cell viability assay (MTT assay).....</b>	<b>27</b>
<b>2.4 RTqPCR.....</b>	<b>28</b>
2.4.1 Treatment and isolation of total RNA .....	28
2.4.2 cDNA synthesis for qualitative analysis of mRNA .....	29
2.4.3 Quantification of mRNA using real-time PCR.....	30
2.4.4 Real-time PCR data analysis .....	31
<b>2.5 Cell apoptosis assay .....</b>	<b>32</b>
<b>2.6 Scratch Wound assay .....</b>	<b>32</b>
<b>2.7 FCCP Optimization with Mito Stress Test.....</b>	<b>33</b>
<b>2.8 Glycolytic Rate assay.....</b>	<b>34</b>
<b>2.9 Real time ATP Rate assay .....</b>	<b>35</b>
<b>2.10 Mitochondrial Mito Stress Test.....</b>	<b>35</b>
<b>2.11 Statistical Analysis.....</b>	<b>36</b>
<b>CHAPTER 3: RESULTS.....</b>	<b>38</b>
<b>3.1 Effect of MET, TMP and MTX on hepatocellular carcinoma cell viability.....</b>	<b>38</b>
<b>3.2 Effect of MET when combined with TMP or MTX on hepatocellular carcinoma cell viability.....</b>	<b>40</b>
<b>3.3 Effect of MET, TMP, MTX and combinations on Bax, Bcl-2 and p53 mRNA expression in HepG2 cells.....</b>	<b>43</b>
<b>3.4 Effect of MET, TMP, MTX and combinations on the percentage of apoptosis in HepG2 cells.....</b>	<b>45</b>
<b>3.5 Effect of MET, TMP, MTX, alone and in combination, on HepG2 cell migration. ...</b>	<b>48</b>
<b>3.6 Effect of MET, TMP and MTX, alone and in combination, on rates of basal and compensatory glycolysis in HepG2 cells.....</b>	<b>52</b>



<b>3.7 Effect of MET, TMP and MTX and combinations on the total ATP production rate in HepG2 cells.....</b>	<b>54</b>
<b>3.8 Effect of MET, TMP and MTX, alone and in combination, on the glycolytic and mitochondrial ATP production rates in HepG2 cells.....</b>	<b>56</b>
<b>3.9 Effect of MET, TMP, MTX and combinations on AMPK mRNA expression in HepG2 cells.....</b>	<b>59</b>
<b>3.10 Effect of MET, TMP, MTX, alone and in combination, on mitochondrial bioenergetics.....</b>	<b>61</b>
<b>CHAPTER 4: DISCUSSION.....</b>	<b>65</b>
<b>CHAPTER 5: CONCLUSION AND FUTURE PERSPECTIVES.....</b>	<b>71</b>
<b>REFERENCES.....</b>	<b>73</b>
<b>APPENDIX.....</b>	<b>89</b>

## LIST OF TABLES

<b>Table 2.1: Cell culture solutions .....</b>	<b>26</b>
<b>Table 2.2: List of primer sequences and their National Center for Biotechnology Information (NCBI) accession numbers .....</b>	<b>31</b>
<b>Table 3.1: Calculated IC<sub>50</sub> values of tested compounds on HepG2 cell line .....</b>	<b>42</b>

## LIST OF FIGURES

Figure 1.1. Stages leading up to Hepatocellular carcinoma.....	3
Figure 1.2. Schematic diagram elucidating cancer cell metastasis.....	6
Figure 1.3. Hallmarks of cancer. ....	8
Figure 1.4. Warburg effect. ....	10
Figure 1.5. Diagram of mitochondria depicting drugs which inhibit oxidative phosphorylation.....	15
Figure 1.6. Chemical structure of Metformin.....	17
Figure 1.7. Proposed mechanism of action of metformin as an anti-cancer agent.....	20
Figure 1.8. Chemical Structure of Trimethoprim. ....	22
Figure 1.9. Chemical structure of Methotrexate. ....	23
Figure 2.1. Schematic diagram elucidating the methods used in the present study. ....	37
Figure 3.1. Effect of MET (A), TMP (B) and MTX (C) on hepatocellular carcinoma cell viability.....	39
Figure 3.2. Effect of MET when combined with TMP (A) or MTX (B) on hepatocellular carcinoma cell viability.....	41
Figure 3.3. Effect of MET, TMP, MTX and combinations on Bax (A), Bcl-2 (B) and p53 (C) mRNA expression in HepG2 cells.....	44
Figure 3.4. Effect of MET, TMP, MTX and combinations on the percentage of apoptosis in HepG2 cells.....	46
Figure 3.5. Effect of MET, TMP, MTX, alone and in combination, on HepG2 cell migration. ....	49
Figure 3.6. Effect of MET, TMP and MTX, alone and in combination, on rates of basal and compensatory glycolysis in HepG2 cells. ....	53
Figure 3.7. Effect of MET, TMP and MTX and combinations on the total ATP production rate in HepG2 cells. ....	55
Figure 3.8. Effect of MET, TMP and MTX, alone and in combination, on the glycolytic and mitochondrial ATP production rates in HepG2 cells. ....	57
Figure 3.9. Effect of MET, TMP, MTX and combinations on AMPK mRNA expression in HepG2 cells.....	60

<b>Figure 3.10. Effect of MET, TMP, MTX, alone and in combination, on mitochondrial bioenergetics.....</b>	<b>62</b>
<b>Figure 3.11. Diagram illustrating the effects of combining MET with either antifolate agents (TMP or MTX).....</b>	<b>64</b>
<b>Figure 5.1. Schematic diagram elucidating the proposed mechanism of action of the tested compounds on the mitochondria and folate pathway.....</b>	<b>72</b>

## LIST OF ABBREVIATIONS

<b>2-DG</b>	2-deoxy-glucose
<b>ABB</b>	Annexin binding buffer
<b>ACC</b>	Acetyl-CoA carboxylase
<b>ADA</b>	American Diabetes Association
<b>ADP</b>	Adenosine diphosphate
<b>AMP</b>	Adenosine monophosphate
<b>AMPK</b>	AMP- activated protein kinase
<b>ANOVA</b>	Analysis of variance
<b>ATO</b>	Arsenic trioxide
<b>ATP</b>	Adenosine triphosphate
<b>BAX</b>	BCL-2-associated X protein
<b>Bcl-2</b>	B-cell lymphoma-2
<b>BR</b>	Basal respiration
<b>BSA</b>	Bovine serum albumin
<b>Caspases</b>	Cysteine-dependent aspartate-directed proteases
<b>cDNA</b>	Complementary deoxyribonucleic acid
<b>CI</b>	Confidence interval
<b>Ct</b>	Cycle threshold
<b>DEN</b>	Diethylnitrosamine
<b>DHFR</b>	Dihydrofolate reductase
<b>DMEM</b>	Dulbecco's Modified Eagle Medium
<b>DMSO</b>	Dimethyl sulfoxide
<b>ECAR</b>	Extracellular acidification rate
<b>ECM</b>	Extracellular matrix
<b>EDTA</b>	Ethylenediaminetetraacetic acid
<b>ETC</b>	Electron transport chain
<b>FADH</b>	Flavin adenine dinucleotide
<b>FBS</b>	Fetal bovine serum
<b>FCCP</b>	Fluoro-carbonyl cyanide phenylhydrazone

<b>FDA</b>	US Food and Drug Administration
<b>FITC</b>	Fluorescein isothiocyanate
<b>GCK</b>	Glucokinase
<b>GLUT-4</b>	Glucose transporter type 4
<b>HBV</b>	Hepatitis B virus
<b>HCC</b>	Hepatocellular carcinoma
<b>HIF</b>	Hypoxia-inducible transcription factor
<b>HK2</b>	Hexokinase 2
<b>IC<sub>50</sub></b>	Half maximal inhibitory concentration
<b>MET</b>	Metformin
<b>mM</b>	Millimolar
<b>MR</b>	Maximal respiration
<b>mRNA</b>	Messenger RNA
<b>MST</b>	Mitochondrial Stress Test
<b>mTOR</b>	Mechanistic target of rapamycin
<b>mtDNA</b>	Mitochondrial DNA
<b>MTT</b>	3-(4,5-dimethylthiazol-2-yl)-2,5-diphenyltetrazolium bromide
<b>MTX</b>	Methotrexate
<b>NADH</b>	Nicotinamide adenine dinucleotide + hydrogen
<b>NAFLD</b>	Nonalcoholic fatty liver disease
<b>NIDDM</b>	Non-insulin-dependent diabetes mellitus
<b>OCR</b>	Oxygen consumption rate
<b>OCT</b>	Organic cation transporter
<b>OLT</b>	Orthotopic liver transplantation
<b>OXPHOS</b>	Oxidative phosphorylation
<b>PBS</b>	Phosphate Buffered Saline
<b>PFK-2</b>	Phosphofructokinase-2
<b>PI</b>	Propidium iodide
<b>PS</b>	Phosphatidylserine
<b>qRT-PCR</b>	Real-time polymerase chain reaction

<b>Rb</b>	Retinoblastoma
<b>RNA</b>	Ribonucleic acid
<b>ROS</b>	Reactive oxygen species
<b>Rot/AA</b>	Rotenone + Antimycin A
<b>RT</b>	Reverse transcription
<b>RT</b>	Room temperature
<b>SEM</b>	Standard error of mean
<b>T<sub>m</sub></b>	Melting temperature
<b>TMP</b>	Trimethoprim
<b>VEGF</b>	Vascular endothelial growth factor

## **CHAPTER 1: INTRODUCTION AND LITERATURE REVIEW**

There is great interest in repurposing drugs for use in cancer. In this chapter, scientific literature regarding hepatocellular carcinoma and the drugs of interest (metformin, trimethoprim, and methotrexate) will be reviewed, with emphasis on how they together contribute to abrogating cancer survival and metastasis.

### **1.1 Hepatocellular carcinoma (HCC)**

HCC, a liver disease predominant in patients suffering from cirrhosis and chronic liver disease, is a prominent cause of worldwide deaths which occur due to cancer. As the third main cause of cancer world-wide, HCC occurs most frequently in Asia and Africa (Altekruse, McGlynn, & Reichman, 2009; Dhanasekaran, Limaye, & Cabrera, 2012). Due to its high mortality rates, HCC poses as a worldwide health burden. As patients with HCC are generally diagnosed at later stages of the disease, the average survival time is 11 months (Greten et al., 2005). Some researchers have informatively suggested that the development of HCC originates from the concept that hepatic stem cells proliferate due to continuous regeneration induced by viral injury (Waller, Deshpande, & Pysopoulos, 2015). Hence, HCC is known for the inflammation, fibrosis, and necrosis of hepatic cells due to the presence of hepatic cirrhosis or hepatitis B virus (HBV), which are vital risk factors in the progression of HCC. Furthermore, HBV can be transmitted from mother to child during delivery and via blood; either transfusions and/or injections (Balogh et al., 2016).

Both surgical and nonsurgical therapies currently available have increased the overall wellbeing of patients. Although HCC is the only solid tumor which can be treated with transplantation, surgical treatments such as orthotopic liver transplantation (OLT) have proven inefficient for therapy due to the shortage in the availability of organs (Balogh et al., 2016). Current nonsurgical approaches to HCC include biological agents such as sorafenib, a tyrosine kinase inhibitor, which blocks threonine kinase isoforms as well as the vascular endothelial growth factor (VEGF) receptor 2 and 3 to decrease angiogenesis and proliferation of tumors (Cheng et al., 2009). Patients who do not qualify for OLT and have not benefited from localized therapies are prescribed sorafenib (Cheng et al., 2009). Though proven effective, sorafenib comes with undesirable side effects such as nausea, vomiting, hypertension, weight loss and anorexia (Liver, 2012). Therefore, we are still



in need of a more efficient treatment to combat HCC (Schlachterman, Craft, Hilgenfeldt, Mitra, & Cabrera, 2015).

### **1.1.1 Risk factors**

#### *Hepatitis B and Hepatitis C virus*

Hepatitis B and hepatitis C viruses, which are responsible for 80% of all HCC cases globally, are the most prominent risk factors of HCC in individuals (El-Serag, 2012; J. D. Yang & Roberts, 2010). Hepatitis C virus has also been known to be the leading cause of HCC in high-risk continents, such as Africa and Asia (Park et al., 2015; J. D. Yang et al., 2015). The World Health Organization (WHO) claimed that one out of three people around the globe have been infected by HBV or HCV, which led to acute hepatitis, chronic hepatitis, cirrhosis or HCC (Hajarizadeh, Grebely, & Dore, 2013; World Health Organization, 2012). Of note, in the Middle East, specifically Egypt, HCV is the leading virus-related cause of HCC (J. D. Yang et al., 2017).

#### *Alcohol consumption*

Aside from viral factors, the development of HCC is also directly associated with alcohol consumption (Morgan, Mandayam, & Jamal, 2004). Roughly around 50% of HCC victims in Europe have been linked to alcohol abuse, as alcohol is metabolized in the liver (Jewell & Sheron, 2010). An increase in the toxic metabolite acetaldehyde may induce mutagenicity along with the increase in production of ROS (Matsushita & Takaki, 2019). Though many studies have been done to shed light on how ethanol contributes to the initiation of HCC, the exact mechanism remains unknown.

#### *Gender*

Women are claimed to have a lower risk of hepatocellular carcinoma than men. Some studies have posed the idea that estrogen works to inhibit growth and proliferation of hepatocellular carcinoma, rendering females less susceptible to disease than males (Ruggieri, Barbati, & Malorni, 2010). Furthermore, a meta-analysis study was previously conducted to investigate the function of the estrogen pathway on the pathogenesis of HCC. It was shown that variation in the ESR1 (estrogen receptor 1) gene was directly related to an increase risk of HCC (H. Sun et al., 2015). Estrogen

replacement reduced the risk of HCC and increased survival in a case-control study conducted (M. M. Hassan et al., 2017). Furthermore, males are more susceptible to both HBV and HCV viruses, increasing their risk of HCC (Ozakyol, 2017).

### *Non-alcoholic fatty liver disease (NAFLD)*

Chronic liver disease if left untreated may lead to fibrosis, cirrhosis and eventually hepatocellular carcinoma (Figure 1.1) (Ramakrishna et al., 2013). In one study, researchers elucidated that NAFLD increased the risk of HCC incidence by 2.6 folds (Younossi et al., 2015). Nonetheless, it is worth mentioning that this association was seen in elderly patients. The inflammation caused due to cirrhosis provides a favorable environment for cancer growth and progression, though the exact link between inflammation and cancer remains unknown.

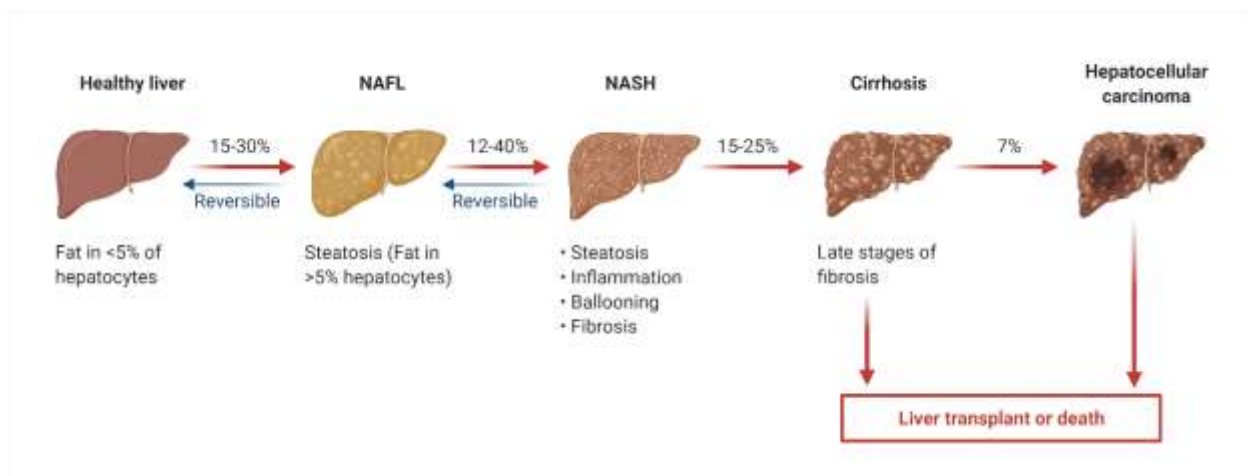


**Figure 1.1. Stages leading up to Hepatocellular carcinoma.**

**Reprinted from “Non-alcoholic Fatty Liver Disease (NAFLD) Spectrum”,  
by BioRender.com (2021)**

### *Diabetes*

Diabetes mellitus is linked to an elevated risk of HCC (El-Serag, Hampel, & Javadi, 2006; Huang et al., 2018; J. D. Yang et al., 2016). Insulin resistance is hypothesized to have a role in hepatocarcinogenesis because it causes an increase in reactive oxygen species and, as a result, increases inflammation (Balkwill & Mantovani, 2001; Hirosumi et al., 2002; Hui, Zatloukal, Scheuch, Stepniak, & Wagner, 2008). According to one study, diabetes raises the risk of HCC even in patients diagnosed with non-HCV cirrhosis (J. D. Yang et al., 2016).

### *Other causes*

Chronic biliary disease and hereditary liver diseases can also induce cirrhosis and stimulate the growth of HCC, but these causes only account for less than 10% of patients with HCC worldwide (J. D. Yang & Roberts, 2010).

## **1.2 Hallmarks of cancer**

In 2000, a paper published by Hanahan and Weinberg summarized the main characteristics of cancer cells and hence originated the term the hallmarks of cancer (Hanahan & Weinberg, 2000). An updated version was later published in 2011 with the addition of two more hallmarks (Hanahan & Weinberg, 2011). As cancer cells face a variety of stresses, such as hypoxia, nutrient shortage and DNA destruction in becoming entirely malignant, they tend to react in a number of ways to conform to the stressful environment in order to survive and metastasize. Both are some of the most important hallmarks of cancer which influence cancer cell survival and proliferation.

### *Limitless replicative potential*

To control proliferation and sustain tissue homeostasis, normal cells rely on growth signaling from a tightly regulated cell cycle. Cancer cells, on the contrary, possess unlimited replicative potential (Kelland, 2007). Cancer cells cannot multiply unless the cell cycle is disrupted and checkpoints are destroyed (Malumbres & Barbacid, 2009). The retinoblastoma (Rb) protein, commonly inactivated in various cancers, is one of the most critical regulators (Weinberg, 1995). The Rb family, including RAS, has been shown to play several roles including maintaining genomic stability, regulation of apoptosis and suppressing invasion and metastasis (Dick & Rubin, 2013; Indovina, Marcelli, Casini, Rizzo, & Giordano, 2013).

Furthermore, the most commonly mutated gene, with mutations seen in more than fifty percent of sequenced tumors, is the p53 gene (M. P. Kim, Zhang, & Lozano, 2015; Stracquadanio et al., 2016). P53 detects a variety of stresses such as hypoxia, nutrient deficiency and abnormal signaling and acts according to the condition at hand. After halting further proliferation, p53 is activated and may trigger repair process; contrastingly, if the damage is irreversible, p53 initiates cell death (Haupt, Raghu, & Haupt, 2016; Kruiswijk, Labuschagne, & Vousden, 2015)

### *Apoptosis evasion*

Apoptotic cell death, a response to irreversible DNA destruction, unregulated proliferation and matrix detachment, is a natural phenomenon that preserves tissue homeostasis (Green & Evan, 2002; Lopez & Tait, 2015). In cancer, this balance is severely impaired. There are two major pathways of apoptosis; the death receptor pathway, which involves the association of cell surface receptors with their respective ligands, also known as the extrinsic pathway. The more relevant pathway, known as the intrinsic pathway, involves the mitochondrial release of cytochrome c. The latter involves changes in the balance of pro-apoptotic and anti-apoptotic proteins. When the levels of pro-apoptotic proteins outweigh the levels of anti-apoptotic proteins, outer mitochondrial membrane releases cytochrome c. Both pathways involve subsequent caspase-3 activation, which effectively completes the process of cell death rapidly by cleaving proteins (Jain, Geneste, Gautier, Depil, & Campone, 2013).

Cancer cells can evade the apoptotic response through a variety of pathways. The inactivation of mutations in the p53 gene render the cell resistant to a variety of apoptotic stimuli. Furthermore, anti-apoptotic proteins are upregulated or pro-apoptotic proteins are lost in different tumors. Nonetheless, it is worth mentioning that while in fact such changes result in better tumor survival, cancer cells are not immune to apoptotic signals. Therefore, many chemotherapeutics target the apoptotic pathway in an attempt to combat extensive cancer cell proliferation (Llambi & Green, 2011; Sarosiek et al., 2017).

### *Tissue invasion and metastasis*

The tendency to infiltrate adjacent tissue and seed distant sites to form secondary tumors is a distinguishing characteristic of malignancies. Around 90% of cancer-related deaths are caused by metastatic diseases (Sporn, 1996; Steeg, 2006). Cancer cells must penetrate the extracellular matrix (ECM), intravasate into tumor vasculature, survive through blood circulation, extravasate at distant organs, develop micrometastases and colonize in order to spread to other areas of the body (Figure 1.2). (Massagué & Obenauf, 2016; Valastyan & Weinberg, 2011). For this reason, chemotherapeutic agents are used to limit cancer cell motility and decrease tumorigenesis in distant areas.

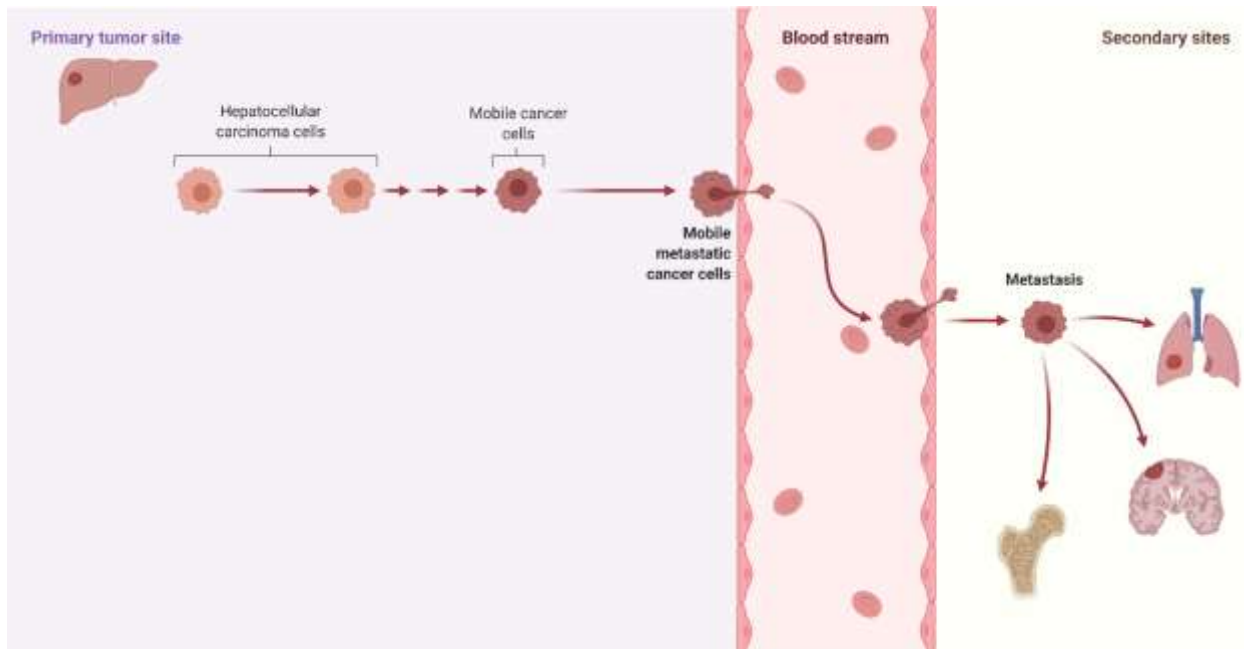


**Figure 1.2. Schematic diagram elucidating cancer cell metastasis**

**Reprinted and modified from “Cancer Progression and Metastasis”, by BioRender.com (2021)**

### *Angiogenesis*

Angiogenesis is the mechanism of endothelial cells sprouting, dividing and proliferating from pre-existing vessels (Carmeliet, 2000). It is used to expand vascular networks in embryogenesis as well as in wound healing and inflammation (Ribatti, Nico, & Crivellato, 2015). In such cases, as opposed to cancer, angiogenesis can be shut off. In malignancies, angiogenesis is continuously activated. Angiogenesis is regulated through the presence of pro-angiogenic and anti-angiogenic factors. When a stimulus increases the levels of pro-angiogenic factors, angiogenesis occurs (Carmeliet & Jain, 2000). Hypoxia is the most powerful cause of angiogenesis. Endothelial cells have several oxygen-sensing activities, the most significant of which interacts with the hypoxia-inducible transcription factor (HIF) family, which regulates the expression of several genes involved in angiogenesis, cell survival, metabolism, and inflammation (Fraisl, Mazzone, Schmidt, & Carmeliet, 2009; Y. Yang, Sun, Wang, & Jiao, 2013). Given that tumors are characterized by hypoxia, it is no surprise that HIF levels are higher in many cancers, which correlates with a low clinical prognosis (Hashimoto & Shibasaki, 2015). Other triggers of angiogenesis in tumors include metabolic rewiring of endothelial cells, resulting in genetic changes regulating angiogenic

receptor production, mechanical tension and inflammatory cell infiltration (Carmeliet & Jain, 2000). These effects may change over the course of a tumor's growth as they may be tissue specific (Petrovic, 2016).

VEGF is one of the most overly expressed pro-angiogenic molecules in a variety of tumors (Ferrara, Gerber, & LeCouter, 2003; Sakurai & Kudo, 2011). Upon stimulation, VEGF causes endothelial cell proliferation and migration. Moreover, there are various other effectors that act in conjunction with VEGF signaling (Yujie Zhao & Adjei, 2015). In addition, the newly formed vessels are not the same as the usual vessels from which they originated from (Hida, Maishi, Torii, & Hida, 2016). Wider in diameter and containing endothelial cells of different layers, the newly formed vessels cause leakiness. Consequently, blood supply is disrupted, resulting in hypoxia and acidosis in some areas. Potentiating angiogenesis, reducing therapeutic efficacy, and enabling resistant clonal expansion are all consequences of these traumatic environments (Naoyo Nishida, Hirohisa Yano, Takashi Nishida, Toshiharu Kamura, & Masamichi Kojiro, 2006).

#### *Deregulating cellular energetics*

Tumor cells, which generally prefer to utilize glycolysis to produce ATP, have once been thought to contain severely impacted mitochondria. On the contrary, it is now known that tumor cells generally have fully functional mitochondria (Cairns, Harris, & Mak, 2011). For this reason, many studies have been undertaken to target mitochondrial DNA, in an attempt to decrease tumorigenesis both *in vivo* and *in vitro* (Hay, 2016; Zong, Rabinowitz, & White, 2016). In this manner, oxidative phosphorylation works in tandem with glycolysis to meet the cancer cells' high energy demands. Despite the cancer cells' control over the two pathways of energy production, when the TCA cycle becomes oversaturated, ROS is generated (DeBerardinis & Chandel, 2016). Although moderate levels of ROS are beneficial to cancer by facilitating cancer growth (Sabharwal & Schumacker, 2014), high levels are toxic to cancer cells. In this manner, cancer cells increase their antioxidant ability to limit excessive ROS levels, which are lethal to the cells (Zong et al., 2016).

In conclusion, tumor cells are immortalized and have the capability of unlimited replicative potential, which is acquired during tumorigenesis.

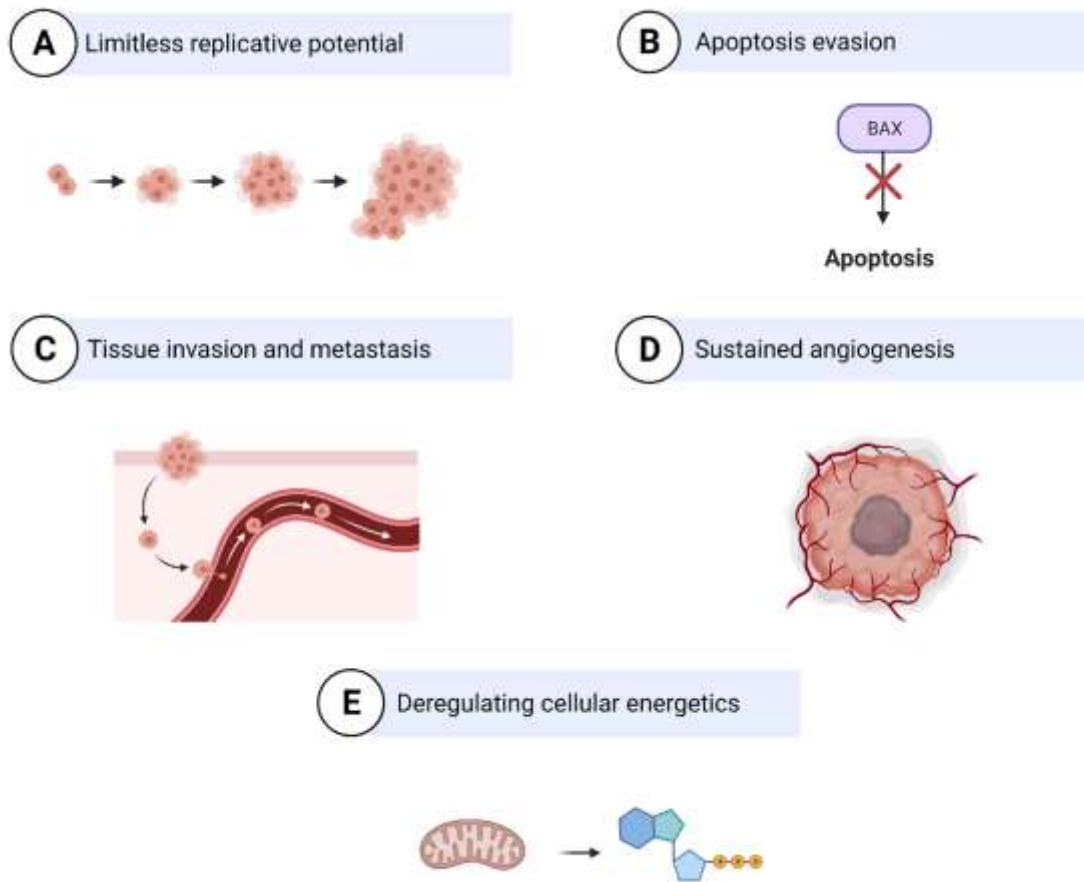


**Figure 1.3. Hallmarks of cancer.**

Reprinted and modified from “The Hallmarks of Cancer (Classical)”, by BioRender.com (2021)

### 1.3 Metabolic pathway in cancer

In the treatment of hepatocellular carcinoma, numerous directions have been taken to prevent the spread of cancerous cells. Furthermore, the detrimental effects of cancer are closely related to an increase in mitochondrial function, critical for the generation of adequate amounts of ATP. Increase mitochondrial function is also known to produce more oxidative stress as it is both the producer and target of reactive oxygen species (ROS) (Marchi et al., 2012; Murphy, 2009; Scherz-Shouval & Elazar, 2007; Y. Yang et al., 2016).

It has been well established that in comparison to normal cells, cancer cells undergo an increase in

glycolysis, hence exhibiting metabolic alteration, a phenomenon which is commonly observed in cancer, known as the Warburg effect (Pelicano, Martin, Xu, & Huang, 2006). This shift in the metabolic pathway of cancer cells allows for the increase in survival and metastasis of cancer. The fact that cancer cells generate ATP via glycolysis far more than normal cells do, regardless of adequate oxygen levels, may be due to various factors such as mitochondrial toxicity, but the exact mechanism of which remains not fully understood (Yu, Chen, Sun, Wang, & Chen, 2017). Notably, one *in vivo* study showed that tumors take up 10-fold more glucose compared to normal tissues (Yalcin, Telang, Clem, & Chesney, 2009).

One study demonstrated this shift by linking it to the loss of p53 function, the change in intracellular pH, hypoxic conditions inducing anaerobic metabolism and mitochondrial disturbances. It may also be that excess lactic acid production consequently causes a decrease in extracellular pH, causing apoptosis in normally functioning adjacent cells, as long-term exposure to acidic environments may cause apoptosis to normal cells (Gatenby & Gillies, 2004). Therefore, low extracellular pH denotes negative prognosis in terms of cancer metastasis and survival. Tumors may even favor the acidic environment as it works to increase the aggressiveness of cancer cells. Moreover, since glycolysis only produces two ATP molecules per glucose, cancer cells must consume higher amounts of glucose to maintain enough ATP to supply for the increase in proliferation, one of the hallmarks of cancer. Therefore, it has also been used clinically in the diagnosis of tumors (Tekade & Sun, 2017).



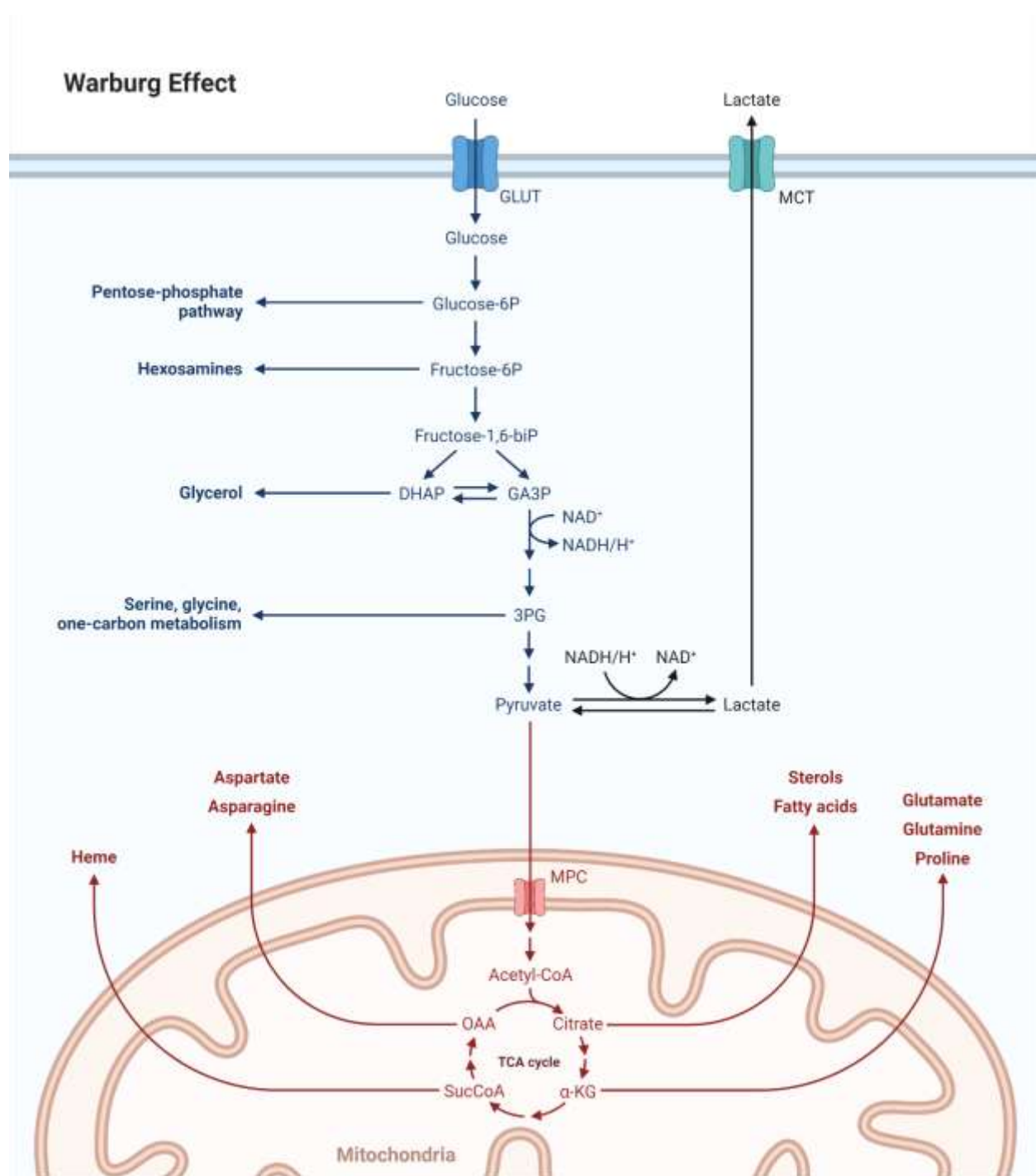


**Figure 1.4. Warburg effect.**

Reprinted from “Warburg effect”, by BioRender.com (2021)

### **1.3.1 Glycolysis**

Glycolysis, fundamentally, consists of a set of reactions that utilizes glucose to produce energy. Glucose is first taken up by transporters and converted into glucose-6-phosphate by an enzyme known as hexokinase. Next, through a series of reactions, glucose is metabolized into pyruvate, lactate, hydrogen ions, forming 2 ATP molecules per one glucose molecule. In aerobic conditions, pyruvate is then oxidized to  $\text{HCO}_3^-$ , generating 36 more ATP molecules per glucose molecule (Ganapathy-Kanniappan & Geschwind, 2013; Gatenby & Gillies, 2004; Pelicano et al., 2006). The reliance on glycolysis that cancer cells exhibit to proliferate and spread has led us to believe that the inhibition of glycolysis may selectively target cancer cells (Gatenby & Gillies, 2007). In this study, we used experimental systems to measure the amount of glycolytic inhibition after the treatment of HepG2 cells to various drug combinations.

### **1.3.2 Oxidative phosphorylation**

Mitochondria, the powerhouses of the cell, are vital organelles that are important in metabolism and energy production through respiration. For this reason, mitochondrial dysfunction plays a role in many diseases, one of which is cancer. ATP, the primary energy source in cells, is created through glycolysis in the cytosol and oxidative phosphorylation (OXPHOS) in the mitochondria. Under basal conditions, the mitochondria metabolize pyruvate which was produced from glycolysis by undergoing oxidation reactions, yielding  $\text{CO}_2$  and water. Electrons, obtained via intermediates of the Krebs cycle, are donated to nicotinamide adenine dinucleotide and flavin adenine dinucleotide to yield NADH and  $\text{FADH}_2$ . They are both coenzymes which contain electrons that are supplied to electron carriers in the electron transport chain (ETC). There are four sets of enzyme complexes designated I, II, III, and IV in the inner mitochondrial membrane. Complex I, known as NADH dehydrogenase, of the ETC is found in the inner mitochondrial membrane and removes hydrogen from the reduced form of the nicotinamide adenine dinucleotide. The electrons provided by NADH and  $\text{FADH}_2$  proceed along the ETC, creating energy along the way. Complex II is known as succinate dehydrogenase, which from its name, removes hydrogen ions from succinate, rendering the formation of fumarate, one of the steps of the Krebs cycle. By doing so,  $\text{FADH}$  is produced, and as previously stated, serves to donate electrons to the ETC.

Cytochrome reductase, complex III of the ETC, contains cytochrome B, C1 and C. Complex III accepts electrons from the ETC and transmits them to cytochrome C, which then delivers the electrons to the ETC's complex IV. Complex IV, also known as cytochrome C oxidase, is a heme and copper-containing enzyme that accepts electrons from cytochrome C and uses them to reduce  $O_2$  to  $H_2O$ . This energy is utilized to transport hydrogen ions into the mitochondria's intermembrane space, establishing a positive charge in the intermembrane space and a negative charge in the matrix, resulting in an electrochemical gradient. This proton gradient supplies energy which is enough to drive ATP synthase. As the inner mitochondria is impermeable to hydrogen ions, the ATP synthase pumps hydrogen ions back to the matrix through  $F_o$  channel in the ATP synthase complex, leading to conformational changes of the enzyme ATP synthases, allowing for the production of ATP from  $ADP + P_i$ . Therefore, electron transport and phosphorylation are tightly coupled, constituting what is known as OXPHOS metabolic pathway (Chance & Williams, 1956; Hatefi, 1985; Senior, 1988).

Metformin, which primarily targets the mitochondria within the cell, was shown to inhibit respiratory complex I in the ETC, NADH dehydrogenase, thereby inhibiting electron flow through the ETC. As a result, AMP levels increase due to the decrease in NADH oxidation and proton-driven ATP synthesis by oxidative phosphorylation. The mechanism of which metformin enters the mitochondria is not clearly known, as no specific mitochondrial carrier for metformin has been identified.

One study demonstrated the importance of enzymes responsible for glycolysis and OXPHOS in hepatocellular carcinoma. Glucokinase (GCK), the major hexokinase in normal hepatocytes, is responsible for converting glucose to glucose-6-phosphate, the first step in glycolysis. On the other hand, HCC cells express HK2 more prominently, thereby differentiating both cell types. They found that HK2 expression was directly proportional to the progression of HCC, widely expressed in later stages of the disease, independent of its cause. This further confirmed that it may allow for safer and more effective targeted therapy against HCC. To back up their assumptions on the role of HK2 in the development of disease, they created a mouse model which did not possess HK2 and found that it in fact did not allow for hepatocarcinogenesis. Due to metabolic shift, OXPHOS was more widely used as a source of ATP production. To eradicate HCC cells, metformin was

used as a complex I inhibitor of OXPHOS, inhibiting tumor growth *in vivo* (DeWaal et al., 2018).

### *Basal respiration*

The oxygen consumption rate (OCR) of basal respiration is determined by assessing OCR without the presence of any mitochondrial inhibitors (Underwood, Redell, Zhao, Moore, & Dash, 2020). Mitochondrial inhibitors may be used to measure four important mitochondrial respiration parameters: baseline, ATP production-linked, maximum, and proton leak-linked OCR. (Smolina, Bruton, Kostareva, & Sejersen, 2017). To estimate the proportion of basal respiration which is a result of ATP synthesis via complex V, the addition of an ATP synthase inhibitor, oligomycin, is used (Leung & Chu, 2018).

### *ATP-linked respiration*

ATP-linked respiration is governed by the amount of energy demand, the extent of ATP synthesis and the quantity of substrate present. The amount of ATP the cell needs in order to function differs from one cell line to another, one cancerous type to another, depending on the extent of ATP needed to undergo key processes such as metastasis in the case of cancer (Divakaruni, Paradyse, Ferrick, Murphy, & Jastroch, 2014). Furthermore, inhibition via administration of an inhibitor of ATP synthase can alter the rate of ATP synthesis. Moreover, decrease in production of NADH or FADH<sub>2</sub> via the TCA cycle could render a lower supply of electron donors essential for the ETC activity, and consequently, ATP-linked respiration. Furthermore, fluoro-carbonyl cyanide phenylhydrazone (FCCP) administration can detect changes in substrate supply and oxidation (Gu, Ma, Liu, & Wan, 2021).

### *Proton-leak respiration*

Protons, when pushed from the mitochondrial matrix to the intermembrane space via complex I, III, and IV, create an electrochemical gradient that not only allows ATP synthase (complex V), to convert ADP into ATP, but also stimulates the ETC complexes. This occurs due to proton leaks, consuming the membrane potential, uncoupling the ETC from ATP synthase. Therefore, oxidation of NADH and FADH<sub>2</sub> still occurs even in the presence of oligomycin.

### *Maximal respiration*

Determining how pharmacological therapeutics can modify metabolism can be greatly seen in comparing the maximal respiration of HepG2 cells with and without potential chemotherapeutics. Maximal respiration is the maximum capacity that the electron respiratory chain can reach. It is calculated after the injection of FCCP (Gu et al., 2021).

#### *Spare respiratory capacity*

Reserve capacity, the difference between ATP production via OXPHOS at maximal respiration and basal respiration, is the amount of ATP able to be generated essentially in times of ATP demand. Under conditions of stress, cells require additional energy to survive. Maximal respiration is a function of substrate supply and oxidation (Gu et al., 2021).

#### *Non-mitochondrial respiration*

Oxygen consumption, independent of mitochondrial respiration, is due to the action of oxidases. Non-mitochondrial respiration may be determined by shutting down the ETC entirely using complex I and III inhibitors, such as Rotenone and Antimycin A (Rot/AA). The extent of non-mitochondrial respiration depends primarily on the cell type being used; some of which may possess oxidases (NADPH oxidase) more actively, such as monocytes and lymphocytes (Kramer, Ravi, Chacko, Johnson, & Darley-Usmar, 2014).

### **1.3.2.1 Drugs that inhibit OXPHOS**

#### *Oligomycin*

Oligomycin, an ATP synthase inhibitor, was first reported in the late 1950s (Lardy, Johnson, & McMurray, 1958). Targeting the final complex in the OXPHOS pathway, oligomycin blocks the proton channel of complex V (inhibiting proton entry into the mitochondrial matrix), thereby inhibiting phosphorylation of ADP into ATP, decreasing energy production. As electron transport and phosphorylation are tightly coupled, electron transport ceases as protons are no longer able to be pumped across the membrane under very steep gradients; therefore, confirming the finding that electron transport across complex I-IV depends on the formation of ATP via complex V (Gu et al., 2021).

### *Rotenone/Antimycin A*

Rotenone, a natural compound, is obtained from the species *Lonchocarpus* and *Derris*. It was first used as a pesticide, but its use was later inhibited due to its toxic effects. Rotenone inhibits complex I by preventing electrons from passing from iron-sulfur centers in complex I to ubiquinone, effecting electron transport and hence ATP production. This inhibition also results in decreased oxygen consumption. Furthermore, rotenone has been seen to cause apoptosis by inducing ROS production due to the inadequate electron transfer along the ETC (Heinz et al., 2017).

### *FCCP*

FCCP, a potent uncoupler of mitochondrial OXPHOS, works to make the inner mitochondrial membrane permeable for protons (interfering with the proton gradient). This consequently allows for maximum electron flux through the ETC and thereby disrupts ATP synthesis (Gu et al., 2021).

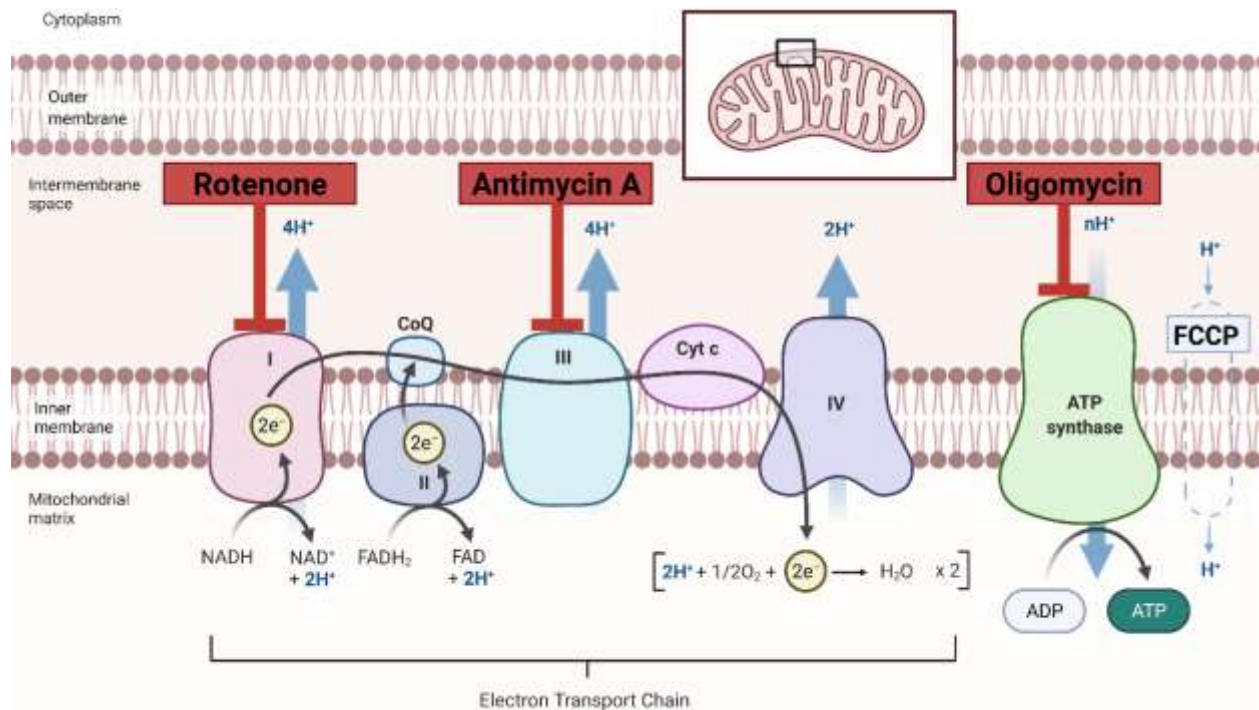


**Figure 1.5. Diagram of mitochondria depicting drugs which inhibit oxidative phosphorylation.**

Reprinted and modified from “Electron Transport Chain”, by BioRender.com (2021)

## **1.4 The need for drug repurposing**

In light of creating a safer, more effective and economical alternative to drug discovery, drug repositioning has posed to be efficient in the treatment of numerous diseases worldwide as de-novo drug discovery can take up to ten to seventeen years for a single compound of interest (Tobinick, 2009). Furthermore, the high cost in determining the safety of novel drugs hinders drug development in many cases. Drug repositioning has posed as an interesting and beneficial approach to drug discovery as it works to recycle drugs in the aim of tackling debilitating diseases. As a result, the primary goal of this research was to look for putative linkages between pharmaceutical medicines and key HCC intermediates.

In one study, computational repositioning was implemented in the treatment of HCC as mice and human cell lines were treated with niclosamide ethanolamine, originally an anthelmintic, and was proven to be helpful in altering the expression of genes which are up-regulated or down-regulated in HCC in favor of decreasing the viability of HCC cells and eventually decreasing the size of the tumor significantly. This posed the idea that niclosamide ethanolamine is a probable anti-tumor agent (B. Chen et al., 2017).

## **1.5 Metformin as an anti-diabetic agent**

Metformin (1,1-dimethyl biguanide) (Figure 1.6), an orally administered drug, is used to decrease the level of blood glucose in patients with non-insulin-dependent diabetes mellitus (NIDDM) by improving insulin sensitivity and decreasing insulin resistance. Recommended as first-line oral therapy in the treatment of diabetes by the American Diabetes Association (ADA), metformin lowers blood glucose levels by blocking hepatic glucose synthesis while also enhancing glucose absorption and use by skeletal muscles. This reduces insulin resistance in peripheral tissues and restores the body's insulin responsiveness (Dowling, Goodwin, & Stambolic, 2011). Moreover, as anti-diabetic drug, metformin exhibits insulin like actions and reduces gluconeogenesis, which results in decreased glucose levels (Zi et al., 2018). Patients with type II diabetes mellitus are likely to develop cancer; therefore, the development of anti-diabetic agents, including metformin, was undertaken to reduce the risk of cancer. Metformin suppresses not only serum glucose level but

according to several studies it has been explained that metformin can be used to treat cancer (Gong et al., 2014).

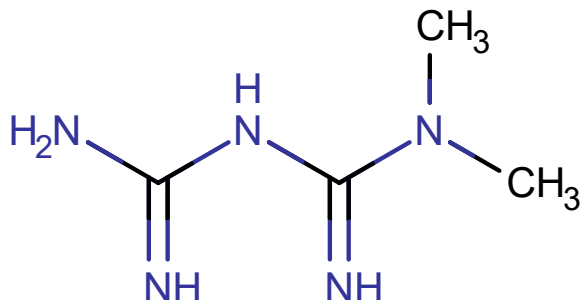


**Figure 1.6. Chemical structure of Metformin.**

**(Wishart et al., 2006)**

Metformin exerts its anti-hyperglycemic action by suppressing the production of hepatic glucose, in a process known as hepatic gluconeogenesis (Foretz, Guigas, Bertrand, Pollak, & Viollet, 2014). As previously stated, metformin inhibits complex I of the ETC and consequently decreases ATP production by OXPHOS. This ultimately disrupts the AMP:ATP ratio, resulting in the activation of 5' AMP- activated protein kinase (AMPK), an enzyme which constantly detects the cellular energy status by monitoring AMP, ADP, and ATP levels (Hardie, 2014). To counteract the improper energy balance upon metformin administration, AMPK works to restore ATP levels by impeding biosynthetic pathways and promoting pathways which restore energy balance. AMPK stimulates key processes such as glycolysis,  $\beta$ - oxidation of fatty acids, mitochondrial biogenesis and glucose uptake, while it also switches off protein, glycogen and sterol synthesis in order to salvage ATP. AMPK phosphorylates enzymes such as acetyl-CoA carboxylase (ACC) to promote fatty acid oxidation and inhibit fatty acid synthesis, hence altering insulin signaling; furthermore, AMPK initiates glycolysis through the phosphorylation of phosphofructokinase-2 (PFK-2). Furthermore, AMPK promotes the translocation of GLUT4 from intracellular vesicles to the plasma membrane, allowing hepatocytes, skeletal muscles, and adipocytes to take up more glucose. The nature of metformin in that it allows for the activation of AMPK which consequently effects crucial pathways renders it a potent hypoglycemic drug.



### **1.5.1 The discovery of metformin as an anti-diabetic agent**

*Galega officinalis*, French lilac, was first used as an herbal therapeutic agent which helped alleviate polyuria, one of the hallmarks associated to diabetes mellitus. Owing to its abundant content of guanidine, this plant was used in the treatment of hyperglycemia. Though proven to be too toxic for therapeutic use, it was nonetheless the beginning of the development of metformin, which posed much less side effects and thereby became authorized for use in the United States in 1995 (Witters, 2001).

### **1.5.2 Safety profile**

Metformin has widely gained acceptance in the treatment of diabetes due to its cheap cost and more importantly, favorable safety profile (Rizos & Elisaf, 2013). The main adverse effects of metformin are mild and transient gastrointestinal symptoms. Fortunately, lactic acidosis, greatly associated with the administration of phenformin and buformin, is rare to occur with metformin treatment (Foretz et al., 2014). Furthermore, unlike various anti-hyperglycemic agents, such as sulfonylureas, metformin is not known to induce hypoglycemic events or weight gain. For these reasons, metformin is readily prescribed to diabetic patients. Given its well-known clinical safety profile as an anti-diabetic drug, low cost and profound effectiveness, metformin represents a promising candidate to be used in combination with anti-folates in the treatment of HCC.

### **1.5.3 Metformin as an anti-cancer agent**

Diabetes and cancer are two of the most prevalent debilitating diseases influencing all races and genders and increasing the burden of chronic diseases worldwide. Many studies have been done to highlight the mechanism of which diabetes may be correlated to cancer, yet the exact mechanism remains unknown. Results from numerous studies also have been also seen to differ with relation to the type of cancer, some cancer types showing a higher risk of incidence than others.

Metformin's anticancer effect was originally discovered in a retrospective study of diabetic patients with cancer. This study depicted that diabetic patients who were prescribed metformin had a lower risk of developing various malignancies than those who were treated using other anti-

diabetic agents (Evans, Donnelly, Emslie-Smith, Alessi, & Morris, 2005). Further research has revealed that metformin halts the growth of a wide spectrum of cancer cells, including breast, prostate, colon and glioma through AMPK activation, mTOR signaling inhibition and reduced cyclin expression (Buzzai et al., 2007; Liu et al., 2012; Mazurek et al., 2020; Nangia-Makker et al., 2014; Rich, 2007; Sahra et al., 2008; Whitburn, Edwards, & Sooriakumaran, 2017).

Furthermore, studies have shown that hyperglycemia may initiate DNA damage, increase levels of ROS, impair DNA repair and interfere with numerous tumor suppressor genes (Basu, 2018; Ramteke, Deb, Shepal, & Bhat, 2019). Evidence depicts an increase in AKT oncogene and DNA damage following induction of type 1 diabetes hyperglycemia in proximal tubular epithelial cells (Ramteke et al., 2019). As hyperglycemia may increase the risk of DNA mutations, it can lead to increasing the risk of cancer in diabetic patients. One study elucidated that diabetic mice show an increase in mitochondrial DNA (mtDNA) mutations in oocytes (Li et al., 2018).

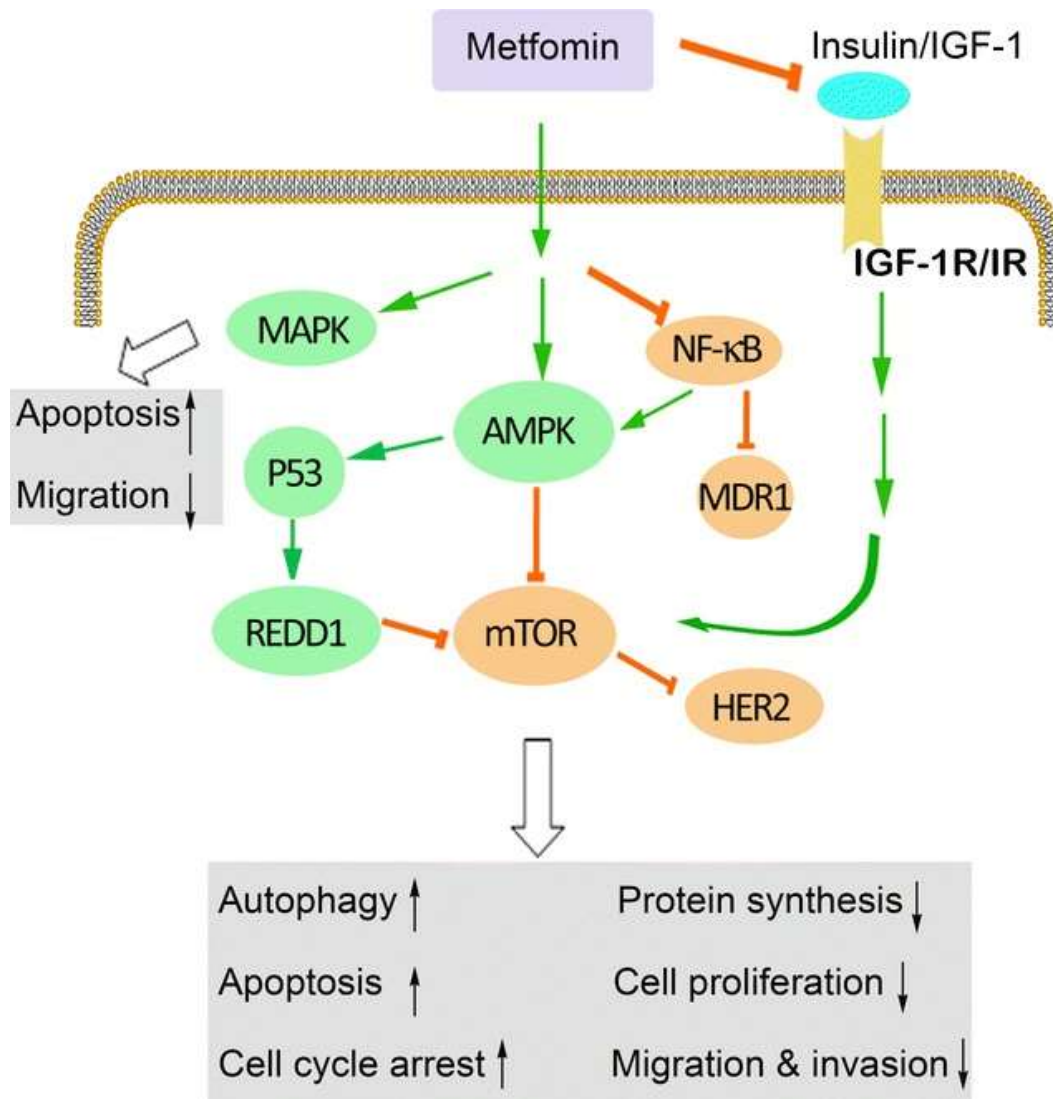


**Figure 1.7. Proposed mechanism of action of metformin as an anti-cancer agent.**

**(Lei et al., 2017)**

Another study depicted that low-dose metformin protects treated diabetes mellitus patients from various malignancies, including colorectal cancer in women, HCC in men, and pancreatic cancer. This was apparent in a population with an increased prevalence of diabetes mellitus (DM) and a higher risk of cancer (Lee et al., 2011). Metformin has also been shown to reduce various types of cancer incidence and mortality, improve cancer cell responsiveness to radiation and chemotherapy, reduce malignancy and lower the chance of recurrence (Sarai, Asadi, Kakar, & Moradi-Kor, 2019).

Furthermore, one study depicted that in response to metformin, de novo synthesis of glutathione,

a folate-dependent process linked to one-carbon metabolism, was also decreased (Bruna Corominas-Faja et al., 2012). Accordingly, these findings imply that metformin can also act as an antifolate chemotherapeutic drug.

In a nutshell, current data suggest that the role of metformin as a cancer prophylactic may not encompass all types of cancers, though several clinical trials are currently studying the credibility of these findings.

## **1.6 Antifolates**

Folates, primarily present in the plasma as 5-methyl tetrahydrofolate, are one-carbon donors, which are essential for the de novo synthesis of nucleotides (purines and pyrimidines), and hence cell division (Zi et al., 2018). Dihydrofolate reductase (DHFR) has been studied for years as a target for antibacterial and antifungal therapies. Its function in cancer treatment has been revealed because it supplies a methyl group required for the de novo production of purines, thymidylic acid, and certain amino acids (Blakley & Benkovic, 1984). DNA consists mainly of three parts; the sugar part, phosphate part and a nitrogen base forming what is known as a nucleotide. The DNA forms a double strand, the sides of which consist of the sugar and phosphate parts, while the center consists of the nitrogen bases. Phosphate and sugar parts are linked together by strong covalent bonds, whereas the nitrogen bases are linked together by weak hydrogen bonds twisting the two strands together, rendering the DNA a double helix (Rojas Quintero et al., 2014). The group of chemotherapeutic drugs, known as anti-metabolites, blocks the enzyme DHFR essential for cell proliferation, halting cells from making and repairing DNA, rendering them cytotoxic agents.

### **1.6.1 Trimethoprim (TMP)**

Trimethoprim (a synthetic compound), used widely for the treatment of microbial infections, has been shown to inhibit various respiratory and urinary tract pathogens by blocking the synthesis of tetrahydrofolate, the active form of folic acid (Darrell, Garrod, & Waterworth, 1968; Smilack, 1999). Unlike other anti-folate agents, TMP, which belongs to the class of compounds known as diaminopyrimidines, is structurally smaller and different than folate (Huovinen, 1987). It is widely

administered in combination with sulfamethoxazole, providing therapeutic and prophylactic potency. TMP was first used in the therapeutic treatment of *Proteus* septicemia, where it was combined with polymyxin and sulfonamides (Huovinen, 1987). This combination has also been used for the treatment of HIV and AIDS (Iyer, Milhous, Cortese, Kublin, & Plowe, 2001). More commonly known to be used as prophylaxis for *Pneumocystis carinii* infection, resistance to this combination has rapidly increased by the years (Eliopoulos & Huovinen, 2001). Moreover, TMP was shown to cause significant cytotoxicity in bladder cancer cells, suggesting the use of antifolate agents in preventing cancer cell seeding, and hence recurrence (Kamat & Lamm, 2004).

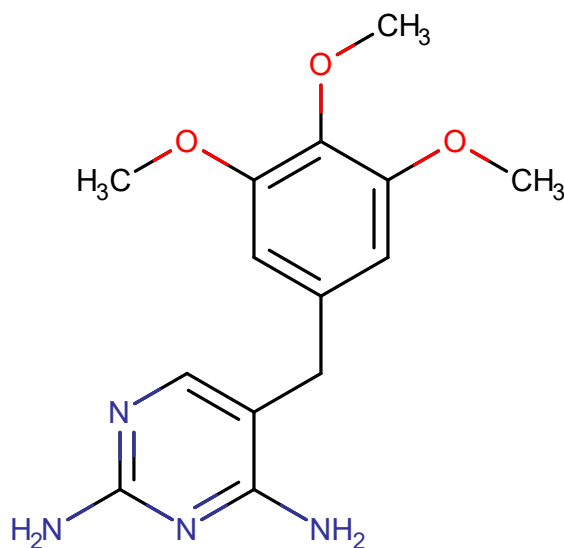


**Figure 1.8. Chemical Structure of Trimethoprim.**

(Wishart et al., 2006)

### 1.6.2 Methotrexate (MTX)

Methotrexate, which potently blocks DHFR (an enzyme that catalyzes the reduction of dihydrofolate to tetrahydrofolate), was used to treat childhood acute leukemia (McGuire, 2003). MTX was originally developed as a chemotherapeutic agent, but the mechanisms by which it can induce other potent activities, at a much lower dose, can vary significantly from those used to treat malignant diseases. As a folic acid antagonist, MTX has also been used to treat psoriasis and psoriatic erythroderma (C.-h. Yang, Yang, Jaing, & Chan, 2000). Moreover, MTX has often been

used in the treatment of rheumatoid arthritis, owing to its anti-inflammatory effects. Even though not a single pathway can account for the distinct actions of MTX as an anti-inflammatory agent, the release of adenosine from cells has been shown in various *in vitro* and *in vivo* studies (Chan & Cronstein, 2010). MTX has also been used in combination with other antirheumatic agents and reported to have a more intense response, when compared to the use of either drug alone (Cronstein, 2005). Methotrexate, blocks purine and pyrimidine synthesis, which explains its efficacy as a chemotherapeutic agent, as well as some of its side effects (Tian & Cronstein, 2007).

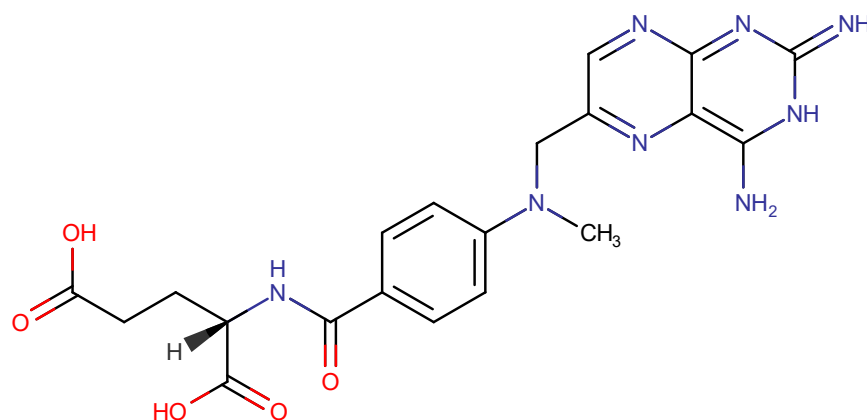


**Figure 1.9. Chemical structure of Methotrexate.**

**(Wishart et al., 2006)**

### **1.6.3 Metformin as an anti-folate agent**

As previously mentioned, metformin causes the inhibition of many different pathways as a result of AMPK activation; one of which is the folate pathway (B. Corominas-Faja et al., 2012); hence, metformin treatment not only affects DNA synthesis, but also influences its regulation and repair. Upon administration of metformin, the levels of nucleotides decrease, hence initiating cancer cell death through the inhibition of DNA formation. Nevertheless, previously formed nucleotides (addition of thymidine and hypoxanthine to cancer cells) are capable of restoring cancer cells' viability and ability to synthesize DNA, and hence reverse the anti-cancer effects of metformin (B. Corominas-Faja et al., 2012).

Furthermore, long term treatment of metformin results in decreased vitamin B12 levels, which is an essential co-factor in the donation of one carbon atom; therefore, the decreased level of vitamin

B12 also contributes to decreased purine and pyrimidine synthesis (Rojas Quintero et al., 2014). Since cancer cells rely on nucleotide formation for DNA synthesis, which occurs at a higher rate than in normal cells, metformin is believed to have a targeted effect on cancer cells. However, targeting cancer cells is not exclusive to cancer as rapidly dividing cells may also be affected (B. Corominas-Faja et al., 2012).

## **1.7 Rationale**

As HCC incidence and mortality rates continue to rise, the need for the development of innovative therapeutic options, with relatively safe profiles and potential anti-cancer effects, are required. Among new therapeutic approaches, the combination of FDA approved drugs as potential chemotherapeutics which impact the apoptotic pathways, migration and cellular bioenergetics of cancer cells, poses as an effective alternative. Due to their low cost, these combinations may be of great interest to developing countries with high prevalence of HCC. To the best of our knowledge, MET has never been used in conjunction with antifolates in the treatment of HCC and the impact of this combination on cellular energetics has not been examined using Seahorse analysis.

## **1.8 Hypothesis**

We hypothesize that combining metformin with antifolates, trimethoprim or methotrexate, will potentiate the anti-cancer effect of metformin on hepatocellular carcinoma.

## **1.9 Aims and Objectives**

This study aims to not only offer a deeper understanding into the molecular pathways involved in the use of drug combinations, but also provide us with a safe and alternative method in tackling HCC among patients. We aimed to examine the use of MET, TMP and MTX, alone and in combination, as potential therapeutic agents against HCC.

Additionally, the specific aims of the present study were:

1. Determine the cytotoxicity of tested compounds, alone and in combination, against HepG2 cell line.

2. Examine the effects of MET, TMP, MTX and respective combinations on Bax, Bcl-2, p53 and AMPK mRNA expression levels using real-time PCR.
3. Investigate the potential pro-apoptotic effects of tested compounds on HepG2 cells by flow cytometry.
4. Explore the anti-cancer effects of tested compounds on the migration ability of HepG2 cells.
5. Identify the effects of MET, TMP, MTX and combinations on the bioenergetics (glycolysis, total ATP production and mitochondrial function) of HepG2 cells by Seahorse Analysis.



## CHAPTER 2: MATERIALS AND METHODS

### 2.1 Materials

Metformin and Trimethoprim were kind donations from Nile Company for Pharmaceuticals and Chemical Industries (Cairo, Egypt). Methotrexate vials 50 mg/2 mL (Mylan-Merck Generiques) were purchased, in their formulated commercial preparations, from a community pharmacy (Cairo, Egypt). RevertAid cDNA kit (K1621), PowerUP SYBR Green Master Mix (A25741), mRNA primers (10629186; designed by NCBI primer blast tool), Dulbecco's Modified Eagle Medium Gibco™ DMEM, High Glucose (41965-039), Fetal Bovine Serum Gibco™ FBS (10270-106), Dimethyl sulfoxide DMSO (67-68-5), Chloroform (HPLC grade; C607SK-1), Isopropanol (HPLC grade; BP26324), and Ethanol (HPLC grade; 64-17-5) were all purchased from ThermoFisher Scientific (MA, USA). QIAzol lysis buffer (79306), RNase/DNase free water (129114) were purchased from Qiagen (Hilden, Germany). Penicillin-Streptomycin Mixture Pen/Strep (09-757F), and Phosphate Buffered Saline (1X) (PBS) (17-516Q) were obtained from Lonza-Bioscience (Billerica, MA, USA). Seahorse cell mito stress kit containing oligomycin, carbonyl cyanide p-trifluoromethoxyphenylhydrazone (FCCP), Rot/AA and glycolytic rate assay kit including Rot/AA and 2-deoxyglucose (2-DG) were obtained from Seahorse Bioscience Inc. (Basel, Switzerland). XF96 cell culture plates, sensor cartridges and XF base medium were also procured from Seahorse Bioscience Inc. Annexin V and propidium iodide (PI) were purchased from ThermoFisher Scientific (MA, USA).

**Table 2.1: Cell culture solutions**

<b>Solution</b>	<b>Formula</b>
DMEM	1x Dulbecco's Modified Eagle Medium [+] 4.5g/L D-Glucose, L-Glutamine [-] Pyruvate (Gibco®)
Complete DMEM media	1x Dulbecco's Modified Eagle Medium [+] 4.5g/L D-Glucose, L-Glutamine [-] Pyruvate (Gibco®) + 10% Fetal Bovine serum (Gibco®) + 100 U/ml of penicillin + 0.1 U/ml streptomycin
PBS	1x Sterile PBS solution (Lonza-Bioscience)

Trypsin	1x Trypsin (0.25%) with EDTA (Gibco®)
Freezing media	10% DMSO in FBS; 9 ml FBS + 1 mL DMSO

## 2.2 Cell culture

HepG2 cells (ATCC® HB-8065) were obtained from the National Research Centre (NRC) Cairo, Egypt. HepG2 cells were cultured in 75 cm<sup>2</sup> flasks in a 5% CO<sub>2</sub> incubator at 37°C, until they reached 80% confluency. HepG2 cells were grown in Dulbecco's modified Eagle's medium (DMEM) high glucose media (Gibco®, Thermo Fisher Scientific) supplemented with 10% fetal bovine serum (FBS) (Gibco), 1% Pen-Strep (100 units/mL penicillin, and 100 µg/mL streptomycin (Gibco, MA, USA).

Cells were stored either in liquid nitrogen or in a -80°C freezer. To thaw cells for use, cells were placed in a water bath at 37°C and resuspended in 5 mL of complete medium.

## 2.3 Cell viability assay (MTT assay)

Once cells reached confluency, T-75 flasks containing HepG2 cells were washed with 5 mL of 1x PBS twice. Next, 5 mL of Trypsin/EDTA solution was added to detach the cells from the surface of the flask and left in the incubator for 5 min at 37°C. Equal volume of media was then added to the flask to deactivate trypsin. The cell suspension was then centrifuged at 280 x g for 7 min to form a cell pellet. The pellet was then resuspended in fresh DMEM media. To precisely assess the seeding density, cells were counted using trypan blue; alive cells were excluded from this dye because they contain an intact cell membrane as opposed to dead cells. (Koopman et al., 1994). To measure the inhibition rates of cells to single drug and dual drugs, HepG2 cells were seeded in 96-well plates at a density of 15,000 cells/well. Twenty-four hours later, adherent cells were treated with increasing concentrations of single drugs: MET (12.5, 25, 50, 100, 200 mM), TMP (32.29, 64.58, 129.17, 258.34, 516.67 µM) and MTX (1.56, 3.125, 6.25, 12.5, 25, 50 mM) in fresh DMEM media. MET powder and MTX solutions were directly dissolved or diluted in complete DMEM media. For TMP, a 100 mg/mL stock solution in dimethyl sulfoxide (DMSO) was prepared and then diluted in cell culture medium until the final concentration of DMSO did not exceed 0.3% per well. The culture medium for dual drugs was composed of increasing concentrations of MET (12.5,

25, 50, 100, 200 mM) and either 516.67  $\mu$ M TMP or 1.5 mM MTX. Following 24 hours (h) incubation with the drugs, culture medium was replaced with 100  $\mu$ L/ well of 10 mg/ml MTT (3-(4,5-Dimethylthiazol-2-yl)-2,5-diphenyltetrazolium bromide) solution prepared in complete DMEM medium. Cells were then incubated for 1 h inside the incubator at 37°C. MTT, a yellow tetrazolium, dye, is reduced by the action of an enzyme known as mitochondrial dehydrogenase, present in the mitochondrial of viable cells, into purple formazan (Kumar, Nagarajan, & Uchil, 2018). As a result, the color intensity as a result of the formation of formazan crystals is proportional to the number of live cells. MTT media was then removed from the wells and formazan crystals were dissolved in 100  $\mu$ L/well DMSO. A Nano SPECTROstar microplate reader (BMG LABTECH, Ortenberg, Germany) was used to detect optical density (absorbance) at 570 nm. The following formula was used to calculate cell viability:

$$\% \text{ Viability} = \frac{\text{Absorbance of treated cell} - \text{absorbance of blank}}{\text{Absorbance of untreated control} - \text{absorbance of blank}} \times 100$$

The untreated control was demonstrated as the wells containing cells only, while the blank was depicted as wells containing no cells.

Furthermore, the IC<sub>50</sub> of the drugs when used as monotherapies or in combination were determined *via* GraphPad Prism software using the non-linear regression analysis.

## 2.4 RTqPCR

### 2.4.1 Treatment and isolation of total RNA

HepG2 cells were seeded in 6-well plates overnight at a seeding density of 250,000 cells/well. Cells were then treated with MET, TMP or MTX and the combinations at concentrations of 20 mM, 516.67  $\mu$ M and 10 mM, respectively for 48 h. Total RNA was then isolated using QIAzol Lysis Reagent, Qiagen, Hilden, Germany) according to the manufacturer's instructions. QIAzol (600  $\mu$ L) was added into each well and cell lysates were then collected in separate Eppendorf tubes. In each tube, 120  $\mu$ L of chloroform (HPLC grade, Thermo Fischer Scientific, MA, USA) was

added and the tubes were shaken vigorously for 15 s and left at room temperature for 3 min. The tubes were then centrifuged at 12000 x g for 15 min at 4°C. The mixture divided into three layers after centrifugation: a bottom phenol red-chloroform phase, an interphase and a colorless top aqueous phase. The RNA-containing aqueous phase was then transferred to a fresh set of Eppendorf tubes. Then, 150 µL of isopropanol (HPLC grade, Thermo Fischer Scientific, MA, USA) was added to each tube and mixed well. The tubes were incubated at room temperature for 10 min and then centrifuged at 12000 x g for 10 min at 4°C. After centrifugation, the total RNA was precipitated at the bottom and the supernatant was discarded. The RNA pellet was then washed with 75% ethanol, which was prepared in nuclease free water, and centrifuged at 7500 x g for 5 min at 4°C. The supernatant containing ethanol was then discarded and the tube containing the RNA pellet was left to air dry for 5-10 mins, to avoid RNA crystallization. The pellet was then resuspended in 30 µL nuclease free water (Qiagen, Hilden, Germany) and incubated in a heat block at 60°C for 15 min. RNA samples were then assessed to detect purity by measuring the absorbance of the RNA samples at 260 nm (ng/µL) and calculating the  $A_{260/280}$  ratio which was measured using NanoDrop Spectrophotometer (BMGLABTECH, Ortenberg, Germany). Finally, RNA was stored at -80°C until further use.

#### **2.4.2 cDNA synthesis for qualitative analysis of mRNA**

The Revertaid cDNA synthesis kit (K1621; ThermoFisher Scientific, MA, USA) was used, according to the manufacturer's instructions, to synthesize the cDNA for real-time quantification. A 20 µL mixture was made containing: 1 µg of total RNA diluted with nuclease free water up to a total volume of 10 µL and 10 µL of the cDNA master mix. The cDNA master mix contained: 4.0 µL 5× reverse transcription (RT) buffer, 2 µL 10mM dNTP mix (100 mM), 1.0 µL RT random Hexamer primers and 1.0 µL Oligo (dt)18 primer, 1.0 µL RevertAid M-MuLV RT (200 U/µL) reverse transcriptase, 1.0 µL RiboLock RNase Inhibitor (20 U/µL). Following a 5 min incubation at room temperature, the mixture was incubated for 60 min at 42°C, followed by 5 min incubation at 70°C to terminate the reaction, and then cooled to 4°C in the Thermal cycler (Applied Biosystems). The reaction was then stored at -20°C to avoid cDNA degradation. The synthesized cDNA was then diluted at a ratio of 1:3 by adding 40 µL nuclease-free water.

### 2.4.3 Quantification of mRNA using real-time PCR

The real-time PCR was carried out on an ABI Prism 7500 system (Applied Biosystems, CA, USA), using PowerUP SYBR Green Master Mix (A25741; Thermo Scientific, MA, USA). SYBR green, a fluorescent dye, allows for monitoring of the levels of amplified products as it binds to double stranded DNA minor groove and in doing so, emits fluorescence (Morrison, Weis, & Wittwer, 1998). During the exponential rise/phase of the reaction, quantification occurs. Quantitative analysis was performed for the expression of mRNAs Bax, Bcl-2 p53 and AMPK normalized against  $\beta$ -actin. The SYBR green mRNA reaction (12.5  $\mu$ L) consisted of 10  $\mu$ M forward primer (0.375  $\mu$ L), 10  $\mu$ M reverse primer (0.375  $\mu$ L) (rendering a 0.3  $\mu$ M final concentration of each primer), SYBR Green Universal Mastermix (6.25  $\mu$ L), nuclease-free water (2.5  $\mu$ L) and cDNA sample (3  $\mu$ L), which is equivalent to 50 ng cDNA.

The real-time RT-PCR protocol was as follows: a 10 min incubation period at 95°C, followed by 40 PCR cycles of denaturation for 15 sec at 95°C and annealing/extension for 1 min at 60°C. The melting curve, performed to determine the specificity of the primers and PCR product purity, was employed using the following settings: 5 sec at 95°C, followed by 10 sec at 65°C and a continuous heating to 97°C. The online NCBI primer blast tool was used to produce the primer sequences presented in table 2.2 and primers were purchased from ThermoFischer (MA, USA).

Primers were initially centrifuged and suspended in 10-fold the number of their molecular weight, i.e. (X nmoles \* 10)  $\mu$ L of nuclease free water to yield a stock concentration of 100  $\mu$ M. Working solutions were then subsequently prepared by adding 5  $\mu$ L of the 100  $\mu$ M primer stock to 45  $\mu$ L nuclease free water. Following dilution, 0.375  $\mu$ L of the working solution was used in the real-time PCR reaction, as stated above.

**Table 2.2: List of primer sequences and their National Center for Biotechnology Information (NCBI) accession numbers**

Gene name	Primer sequences (5'-3')	Accession number	Tm (°C)
Bax	F: AAGCTGAGCGAGTGTCTCAAG	NM_138764.5	60.34
	R: CAAAGTAGAAAAGGGCGACAAC		58.11
Bcl-2	F: CTTTGAGTTCGGTGGGGTCA	NM_000633.3	59.89
	R: GGGCCGTACAGTTCCACAAA		60.54
p53	F: CCCTTCCCAGAAAACCTACC	NM_001126118.2	57.49
	R: CTCCGTCATGTGCTGTGACT		60.04
AMPK	F: AAGAAAGTCGGCGTCTGTTC	NM_206907.4	58.50
	R: TTCTGGTGCAGCATAGTTGG		58.17
β-actin	F: AGCACAGAGCCTCGCCTTT	NM_001101.5	61.89
	R: CACGATGGAGGGGAAGAC		56.74

#### 2.4.4 Real-time PCR data analysis

The relative quantification approach, commonly known as the  $\Delta\Delta C_t$  technique, was used to evaluate the real-time PCR amplification data. This method depicts the fold change in expression of a gene of interest relative to a reference group, such as untreated samples. Primer dimers, self-priming capabilities, and/or non-specific amplification were investigated in the primers employed in this work. For each reaction, a fluorescent signal buildup was recorded, and a threshold cycle was calculated, which is defined as the number of cycles required for the fluorescent signal to reach background level. Moreover, the  $C_t$  values are inversely linked to the amount of target nucleic acid in the sample (i.e., the lower the  $C_t$  level, the greater the amount of target nucleic acid in the sample). Samples were measured in triplicates and an average  $C_t$  value was calculated for each of the tested compounds.  $\Delta C_t$  values were calculated for each sample by using the following equation:  $C_t$  (gene of interest) –  $C_t$  (housekeeping gene).  $\Delta\Delta C_t$  values were then determined by subtracting the  $\Delta C_t$  of the control (untreated cells) from the  $\Delta C_t$  of the treatment groups. Fold change were calculated as follows:  $2^{-\Delta\Delta C_t} \pm$  standard error of mean (SEM).

## **2.5 Cell apoptosis assay**

Using Annexin V and PI labelling, the percentage of apoptotic cells was determined by measuring phosphatidyl serine externalization on the cell membrane. Annexin V, conjugated to a fluorochrome fluorescein isothiocyanate (FITC), can detect cells that externalize phosphatidylserine (PS) on their outer cell membrane. Furthermore, plasma membrane integrity is compromised in late apoptosis, enabling PI to enter, which is ordinarily excluded by living cells. (Lakshmanan & Batra, 2013). Cells were grown in T25 flasks and subsequently treated with MET, TMP or MTX and the combinations at concentrations of 20 mM, 516.67  $\mu$ M and 10 mM, respectively for 48 h. Then, cells were harvested, washed with cold 1x PBS, centrifuged three times at 280 x g for 7 min and resuspended in 1x Annexin binding buffer (ABB). Aliquots of 100  $\mu$ L were stained with 5  $\mu$ L Annexin V-FITC and 1  $\mu$ L PI stock (100  $\mu$ g/mL) and incubated for 15 min at room temperature in the dark. 1x ABB (400  $\mu$ L) was then added to each sample and analyzed by CytoFlex flow cytometer (Beckman Coulter, CA, USA). according to the manufacturers' instructions. A minimum of 30,000 events were recorded for each sample. The degree of apoptosis was detected in the BL-1 channel, while necrosis was detected in the BL-3 channel. Alive, early apoptotic, late apoptotic and necrotic cells were depicted as annexin V/PI negative, annexin V positive/PI negative, annexin V negative/ PI positive, respectively. Data analysis was performed in CytExpert software.

## **2.6 Scratch Wound assay**

Various conditions needed to be optimized to monitor HepG2 cell migration including seeding density, drug concentrations and incubation periods. Briefly,  $10^6$  HepG2 cells were seeded in 6-well plates and allowed to attach overnight. Once the cells reached confluency, a wound was made by scratching the surface with a 200  $\mu$ L pipette tip held vertically. Cells were then washed twice with PBS to eliminate floating cells. The cells were then treated with complete DMEM medium and either 3 mM MET, 344.45  $\mu$ M TMP or 0.2 mM MTX or the combinations (MET + TMP) and (MET + MTX). The wells which only contained HepG2 cells and DMEM medium were used as controls. The initial wound area was measured at time 0 using an inverted microscope (magnification power of 40x) (Labomed Inc., LA, CA, USA) connected to a digital camera. The wound distance was assessed by ImageJ software. Cells were then further imaged after 24, 48 and

72 h. Percentage of wound closure, which correlates to migration, was determined as the gap area value in respect to the initial scratch area.

$$\text{Percentage of wound closure} = \frac{(A - B)}{A} \times 100$$

The width of the original scratch wound is denoted by A, while the width of the scratch wound at 24, 48, or 72 hours corresponds to B.

## **Mitochondrial Assays**

In order to confirm the effects of MET, TMP, MTX and combinations on mitochondrial toxicity and ATP production, the below assays were done using the Seahorse XFe96 Analyzer (Agilent/Seahorse Bioscience). Lower concentrations of tested compounds, as stated below, were used to assess mitochondrial parameters as higher concentrations initiated cell death and hindered the analysis of mitochondrial function in real-time.

### **2.7 FCCP Optimization with Mito Stress Test**

To conduct the following Seahorse experiments, optimization of FCCP concentration was first done by titration to detect the concentration of FCCP that is required to cause maximal respiration. After warming XFe Assay medium to 37°C and confirming cell morphology as well as uniform seeding of cells by using an inverted microscope, the media above the cells was decanted and cells were washed with XFe Seahorse media. Each well was then filled with assay medium to a final volume of 180 µL/well. Plates were incubated for 45 min in a non-CO<sub>2</sub> incubator. Stock solution of oligomycin (100 µM), a mitochondrial ATP synthase inhibitor, was made by resuspending lyophilized powder in 630 µL of Seahorse media. Stock solution of FCCP (100 µM), a potent mitochondrial uncoupler, was made by resuspending FCCP in 720 µL of Seahorse media. Similarly, Rot/AA (50 µM), which inhibit complex I and III, respectively, were prepared by solubilizing contents in 540 µL of Seahorse media. To prepare 3 mL (1.5 µM/final well conc) of



oligomycin, 450  $\mu\text{L}$  of the stock was taken into a separate tube which contained 2550  $\mu\text{L}$  of media. The same was done to prepare 3 mL (2  $\mu\text{M}$ / final well conc) FCCP and 3 mL (0.5  $\mu\text{M}$ / final well conc) Rot/AA. Different concentrations of FCCP (2, 1, 0.5, 0.25, 0.125  $\mu\text{M}$ ) were prepared by serial dilution in separate tubes. For each of the 10x stock solutions, 20  $\mu\text{L}$  Oligomycin, 22  $\mu\text{L}$  FCCP and 25  $\mu\text{L}$  Rot/AA were loaded into the cartridge injection ports A, B, and C, respectively. The XFe96 well plate was divided into columns of 6 groups in which each 2 columns, belonging to the same group, were injected with the same FCCP concentration. The columns on the left were injected with the lowest FCCP concentration (0.125  $\mu\text{M}$  final concentration in the well), and the concentrations increased accordingly, with the highest concentration of FCCP (2  $\mu\text{M}$  final concentration in the well) injected to the columns on the far right. The remaining concentrations fell in between. An assay template was created on the XF controller, labeling each of the wells. The cartridge was then loaded and left to equilibrate. Once ready, the utility plate was replaced with the cell plate and measurements began. Three baseline rate measures were taken before the first injection and then three rate measurements were recorded following each injection.

## **2.8 Glycolytic Rate assay**

HepG2 cells were grown in complete DMEM medium. Cells were incubated in humidified atmosphere containing 5%  $\text{CO}_2$ . Three days before the experiment, cells were seeded in XF96-well plates (15,000 cells/80  $\mu\text{L}$  medium/well) and left in the incubator to adhere overnight. The next day, the cells were treated with different concentrations MET (3 mM), TMP (86.11  $\mu\text{M}$ ), MTX (1.5) and combinations. Twenty-four hours before the start of the experiment, cartridges were soaked in calibrant solution and left in a non- $\text{CO}_2$  incubator overnight. In addition, the Seahorse XFe96 Analyzer was switched on and left to warm up and equilibrate. On the day of the assay, aliquots of 50 mL of Seahorse media (Seahorse Bioscience) (per plate) were placed in a 37°C water bath until warm. The culture medium on the plates was removed and washed with 150  $\mu\text{L}$  of XF Seahorse media (supplemented with 2 mM glutamine, 1 mM pyruvate and 10 mM glucose). Then, 180  $\mu\text{L}$  of Seahorse media was added to each of the wells and the plates were incubated for 45 min in a non- $\text{CO}_2$  incubator to remove  $\text{CO}_2$  from the media, which may affect pH sensitive measurements. Mitochondrial compounds were diluted with XF media to a final concentration of 5  $\mu\text{M}$  Rot/AA and 500 mM 2-DG and added in the corresponding cartridge ports

(20 and 22  $\mu\text{L}$ , respectively). The cartridge was transferred to the Seahorse XF Analyzer for calibration prior to the start of the assay. The protocol used was as follows:

Three measurement cycles (3 mins Mix, 0 min Wait, 3 mins Measure) – injection through port A (Rot/AA) – three measurement cycles (3 mins Mix, 3 mins Wait, 3 mins Measure) – injection through port B (2-DG) – (3 mins Mix, 0 min Wait, 3 mins Measure).

## **2.9 Real time ATP Rate assay**

HepG2 cells were grown in complete DMEM medium. Cells were incubated in a humidified environment with 5%  $\text{CO}_2$ . Three days before the experiment, cells were seeded in XF96-well plates (15,000 cells/80  $\mu\text{L}$  medium/well) and left in the incubator to adhere overnight. The next day, the cells were treated with different concentrations MET (3 or 6.5 mM), TMP (86.11 or 55  $\mu\text{M}$ ), MTX (1.5 or 3 mM) and combinations. Twenty-four hours before the start of the experiment, cartridges were soaked in calibrant solution and left in a non- $\text{CO}_2$  incubator overnight. In addition, the Seahorse XFe96 Analyzer was switched on and left to warm up and equilibrate. On the day of the assay, aliquots of 50 mL of Seahorse media (Seahorse Bioscience) (per plate) were placed in a 37°C water bath until warm. The culture medium on the plates was removed and washed with 150  $\mu\text{L}$  of Seahorse media. Then, 180  $\mu\text{L}$  of Seahorse media was added to each of the wells and the plates were incubated for 45 min in a non- $\text{CO}_2$  incubator to remove  $\text{CO}_2$  from the media which may alter the pH and interfere with pH sensitive measurements. Mitochondrial compounds were diluted with XF media to a final concentration of 15  $\mu\text{M}$  Oligomycin and 5  $\mu\text{M}$  Rot/AA and added in the corresponding cartridge ports (20 and 22  $\mu\text{L}$ , respectively).

## **2.10 Mitochondrial Mito Stress Test**

Similarly, the Mito Stress Test (MST) was performed using the Seahorse XFe96 Analyzer. Mitochondrial compounds were diluted with XF to a final concentration of 15  $\mu\text{M}$  Oligomycin, 10  $\mu\text{M}$  FCCP and 5  $\mu\text{M}$  Rot/AA and added in the corresponding cartridge ports (20, 22 and 25  $\mu\text{L}$ , respectively). The cell plate was then placed into the analyzer after the XF Assay Cartridge was calibrated and three basal measurements were taken using a 3 min mix, 3 min measure procedure. Oligomycin (1.5  $\mu\text{M}$  final conc/well), FCCP (1  $\mu\text{M}$  final conc/well) and Rot/AA (0.5  $\mu\text{M}$  final

conc/well) were sequentially injected from ports A, B and C onto the wells containing HepG2 cells, with and without treatment (blank). OCR and extracellular acidification rate (ECAR) were measured in XF media, which did not contain buffer as it is essential to accurately measure the drop in pH which correlates to ECAR.

Mitochondrial respiration, which was measured in a single experiment, was determined in terms of basal respiration (BR), ATP production-linked after oligomycin injection, maximal (MR) after FCCP injection, proton leak-linked (PL) OCR, spare respiratory capacity (SRC) and non-mitochondrial respiration (NMR) following Rot/AA injection. Oligomycin, an inhibitor of ATP synthase, reduces OCR, the extent of which depends on the oxygen consumed in ATP production. Rot/AA completely inhibit OCR as they block complex I and III of the ETC. FCCP maximizes mitochondrial respiration by altering the proton gradient present due to the pump of protons from the mitochondrial matrix into the intermembrane space via the complex I, III and IV. Spare respiratory capacity is the difference in OCR between BR and MR. Any remaining OCR is due to non-mitochondrial respiration within the cell.

## **2.11 Statistical Analysis**

Each experiment was repeated at least 3 times with 3 to 6 replicates per treatment (representative data are shown in the results section). Data are depicted as means  $\pm$  SEM for each experiment. For MTT, RT qPCR, apoptosis assay, wound healing assay, and Seahorse analysis, one-way ANOVA was used followed by the Student–Newman–Keuls (SNK) post-hoc test to determine the statistical significance between various groups. Statistical significance was defined as a p-value of less than 0.05. SigmaPlot was used to compare the results obtained from the tested compound groups and their relative controls (Version 12.0; Systat Software, Chicago, IL, USA). Graphs were drawn using SigmaPlot software. XF Glycolytic Rate Assay, XF ATP Rate Assay and XF MST parameters were automatically generated using Wave software (Agilent Technologies) to determine OCR and ECAR values, depicting respiration and acidification rates. Graphs pertaining to the Seahorse data were exported to GraphPad Prism 6 software.

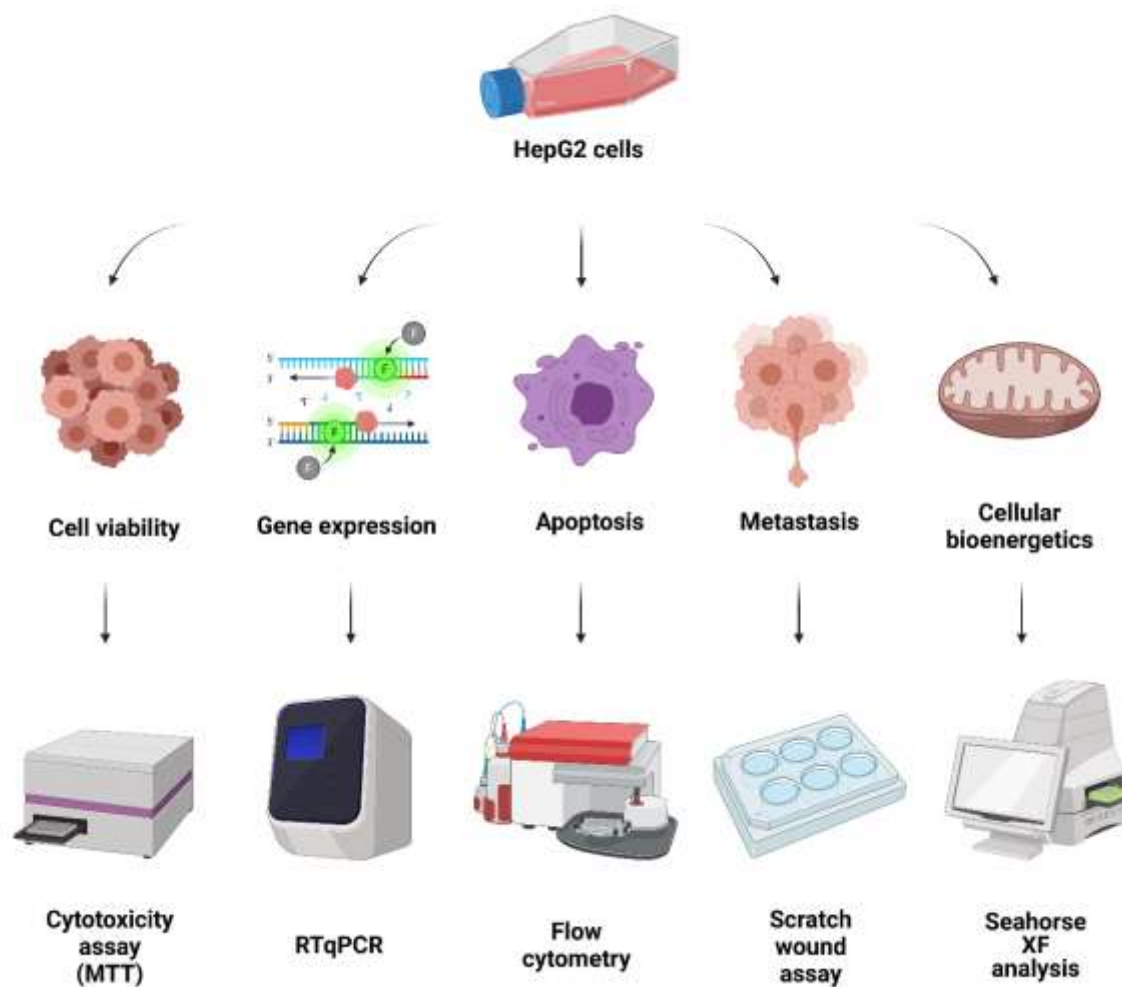


Figure 2.1. Schematic diagram elucidating the methods used in the present study.

(Created with [Biorender.com](https://www.biorender.com))

## CHAPTER 3: RESULTS

### 3.1 Effect of MET, TMP and MTX on hepatocellular carcinoma cell viability.

To evaluate the effect of MET, TMP and MTX on HepG2 cell viability, cells were treated with increasing concentrations of MET (12.5-100 mM), TMP (32.29-516.67  $\mu$ M) and MTX (3.125-50 mM). In a dose-dependent manner, both MET and MTX dramatically decreased HepG2 cell viability (Figures 3.1 A,C). MET individually inhibited cell viability with an  $IC_{50}$  value of 44.08 mM, while MTX inhibited cell viability with an  $IC_{50}$  value of 14.3 mM. As the maximum solubility of TMP in DMSO is 172.22 mM (corresponding to 100% DMSO), which is cytotoxic to the cells, the highest concentration tested of TMP was 516.67  $\mu$ M, corresponding to a final concentration of 0.3% DMSO. Wells serving as control were incubated with 0.3% DMSO, the vehicle only, to ensure that the cytotoxicity was not due to the presence of DMSO. TMP reduced HepG2 cell viability at 32.29  $\mu$ M, then plateaued at the subsequent concentrations. Notably, due to the limited solubility of TMP in DMSO at non-toxic concentrations, the  $IC_{50}$  concentration of TMP was not calculated and is well above the concentrations used in the present study. Hence, all subsequent experiments were conducted using 516.67  $\mu$ M TMP. MTX was used at sub  $IC_{50}$  concentrations, calculated according to the cell viability assay results. Furthermore, MET was used at 20 mM in monitoring cellular apoptosis, as shown in previous studies (Yi Zhao et al., 2018).

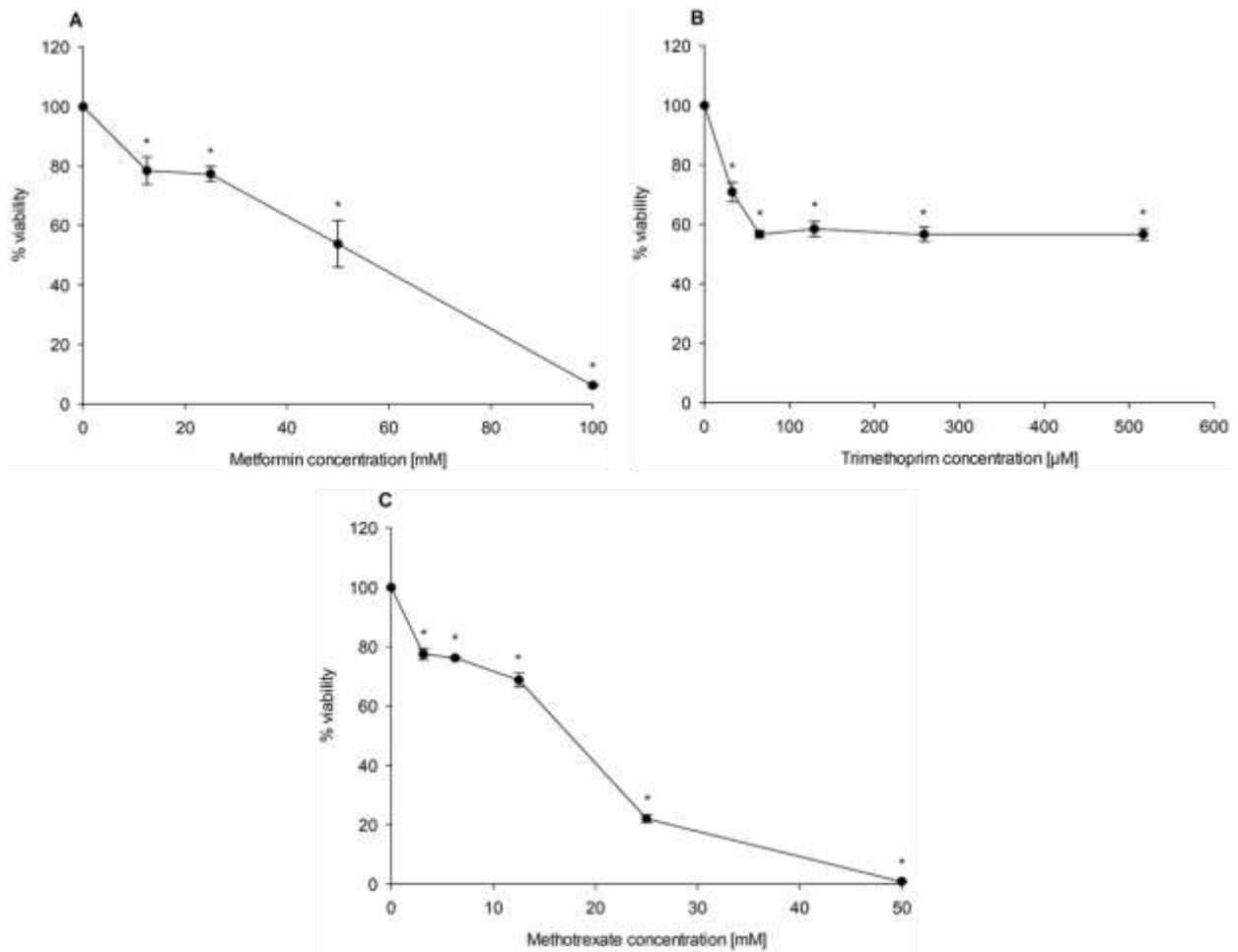


Figure 3.1. Effect of MET (A), TMP (B) and MTX (C) on hepatocellular carcinoma cell viability.

HepG2 cells were exposed to increasing concentrations of MET (12.5-100 mM), MTX (3.125-50 mM) and TMP (32.29-516.67 µM) for 24 h. The MTT assay was done to assess the inhibitory effects of the tested compounds at the used concentrations. Results are expressed as a percentage of the untreated control. The error bars represent the standard error of mean (SEM) (n=6). Comparisons were made using ANOVA followed by Student–Newman–Keuls (SNK) post-hoc test. \*; indicates a statistically significant difference between the control and drug-treated groups at  $p$ -value  $< 0.05$  versus the control group.

### **3.2 Effect of MET when combined with TMP or MTX on hepatocellular carcinoma cell viability.**

To evaluate the cytotoxicity of MET in combination with both antifolate agents, TMP and MTX, cells were co-exposed with increasing concentration of MET (12.5-100 mM) and either 516.67  $\mu$ M TMP or 1.5 mM MTX for 24 h. The MTT test was then used to compare the toxicity of the various combinations to that of MET alone. The  $IC_{50}$  value of MET was decreased from 44.06 mM to 22.73 mM upon the addition of TMP. As presented in figure 3.2, all combinations of MET with TMP had more cytotoxic effects compared to MET individually. Furthermore,  $IC_{50}$  value of MET was decreased from 44.06 mM to 29.29 mM upon the addition of MTX. As shown in the figure below, the combination of MET + TMP and MET + MTX caused a shift in the survival curves to the left. For this reason, the following experiments were conducted using MET (20 mM) in combination with TMP (516.67  $\mu$ M) or MTX (10 mM) to compare the effects of this combination versus metformin used singly in the treatment of HepG2 cells.

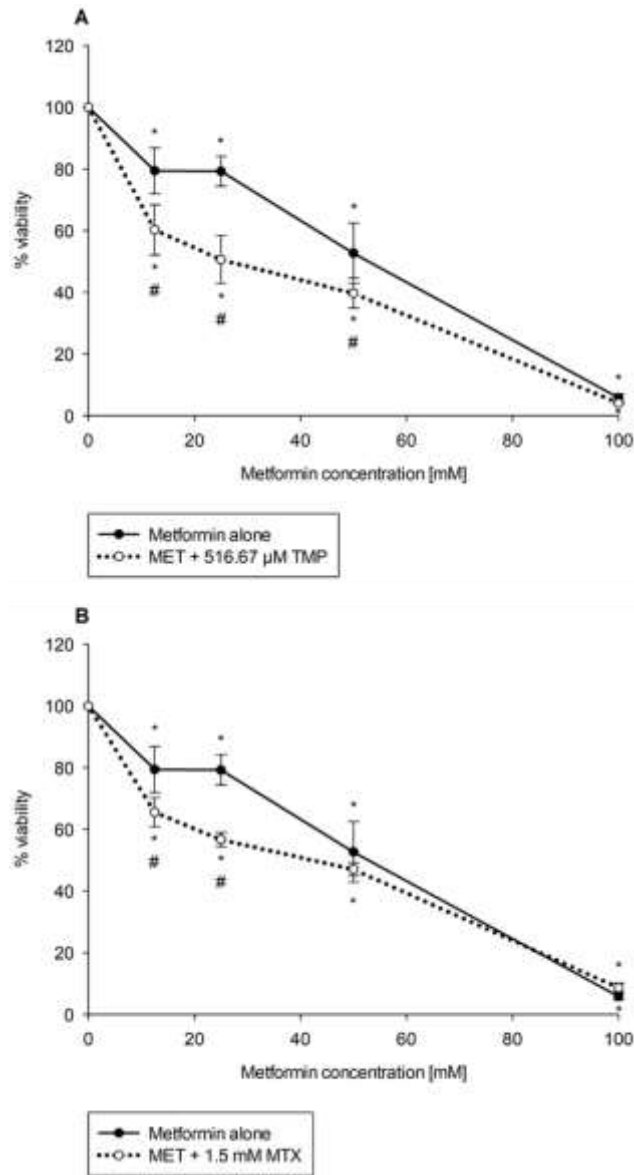


Figure 3.2. Effect of MET when combined with TMP (A) or MTX (B) on hepatocellular carcinoma cell viability.

Cytotoxicity of various concentrations of MET individually or in combination with TMP or MTX in HepG2 cells were shown above. TMP and MTX increase the cytotoxic effect of MET on HepG2 cells *in vitro*. The MTT assay was conducted to assess the combinatory effects of MET (12.5-100 mM) and TMP (516.67 μM) or MTX (1.5 mM) after 24 h. The IC<sub>50</sub> of MET was calculated as 44.06 mM, while upon the addition of TMP, the IC<sub>50</sub> was markedly reduced to 22.73 mM and upon



the addition of MTX, the IC<sub>50</sub> was markedly reduced to 29.29 mM; the error bars represent the SEM (n=6). Comparisons were made using ANOVA followed by Student–Newman–Keuls (SNK) post-hoc test. \*; indicates a statistically significant difference between the control and drug-treated groups at *p*-value < 0.05 versus the control group; #; indicates a statistically significant difference between the MET treated group and other drug-treated groups at *p*-value < 0.05.

**Table 3.1: Calculated IC<sub>50</sub> values of tested compounds on HepG2 cell line**

Tested compound(s)	IC <sub>50</sub>
MET	44.06 mM
TMP	>516.67 μM
MTX	14.3 mM
MET (+TMP)	22.73 mM
MET (+MTX)	29.29 mM

### **3.3 Effect of MET, TMP, MTX and combinations on Bax, Bcl-2 and p53 mRNA expression in HepG2 cells.**

To examine whether the inhibitory effect of drug combinations was due to the activation of key apoptotic markers, HepG2 cells were treated for 48 h with 20 mM MET, 516.67  $\mu$ M TMP, 10 mM MTX and their respective combinations. The levels of expression of apoptosis associated genes, Bax, Bcl-2, p53 were evaluated using the real time quantitative polymerase chain reaction technique. The levels of pro- and anti-apoptotic markers of the Bcl-2 family are principally responsible for mediating this pathway (Czabotar, Lessene, Strasser, & Adams, 2014). The expression of Bax and p53 were significantly ( $P < 0.05$ ) increased in both combinations (using sub  $IC_{50}$  concentrations of each drug), when compared with both the control and cells incubated with MET alone, as shown below (Figure 3.3). Contrastingly, the anti-apoptotic gene Bcl-2 decreased significantly, when compared to the control. Our data revealed that Bax was upregulated by 1.77, 3.79, 3.03, 3.78 and 6.20 folds after treatment with MET, TMP, MTX MET + TMP and MET + MTX, respectively compared to the control. The gene expression of p53 exhibited comparable results and was also upregulated by 1.17, 1.06, 1.27, 1.83 and 2.39 folds following treatment with MET, TMP, MTX MET + TMP and MET + MTX, respectively compared to the control. Furthermore, the gene expression of Bcl-2 was shown to decrease by 0.29, 0.82, 0.4, 0.08 and 0.15 folds when treated with MET, TMP, MTX MET + TMP and MET + MTX, respectively compared to the control. The fold changes of each of the tested compounds, alone or in combination, demonstrated an elevation of major apoptotic markers and a downregulation of an anti-apoptotic gene in a thorough comparison. For both apoptotic markers, combining MET with either TMP or MTX resulted in larger fold change values than MET alone. These data suggest that the tested compounds in combination significantly trigger apoptosis through the mitochondrial apoptotic pathway.

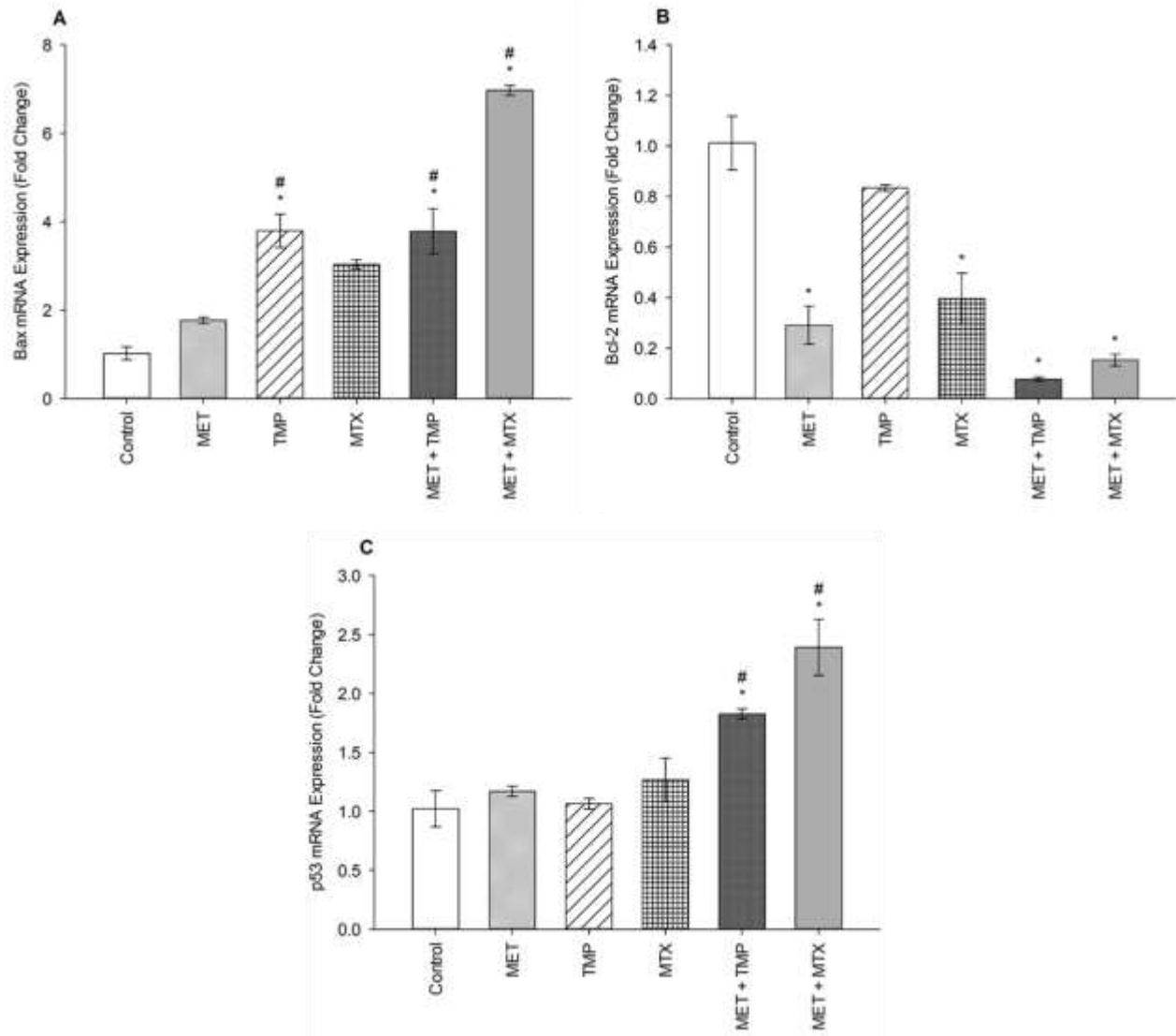


Figure 3.3. Effect of MET, TMP, MTX and combinations on Bax (A), Bcl-2 (B) and p53 (C) mRNA expression in HepG2 cells.

HepG2 cells were treated for 48 h with MET (20 mM), TMP (516.67  $\mu$ M), MTX (10 mM), MET + TMP (20 mM + 516.67  $\mu$ M) or MET + MTX (20 mM + 10 mM). Bax, Bcl-2 and p53 mRNA levels were quantified using qRT-PCR and normalized to  $\beta$ -actin. Data are expressed as mean  $\pm$  SEM (n=3). Comparisons were made with ANOVA followed by Student–Newman–Keuls (SNK) post-hoc test; \*, indicates a statistically significant difference between the control and drug-treated groups at  $p$ -value < 0.05 versus the control group; #, indicates a statistically significant difference between the MET treated group and other drug-treated groups at  $p$ -value < 0.05.

### **3.4 Effect of MET, TMP, MTX and combinations on the percentage of apoptosis in HepG2 cells.**

To examine the role of apoptosis in the cytotoxic effect of MET, TMP, MTX or combinations, the percentage of apoptotic cells was detected via Annexin/PI staining that was measured by the flow cytometry analysis, as previously described. For this aim, cells were exposed to MET (20 mM), TMP (516.67  $\mu$ M), MTX (10 mM), MET + TMP (20 mM + 516.67  $\mu$ M) or MET + MTX (20 mM + 10 mM). When compared to the control and solo MET treatment, our findings demonstrated that cells co-treated with both combinations increased cell death in HepG2 cells. MET significantly increased apoptosis at 20 mM and the percentage of viable cells, early apoptotic, late apoptotic and necrotic cells was  $85.38 \pm 3.88$ ,  $8.82 \pm 2.78$ ,  $4.22 \pm 1.08$ ,  $1.58 \pm 0.08$ , respectively. TMP at 516.67  $\mu$ M induced apoptosis and the percentage of viable cells, early apoptotic, late apoptotic and necrotic cells was  $88.42 \pm 1.37$ ,  $2.35 \pm 0.45$ ,  $3.60 \pm 0.81$ ,  $5.63 \pm 0.16$ , respectively. It is also of interest that cells treated with MTX (10 mM) did not significantly increase apoptosis. Contrastingly, the percentage of early and late apoptotic cells in the combined treatment of MET and TMP was  $4.73 \pm 2.15$  % and  $18.57 \pm 4.44$ , respectively. Moreover, the combination of MET with MTX depicted a rise in the percentage of early apoptotic cells,  $18.69 \pm 1.62$ , while the percentage of late apoptotic cells was nearly the same,  $3.93 \pm 0.41$ . The total percentage of apoptotic cells significantly increased when both drug combinations were used simultaneously ( $P < 0.05$ ), as shown in figure 3.4, as compared with the control or single treatment. These findings suggest that MET combined with TMP or MTX effectively induced early and late apoptosis in hepatocellular carcinoma cells. The findings acquired from the increase in mRNA expression of important apoptotic markers corroborated changes in the proportion of total apoptotic cells assessed by flow cytometry. Hence, the combination of MET and either TMP or MTX considerably inhibited cell growth in HepG2 cells by inducing apoptosis.

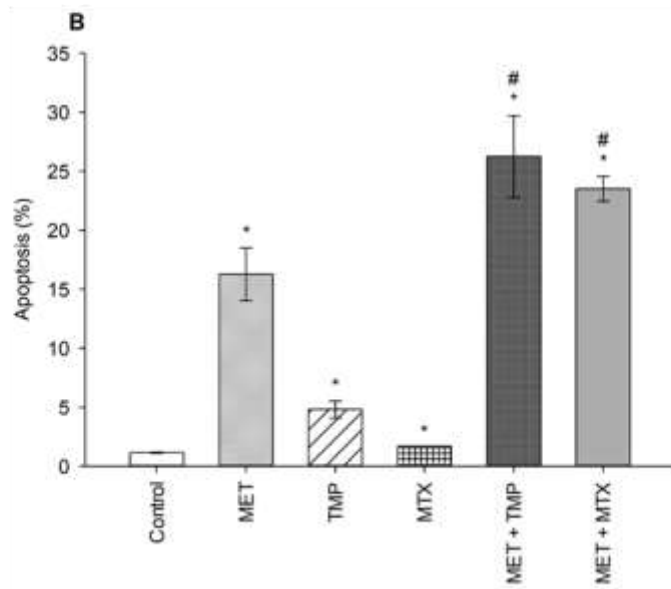
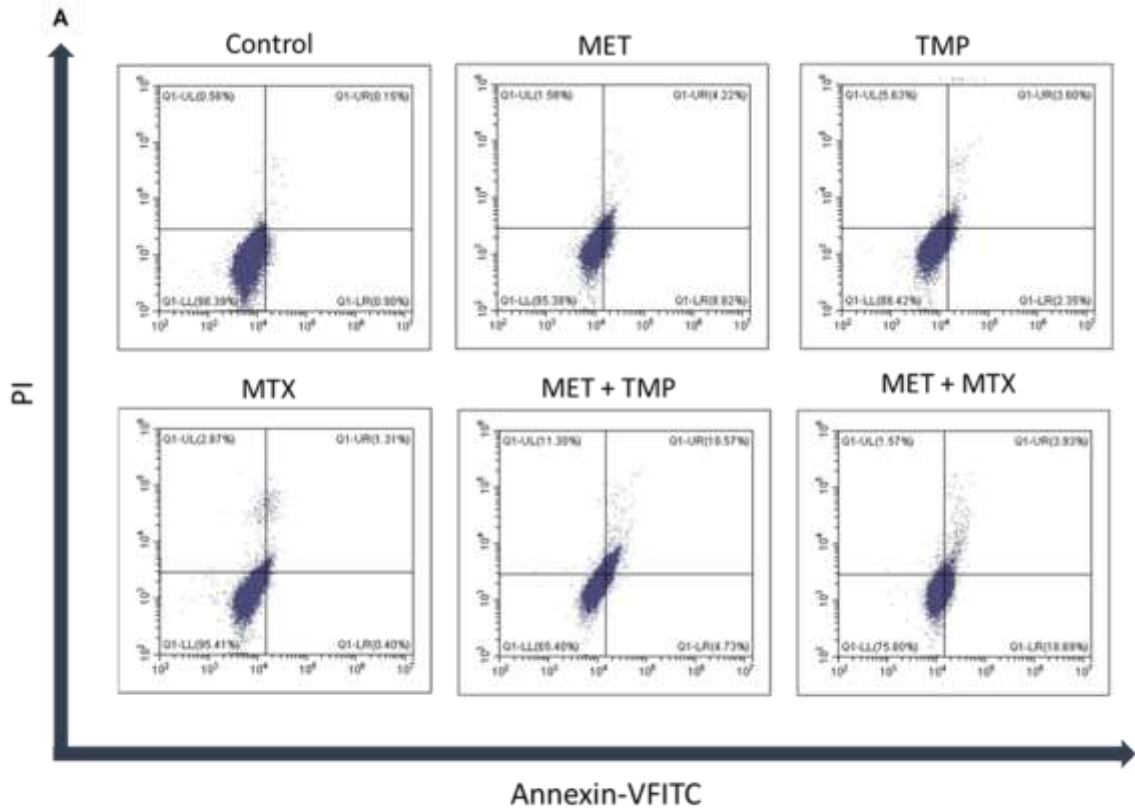


Figure 3.4. Effect of MET, TMP, MTX and combinations on the percentage of apoptosis in HepG2 cells.

(A) Flow cytometry dot plots (Annexin-VFITC against PI) for apoptosis assay. Squares depict

populations of cells; population of viable cells (LL), early apoptotic cells (LR), late apoptotic cells (UR) and necrotic cells (UL). Representative data of three independent experiments ( $n = 3$ ) are shown. MET + TMP and MET + MTX combinations significantly induced a higher total percentage of apoptosis in HepG2 cells, compared to single drug treatments. (B) Total percentage of apoptosis (early + late apoptosis) in different treatment groups. Each bar represents the mean of three independent experiments. HepG2 cells were treated for 48 h with MET (20 mM), TMP (516.67  $\mu$ M), MTX (10 mM), MET + TMP (20 mM + 516.67  $\mu$ M) or MET + MTX (20 mM + 10 mM). Error bars represent the SEM. Some error bars are too small to be seen. Comparisons were made using ANOVA followed by Student–Newman–Keuls (SNK) post-hoc test. \*,  $p$ -value < 0.05 versus control and #,  $p$ -value < 0.05 versus cells treated with MET only.

### **3.5 Effect of MET, TMP, MTX, alone and in combination, on HepG2 cell migration.**

Carcinoma cell migration is due to the cancer cells' ability to undergo various biological processes, specifically related to coordination. As metastasis and angiogenesis are closely related (N. Nishida, H. Yano, T. Nishida, T. Kamura, & M. Kojiro, 2006), therefore, it was crucial to examine the impact of the drugs on hepatocellular motility. The ability of MET, TMP, MTX and respective combinations to alter cell migration was analyzed via the scratch wound healing assay, which investigates the ability of cells to undergo migration and hence, increase tumorigenesis.

The effects of MET, TMP, MTX and combinations on cell migration were observed in hepatocellular carcinoma cell line. After the scratch was made, HepG2 cells were treated with 3 mM MET, 344.45  $\mu$ M TMP or 0.2 mM MTX or the combinations (MET +TMP) and (MET+MTX) and incubated for up to 72 h. Images were taken every 24 h for three consecutive days. Co -presence of MET and TMP resulted in a significantly lower percentage of wound closure when compared to the presence of metformin (3 mM) from  $29.75 \pm 3.94\%$  to  $1.97 \pm 0.53\%$  at 24 h, from  $52.29 \pm 2.2\%$  to  $6.79 \pm 4.56\%$  at 48 h and from  $54.93 \pm 2.83\%$  to  $10.8 \pm 4.70\%$  at 72 h, respectively (Figure 3.5). Contrastingly, MET when combined with MTX inhibited cell migration, to a much less extent when compared to MET alone; from  $29.75 \pm 3.94\%$  to  $11.94 \pm 2.61\%$  at 24 h, from  $52.29 \pm 2.2\%$  to  $38.5 \pm 4.38\%$  at 48 h and from  $54.93 \pm 2.83\%$  to  $41.35 \pm 3.92\%$  at 72 h, respectively. TMP and MTX alone significantly decreased HepG2 cellular migration, when compared to the control at the same time points. TMP alone resulted in a percentage of wound closure of  $25.45 \pm 2.42\%$  at 24 h,  $42.24 \pm 2.19\%$  at 48 h and  $43.86 \pm 3.07\%$  at 72 h. Moreover, MTX caused a percentage of wound closure of  $23.99 \pm 2.92\%$  at 24 h,  $43.43 \pm 2.11\%$  at 48 h and  $44.31 \pm 1.63\%$  at 72 h. Quantification of migration in terms of gap width was done by ImageJ software, as previously mentioned in chapter 2.

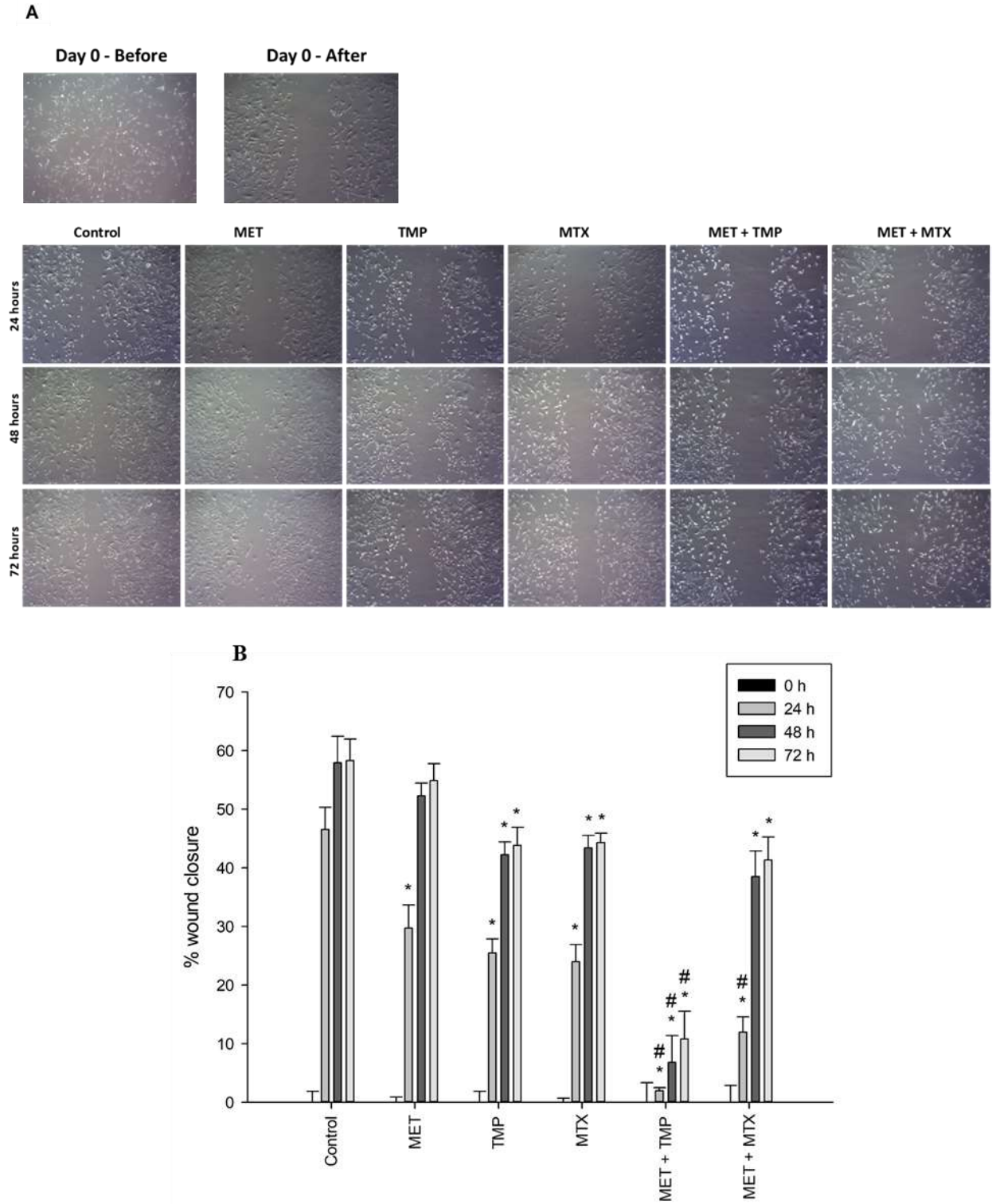


Figure 3.5. Effect of MET, TMP, MTX, alone and in combination, on HepG2 cell migration.



(A) Migration of HepG2 cells in response to the treated compounds was determined by the wound healing assay at 24, 48 and 72 h using an inverted microscope at 40x magnification. (B) Percentage of wound closure was calculated at 0, 24, 48 and 72 h by measuring the gap width with respect to the initial scratch area. Error bars represent the SEM. Comparisons were made using ANOVA followed by Student–Newman–Keuls (SNK) post-hoc test. \*,  $p$ -value < 0.05 versus control at equal time points and #,  $p$ -value < 0.05 versus cells treated with MET only at equal time points.

## **Seahorse XF Extracellular Flux Analysis**

To closely examine the two main energy pathways cells utilize to generate ATP, the rate of glycolysis as well as the mitochondrial function of HepG2 cells were assessed using the Seahorse XF extracellular Flux Analyzer. HepG2 cells were incubated with MET, TMP, MTX, MET + TMP, MET + MTX for 24 h in Seahorse XF tissue culture microplates. Following incubation, cells were examined using the Glycolytic Rate Assay, ATP Rate Assay and Mitochondrial Stress Test (MST). It was possible to measure the ECAR (indicating glycolysis) and OCR (indicating OXPHOS) of live cells in real time, simultaneously, via the fiber-optic probes present on the sensors of the cartridges used in the Seahorse XFe96 Analyzer; one which is oxygen sensitive and the other which is proton sensitive, detecting changes in pH. By doing so, we were able to monitor the metabolism of HCC cells with and without treatment of potential chemotherapeutic agents. Moreover, our data suggest that the combination of MET with the tested antifolate compounds causes more extreme damages to the energy production of HepG2 cancer cells (by decreasing the increase in rate of glycolysis induced by MET), leading to an increase in cell death.

### **3.6 Effect of MET, TMP and MTX, alone and in combination, on rates of basal and compensatory glycolysis in HepG2 cells.**

To examine if the tested compounds influence the Warburg effect, MET, TMP, MTX, MET + TMP and MET + MTX treated groups were examined in terms of rate of glycolysis. MET treated cells exhibited an increase in the rates of basal glycolysis of HepG2 cells. Of significance, the co-treatment of MET with either TMP or MTX caused a significant reduction in the rate of basal glycolysis, when compared to cells treated with MET only. Changes in ECAR were monitored using the Glycolytic Rate Assay (Seahorse Bioscience).

MET alone, or in combination, activated glycolysis up to the maximum level, as shown by the insensitivity to oligomycin. MET caused an increase in basal glycolysis depicted by a 68% increase, when compared to the control (Figure 3.6). Contrastingly, TMP and MTX alone decreased basal glycolysis rates by 11% and 27%, respectively, also when compared to the control. Of significance, co-treatment of MET and TMP or MET and MTX, decreased basal glycolysis rates by 17% and 25%, when compared to MET alone. Furthermore, MET caused a slight decrease in the rates of compensatory glycolysis by 4%, when compared to the control, while TMP and MTX decreased compensatory glycolysis by 14% and 26%, respectively. Rates of compensatory glycolysis were significantly decreased upon co-therapy of MET and TMP or MET and MTX by 13% and 21%, respectively, when compared to MET alone. These data bring to light the suggestion that both TMP and MTX significantly combat the MET-induced shift in glycolysis.

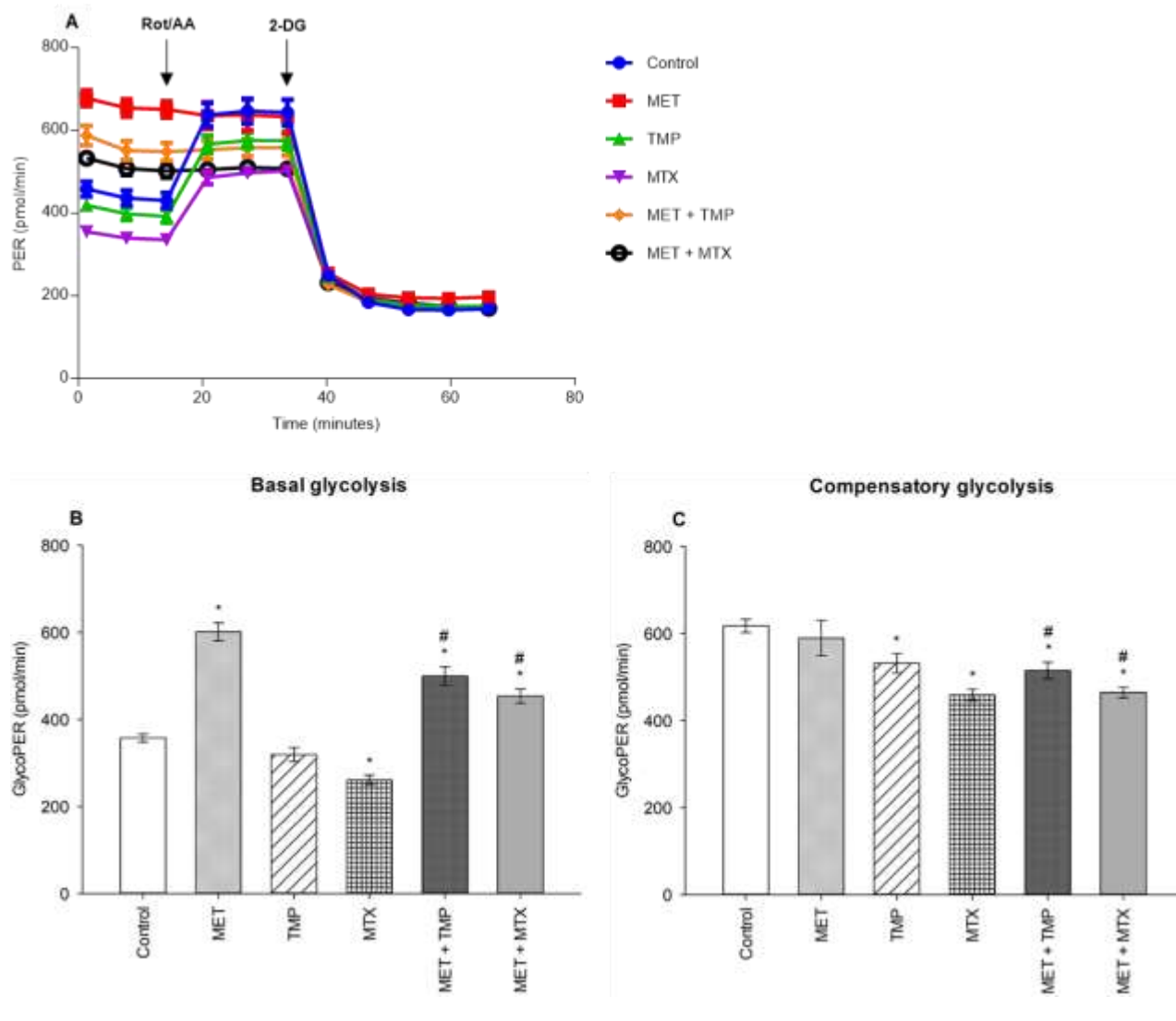


Figure 3.6. Effect of MET, TMP and MTX, alone and in combination, on rates of basal and compensatory glycolysis in HepG2 cells.

Cells were seeded in Seahorse tissue culture microplates, treated with MET (3 mM), TMP (86.11  $\mu$ M), MTX (1.5 mM), MET + TMP (3 mM + 86.11  $\mu$ M) or MET + MTX (3 mM + 1.5 mM) for 24 hours and examined by the Glycolytic Rate Assay in which Rot/AA and 2-DG were added as shown above. (A) Representative Glycolytic Rate Assay profile. (B) Calculated basal glycolytic proton efflux rate (glycoPER). (C) Calculated compensatory glycolytic proton efflux rate (glycoPER). Data are expressed as mean  $\pm$  SEM (n=6). Comparisons were made using ANOVA followed by Student–Newman–Keuls (SNK) post-hoc test. \*, *p*-value < 0.05 versus control and #, *p*-value < 0.05 versus cells treated with MET only.

### **3.7 Effect of MET, TMP and MTX and combinations on the total ATP production rate in HepG2 cells.**

To analyze living cells, sub-IC<sub>50</sub> values were used to measure the total ATP production rates in HepG2 cells. Two concentrations were used for the tested compounds, alone and in combination (Figure 3.7). At low and high concentrations, MET increased total ATP production rates by 30% and 26%, respectively, when compared to the control. Contrastingly, TMP and MTX (at low concentrations) induced a increase in total ATP production rate by 16% and 1%, respectively, when compared to the control. To the contrary, TMP induced a decrease in total ATP production by 23% at high concentrations, while MTX, similarly, induced a decrease by 9%, when compared to the control. MET + TMP and MET + MTX significantly decreased ATP production in a dose dependent manner, compared to MET alone at both low and high concentrations, respectively; MET + TMP (15% and 39%) and MET + MTX (30% and 58%).

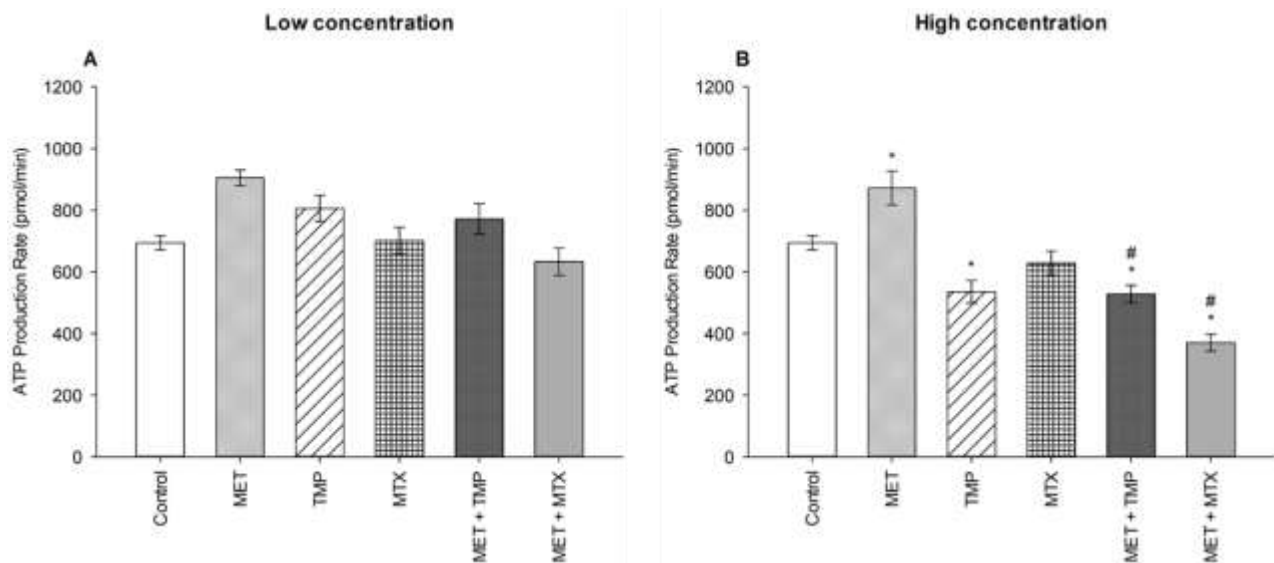


Figure 3.7. Effect of MET, TMP and MTX and combinations on the total ATP production rate in HepG2 cells.

(A) HepG2 cells were treated for 24 h with MET (3 mM), TMP (86.11  $\mu$ M), MTX (1.5 mM), MET + TMP (3 mM + 86.11  $\mu$ M) or MET + MTX (3 mM + 1.5 mM). (B) HepG2 cells were treated for 24 h with MET (6.5 mM), TMP (189.45  $\mu$ M), MTX (3 mM), MET + TMP (6.5 mM + 189.45  $\mu$ M) or MET + MTX (6.5 mM + 3 mM) and measured by Seahorse XF Real-Time ATP rate assay. Data are expressed as mean  $\pm$  SEM (n=6). Comparisons were made using ANOVA followed by Student–Newman–Keuls (SNK) post-hoc test. \*,  $p$ -value < 0.05 versus control and #,  $p$ -value < 0.05 versus cells treated with MET only.

### **3.8 Effect of MET, TMP and MTX, alone and in combination, on the glycolytic and mitochondrial ATP production rates in HepG2 cells.**

Consistent with the results presented in figure 3.6 pertaining to basal and compensatory glycolysis rates, treatment of MET caused an increase in rate of glycolysis, while the combinations led to a decrease in glycolysis rate (Figure 3.8). Both concentrations of MET increased the glycolytic ATP production rate by 57% and 105%, respectively, when compared to the control. Contrastingly, TMP increased glycolysis by 26% at low concentration and decreased the rate of glycolysis by 11% at higher concentrations. Similarly, MTX increased glycolysis by 15% when administered at a low concentration, while decreased the glycolytic rate by 8% at higher concentrations, when compared to the control. Combining MET and TMP or MET and MTX at low concentrations decreased the rate of glycolysis by 12% and 36%, respectively, when compared to MET alone. Interestingly, both combinations (MET + TMP and MET + MTX) effectively led to a more prominent decrease in the rate of glycolysis at higher concentrations; 36% and 55%, respectively when compared to MET alone. Hence, our results confirmed the findings obtained from the Glycolytic Rate Assay depicted above.

Of significance, the rate of mitochondrial ATP production was also impacted as a result of drug treatments. MET and MTX (at low concentrations) decreased mito-ATP production by 0.92% and 13%, respectively when compared to the control. Contrastingly, TMP slightly increased the mito-ATP production rate by 4%. Both combinations, on the other hand, declined these rates by 21% and 19%, when compared to MET alone. Furthermore, MET, TMP and MTX (at high concentrations) elucidated a higher decrease in mito-ATP production by 69%, 38% and 11%, respectively, when compared to the control. Of note, co-treatment of MET + TMP and MET + MTX further led to a decrease in mitochondrial ATP production by 65% and 75%, respectively, when compared to MET alone.

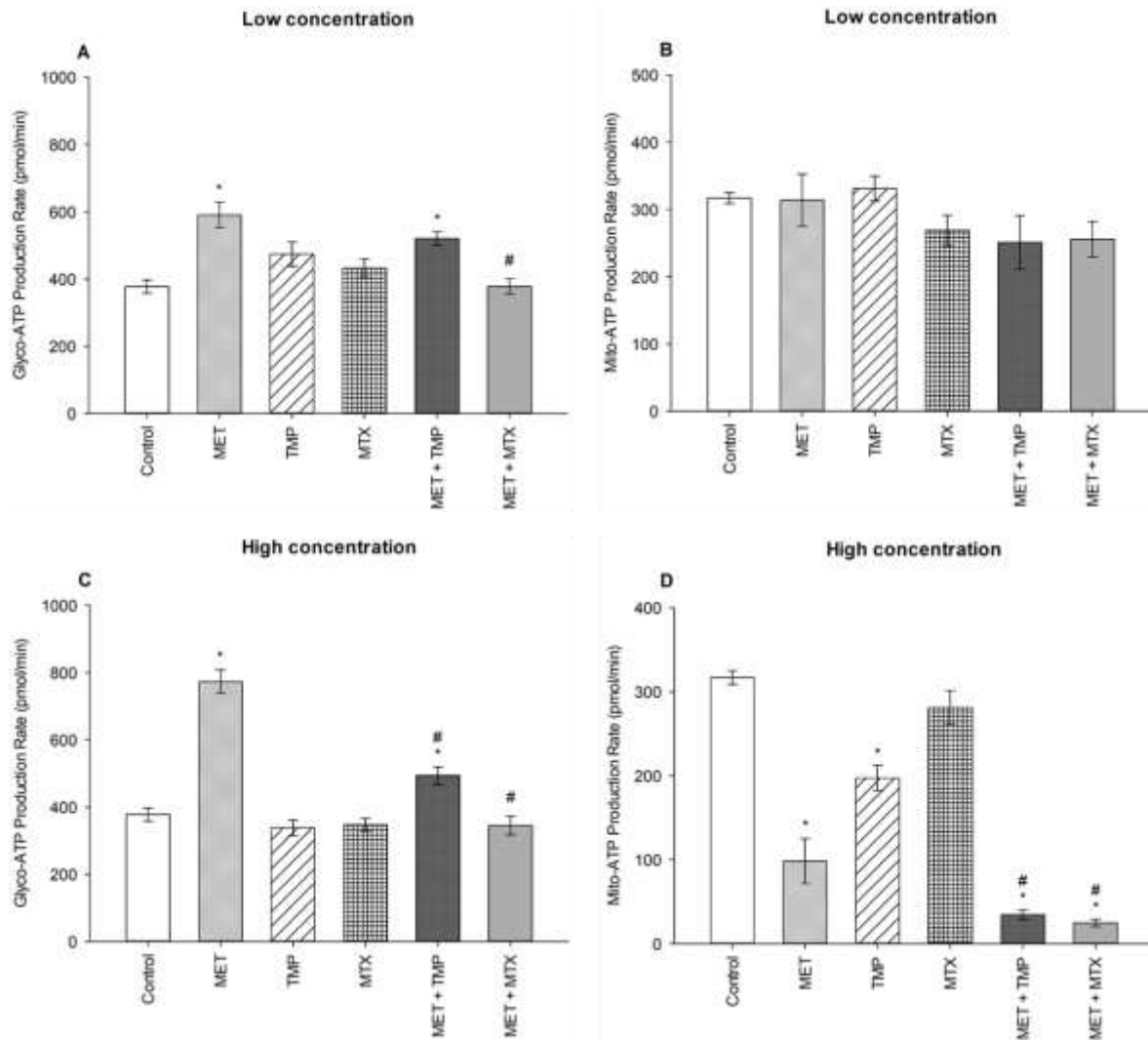


Figure 3.8. Effect of MET, TMP and MTX, alone and in combination, on the glycolytic and mitochondrial ATP production rates in HepG2 cells.

(A, B) Glycolytic and mitochondrial ATP production rates decreased upon co-treatment of MET with TMP or MTX. HepG2 cells were incubated for 24 h with MET (3 mM), TMP (86.11 µM), MTX (1.5 mM), MET + TMP (3 mM + 86.11 µM) or MET + MTX (3 mM + 1.5 mM). (C, D) Percentage of ATP production from glycolysis and mitochondria significantly decreased upon combination of MET with either TMP or MTX, when compared to MET only. HepG2 cells were treated for 24 h with MET (6.5 mM), TMP (189.45 µM), MTX (3 mM), MET + TMP (6.5 mM + 189.45 µM) or MET + MTX (6.5 mM + 3 mM) and measured by Seahorse XF Real-Time ATP rate assays. Data are expressed as mean ± SEM (n=6). Comparisons were made using ANOVA



followed by Student–Newman–Keuls (SNK) post-hoc test. \*,  $p$ -value < 0.05 versus control and #,  $p$ -value < 0.05 versus cells treated with MET only.

### **3.9 Effect of MET, TMP, MTX and combinations on AMPK mRNA expression in HepG2 cells.**

MET is well known to block complex I of the mitochondrial respiratory chain, lowering the ATP/AMP ratio, hence activating AMPK as a result (El-Mir et al., 2000; Owen, Doran, & Halestrap, 2000). Therefore, we decided to monitor the gene expression of AMPK following drug incubation.

In comparison to the control group, AMPK was elevated by 1.29, 1.10, 2.55, 2.11, and 2.03 folds after treatment with MET, TMP, MTX, MET + TMP, and MET + MTX, respectively (Figure 3.9). The increasing pattern in terms of fold change confirmed the results obtain via the ATP Rate assay, though none of the values above were considered significant.

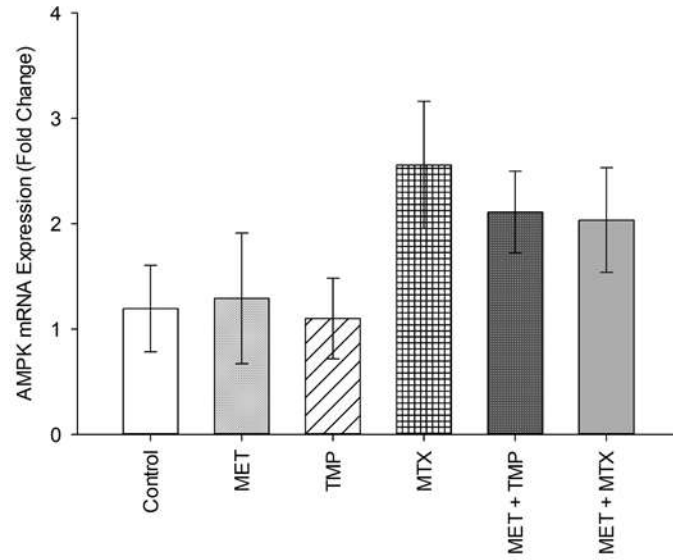


Figure 3.9. Effect of MET, TMP, MTX and combinations on AMPK mRNA expression in HepG2 cells.

HepG2 cells were treated with MET (6.5 mM), TMP (189.45  $\mu$ M), MTX (3 mM), MET + TMP (6.5 mM + 189.45  $\mu$ M) or MET + MTX (6.5 mM + 3 mM). AMPK mRNA levels were quantified using qRT-PCR and normalized to  $\beta$ -actin. Data are expressed as mean  $\pm$  SEM. (n=3).

### **3.10 Effect of MET, TMP, MTX, alone and in combination, on mitochondrial bioenergetics.**

Combining MET to either TMP or MTX leads to inhibition of mitochondrial bioenergetics.

As metformin has been previously known to inhibit OXPHOS, the tested compounds were examined alone and in combination (at high concentrations) to further investigate the effects of the combinations on mitochondrial function using the MST. HepG2 cells were incubated with MET, TMP, MTX or respective combinations at sub-IC<sub>50</sub> concentrations for 24 h. After incubation, cells were placed in a non-CO<sub>2</sub> incubator for 45 minutes before being assayed using the Seahorse XFe96 Analyzer. Real-time measurements of oxygen consumption rate were measured (Figure 3.10). MET caused a decrease in mitochondrial function as elucidated by a sharp reduction in mitochondria basal activity (calculated as the difference between basal OCR and non-mitochondrial OCR), maximal respiration (maximal oxygen consumption rate after the addition of the uncoupler FCCP), proton leak (remaining basal respiration not coupled to ATP production) and spare respiratory capacity (the difference between basal and maximal rates) by 86%, 69%, 42% and 53%, respectively, when compared to the control. Similarly, TMP alone reduced basal respiration, maximal respiration, proton leak and spare respiratory capacity by 64%, 78%, 24% and 91%, respectively, when compared to untreated cells. Furthermore, MTX decreased the above assessed parameters, in the same order, by 16%, 22%, 4% and 28%, respectively, when compared to the control. Interestingly, the mitochondrial inhibitory functions of MET were increased upon the addition of either TMP or MTX. Following 24 h incubation with MET + TMP, cells depicted a basal respiration and maximal respiration reduction by 6% and 86%, respectively, when compared to MET alone. MET + TMP also induced a decrease in proton leak, which reached 25%, while the spare respiratory capacity was completely abolished at 24 h. Moreover, MET when combined with MTX also exhibited a decrease in basal and maximal respiration by 18% and 36%, respectively, when compared to MET alone. In congruence with these findings, the proton leak and spare respiratory capacity were also reduced by 26% and 41% upon co-treatment of tested compounds, compared to MET alone. These data suggest that TMP and MTX may potentiate the detrimental action of MET on mitochondrial function in HepG2 cells.

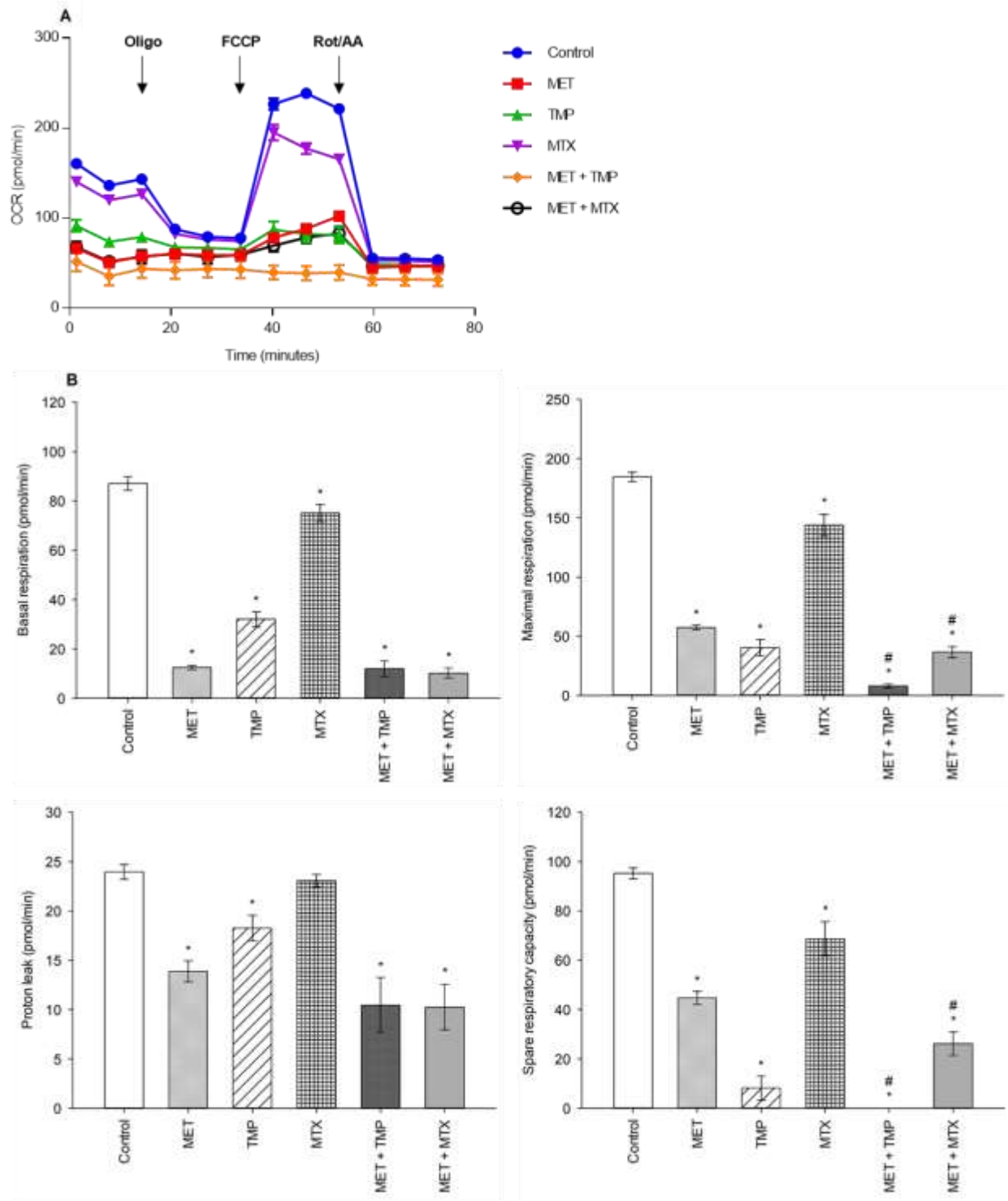


Figure 3.10. Effect of MET, TMP, MTX, alone and in combination, on mitochondrial bioenergetics.

Combining MET to either TMP or MTX leads to inhibition of mitochondrial bioenergetics. (A) The effect of treatment of MET, TMP, MTX and combinations on the rate of mitochondrial respiration (OCR) in HepG2 cells after 24 h. TMP and MTX combined with MET synergistically induced mitochondrial dysfunction in HepG2 cells. A decrease in OCR of cells is seen following combination therapy, when compared to the control. (B) Basal respiratory rate, maximal respiration, proton leak and spare respiratory capacity of HepG2 cells following treatment of MET (6.5 mM), TMP (189.45  $\mu$ M), MTX (3 mM), MET + TMP (6.5 mM + 189.45  $\mu$ M) or MET + MTX (6.5 mM + 3 mM) for 24 h. Following measurements of basal respiration, oligomycin (1.5  $\mu$ M), FCCP (1 mM) and Rot/AA (0.5  $\mu$ M) were injected to measure key mitochondrial parameters. The combination treatment clearly caused a significant decrease in mitochondrial function in HepG2 cells. Data are expressed as mean  $\pm$  SEM (n=6). Comparisons were made using ANOVA followed by Student–Newman–Keuls (SNK) post-hoc test. \*, *p*-value < 0.05 versus control and #, *p*-value < 0.05 versus cells treated with MET only.

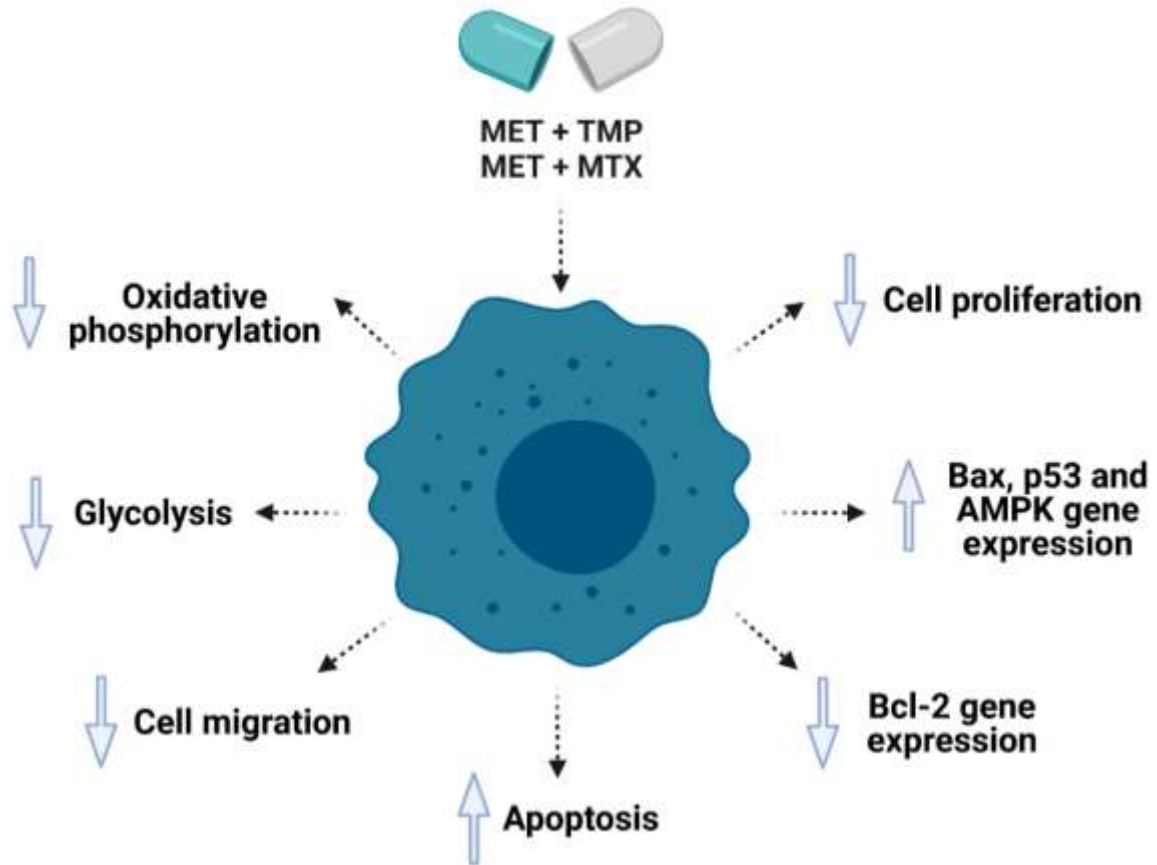


Figure 3.11. Diagram illustrating the effects of combining MET with either antifolate agents (TMP or MTX).

(Created with [Biorender.com](https://www.biorender.com))

## CHAPTER 4: DISCUSSION

In recent years, clinical evidence has emerged that the use of a single therapeutic agent for treatment has proven to be less effective in preventing the recurrence of various cancers (Wu, Sirota, Butte, & Chen, 2014). Moreover, cancer cells are known to exemplify resistance to pharmacological therapeutics through signaling pathways, thereby increasing mortality rates in liver cancer patients (Rexer et al., 2011). Furthermore, HCC, one of the most common types of cancers globally, portrays poor prognosis in currently existing treatment options. Combination therapy hence provides an exciting alternative for improving therapeutic outcomes and reducing recurrence in HCC. Additionally, repurposing FDA approved drugs provides a more economical approach to drug development. The co-treatment of drugs that alter cancer cell metabolism with antifolate agents may yield more effective results (Janjetovic et al., 2011).

MET, used as first-line treatment of type 2 diabetes mellitus, is a safe and economical therapeutic agent which stands to be one of the most widely prescribed drugs worldwide (H. G. Kim et al., 2011; Pryor & Cabreiro, 2015). Several studies have shown the potential of MET as a chemotherapeutic agent in various cancer types, such as breast cancer, lung cancer, gastric and colorectal cancer (Bosco, Antonsen, Sørensen, Pedersen, & Lash, 2011; Libby et al., 2009; Ruitter et al., 2012). In another study, MET served to combat thyroid cancer in a dose dependent manner (González, 2012). Furthermore, Metformin significantly inhibited breast and lung cancer cell proliferation when combined with Paclitaxel by inducing AMPK activation and inhibiting mTOR levels (Rocha et al., 2011).

MET has shown to be more effective in combination with other anti-cancer agents when compared to single therapy; i.e. doxorubicin and cisplatin (G. Chen, Xu, Renko, & Derwahl, 2012). However, MET has not been previously investigated with either TMP or MTX on hepatocellular carcinoma. Therefore, the molecular mechanisms associated with the cytotoxic potential of MET + TMP and MET + MTX were tested to assess the effectiveness of the respective combinations in the treatment of HCC.

In this present investigation, we discovered that treatment of HepG2 cell line with either MET, TMP or MTX directly inhibits cell survival. In addition, the co-treatment of MET and either TMP or MTX effectively inhibited HepG2 cell survival at sub-IC<sub>50</sub> concentrations, causing a reduction



in the IC<sub>50</sub> concentration of MET alone. Our findings were consistent with previous studies that depicted the cytotoxic effects of MET and WP 631 (a structural analogue of doxorubicin) on HepG2 cells (Sliwinska, Rogalska, Marczak, Kasznicki, & Drzewoski, 2015).

Alternatively, the combination of WP 631 and sitagliptin (a dipeptidyl peptidase-4 inhibitor used for patients with diabetes) did not enhance the cytotoxic effects of WP 631 on HepG2 cells. Moreover, our results align strongly with reports of MET in combination with potential chemotherapeutic agents on various breast cancer cell lines (Liu et al., 2012). Another study also reported that the combined treatment of MET with aloin (an extract of Aloe vera) inhibits HCC growth *in vitro* and *in vivo* (R. Sun, Zhai, Ma, & Miao, 2020). Their findings were in uniformity with our results in that MET also elucidated a stronger anti-cancer effect when compared to either drug alone; however, upon combination, the added therapeutic agent increased the cytotoxicity of MET in HepG2 cells. Additionally, MET and curcumin were reported to have inhibited the growth, metastasis and angiogenesis of HCC (Zhang et al., 2018). Co-treatment of MET and sorafenib (an FDA approved drug for the treatment of advanced HCC) also effectively decreased the growth of HCC cells, when compared to each drug alone (Guo et al., 2016; Ling et al., 2014; Ling et al., 2017). Furthermore, another study reported that MET when used in combination with rapamycin decreased cancer cell viability in HepG2 cells by inducing cell apoptosis (Rastegar et al., 2018).

All subsequent experiments were carried out by the calculated sub-IC<sub>50</sub> values of the tested compounds, alone and in combination. Our findings were consistent with the previously mentioned studies which were conducted on HepG2 cells confirming that the combination of MET with both tested antifolate compounds dramatically inhibited cell viability, when compared with single therapy of MET alone. To study the impact of the tested chemotherapeutic agents on the induction of apoptosis, we investigated the effect of MET, TMP, MTX and respective combinations on the expression of p53, Bax and Bcl-2 on HepG2 cells. Apoptosis is initiated via two signaling pathways; intrinsic or extrinsic (Cory & Adams, 2002; Green & Kroemer, 2004).

Bax, Bcl-2 and p53 are associated with mitochondrial-associated intrinsic apoptosis (M. Hassan, Watari, AbuAlmaaty, Ohba, & Sakuragi, 2014). Bax induces apoptotic cell death by forming pores in the mitochondrial outer membrane. Cytochrome C molecules, which are proapoptotic factors, are then able to translocate from the mitochondria to the cytoplasm, disabling the production of ATP and initiating proteolytic caspase cascade (Breckenridge & Xue, 2004). The levels of p53, a

tumor suppressor gene, have also been linked to cell cycle control and DNA repair in several studies. Once activated, p53 has also been seen to induced AMPK-mediated cell cycle arrest (Jones et al., 2005). In this aspect, the combined treatment of cells with MET and either TMP or MTX increased p53 and Bax gene levels, while decreasing Bcl-2 levels. As a result, co-treatment of MET with an antifolate drug (TMP or MTX) on HepG2 cells increased the reduction in cancer cell viability by activating the intrinsic apoptotic pathway. When compared to MET alone, both combinations stimulated apoptosis more prominently.

Our findings are aligned with previous studies which have linked an increase in Bax levels and a reduction in Bcl-2 levels to cytochrome C release as well as enhanced apoptosis (Ibrahim et al., 2014). Similar to the findings presented in the results section, the combination of MET and DSF-Cu (an FDA-approved repurposed medicine used to treat alcohol abusers) boosted the expression of important apoptotic markers, Bax and p53, albeit at lower MET concentrations (Rezaei, Neshasteh-Riz, Mazaheri, Koosha, & Hoormand, 2020). The decrease in MET concentration may be due to the difference in experimental conditions and diverse cell line used. In another recent study, MET when combined with EGCG (epigallocatechin-3-gallate, a polyphenol present in green tea) increased the levels of caspase-3 and decreased levels of survivin, thereby significantly promoting apoptosis in hepatocellular carcinoma cells (Sabry et al., 2019). Additionally, another study found that treating HepG2 cells with ATO (arsenic trioxide, a drug used to treat acute promyelocytic leukemia) boosted apoptosis *in vitro* via lowering Bcl-2 levels (X. Yang, Sun, Tian, Ling, & Wang, 2015).

Flow cytometry was then used to assess apoptosis in HepG2 cells. The percentage of total apoptotic cells in cells treated with the combined therapy was also consistent with the increase in gene expression of pro-apoptotic molecules. The presence of apoptotic or necrotic cells is not the only indication of cytotoxicity of the tested combinations; for this reason, the impact of treatments on the migration of HepG2 cells was also examined.

In line with the previous results, drug combinations potentially inhibited migration of HepG2 cells via decreasing proliferation and increasing the percentage of apoptotic cells. Cell migration, a mechanism involved in the metastatic progression of cancer, is associated with lack of cell-cell adhesion, accelerated migration and cancer cell invasion (Yamaguchi, Wyckoff, & Condeelis, 2005). While higher concentrations of MET elucidate both a decrease in cancer cell viability and

induction of apoptosis, the effect of MET on cancer cell migration is prominent even at lower doses (3 mM causing an inhibition in the wound healing assay) (Figure 3.5), suggesting that MET targets various pathways to differing extents.

Our findings imply the potential effects of MET and combinations on the inhibition of migration of HepG2 cells. Interestingly, upon the addition of MTX to MET, cancer cell migration was not significantly altered, suggesting a potential antagonistic role of MET on the effect of MTX on HepG2 cell migration. Contrastingly, our data suggest a strong effect of MET + TMP on migration by significantly reducing wound closure, demonstrating that the sub-IC<sub>50</sub> concentrations of both drugs may be significant in preventing the metastasis of hepatocellular carcinoma.

In one study, MET slightly enhanced HER+ cell migration, while the combination of MET with aspirin inhibited cancer cell migration in triple-negative breast cancer as well as MCF-7 cell lines, in alignment with our results. In MDA-MB-231 and SK-BR-3 cell lines, however, co-treatment of MET with aspirin did not result in a significant change in migration ability (Amaral, Nery, Leite, de Azevedo Junior, & Campos, 2018). Additionally, another study depicted a reduction in MDA-MB-231 cell migration upon treatment of the same concentration of MET used in the present study (Fan et al., 2015). Therefore, the effects of MET on cancer cell migration, alone or in combination, vary according to the cancer cell type.

Recent research has discovered that metabolic changes are critical for cancer cell survival and proliferation. There is emerging evidence that glycolysis and OXPHOS are essential drivers in cancer cell metastasis (Porporato, Payen, Baset, & Sonveaux, 2016). For this reason, the effect of the tested compounds, alone and in combination, on mitochondrial function was assessed. Cancer cells tend to utilize glycolysis to produce ATP, while also maintain OXPHOS for energy production. This altered cancer metabolism is known as the Warburg effect and is considered one of the hallmarks of cancer (Liberti & Locasale, 2016). Since tumors proliferate more quickly than normal tissues, they require a larger amount of ATP as a source of energy. For this reason, drugs targeting the metabolic pathway of cancer cells pose as potential chemotherapeutics. By blocking the complex I of the ETC, MET has been widely known to inhibit mitochondrial function (Fujita et al., 2019). Consequently, cancer cells treated with MET exhibit an increase in rate of glycolysis as a compensatory mechanism in the aim of increasing ATP production (Andrzejewski, Gravel, Pollak, & St-Pierre, 2014). In cancer cells, preventing this compensatory metabolic event would

directly impact cancer cell survival. We aimed to test whether MET in combination with antifolates would initiate cytotoxicity by decreasing the MET-induced increase in glycolysis, and hence, potentiate cell death. As the Seahorse XFe96 Analyzer measures glycolytic and mitochondrial parameters in real-time, optimization of the respective drug concentrations used was done to ensure adequate measurements of parameters within the allowed range (20-200 OCR). The glycolytic rate assay was conducted after 24 h of incubation with the tested drugs, alone or in combination, to determine the rate of glycolysis in HepG2 cells. When compared to the control, MET dramatically raised the basal rate of glycolysis. In congruity with these findings, previous research that has linked MET to OXPHOS suppression and, as a result, a spike in glycolysis (L. Chen, Ahmad, & Liu, 2016). Furthermore, both TMP and MTX alone decreased basal glycolysis rates, when compared to the control. Combined treatment of MET and TMP or MTX exhibited a considerable reduction in the basal rate of glycolysis in HepG2 cells, when compared to MET alone (Figure 3.6 B).

To further confirm the findings obtained from the glycolytic rate assay, we further went on to perform the ATP rate assay. MET alone induced an increase in the total ATP production rate in HepG2 cells (Figure 3.7). Consistent with our previous findings, both combinations decreased the percentage of total ATP production in HepG2 cells and significantly impacted the percentage of ATP production produced via glycolysis. The ATP rate assay also shed light on the effect of tested compounds on the mitochondrial ATP production. Both combinations elucidated a decrease in the rate of ATP production via the mitochondria (Figure 3.8), yet further analysis was needed to confirm these results. AMPK mRNA expression was also evaluated as AMPK values increase with decrease in ATP levels (Ke, Xu, Li, Luo, & Huang, 2018). Both combinations depicted an increase in AMPK levels, confirming our findings, though they were not significant (Figure 3.9).

We then conducted the MST on HepG2 cells treated with the compounds alone and in combination for 24 h. Following MST, data confirmed that metformin induced mitochondrial injury, consistent with previous findings. Interestingly, both TMP and MTX also inhibited mitochondrial function, but to a lesser extent. Co-treatment of MET and either antifolate resulted in the significant decrease of OCR, compared to the control. Basal respiration as well as proton leak decreased, but not significantly, when compared to MET alone. Contrastingly, maximal respiration and the spare respiratory capacity significantly declined, compared with MET treatment alone (Figure 3.10 B).

These data suggest that MET in combination with antifolates (TMP or MTX) synergistically impact the energy production in HepG2 cells via two main pathways: OXPHOS and glycolysis. Furthermore, the powerful anti-metastatic characteristics of the tested compounds are likely a result of the ability of both combinations to inhibit the mitochondrial bioenergetics. These combinations might be particularly useful in preventing liver cancer metastases and recurrence, as increased oxidative metabolism is linked to increased tumor cell survival and proliferation. Through the inhibition of both energy production routes, cancer cell viability, hence, was significantly reduced.

In conclusion, MET in combination with TMP evoked the highest cytotoxic effects on HepG2 cells, when compared to MET + MTX. The mechanism involved in this co-therapy may potentially be related to a greater inhibition of cell viability, migration and mitochondrial function. Taken together, these data suggest that blocking multiple cellular pathways simultaneously could result in a more potent antitumor effect.

## CHAPTER 5: CONCLUSION AND FUTURE PERSPECTIVES

To the best of our knowledge, no prior studies have been performed examining the cytotoxic effects of combining MET with either TMP or MTX. In this study, the effects of MET alone as opposed to both combinations were compared, underlying the mechanisms involved in this combination *in vitro* on HepG2 cell line. Our findings imply that combining MET with an antifolate agent (TMP or MTX) increases cell death significantly when compared to MET alone. We suggest that the cytotoxic effect of MET when combined with either antifolate agent occurs through the inhibition of cancer cell progression, increase levels of Bax and p53, decrease expression of Bcl-2, rise in the number of total apoptotic cells, inhibition of migration ability, decrease in ATP production, inhibition of the glycolysis pathway and induction of mitochondrial damage. The present findings propose a novel combination for the treatment of hepatocellular carcinoma and possibly other tumor malignancies. Further *in vivo* experiments using DEN (diethylnitrosamine) induced HCC models are recommended to confirm the effects of MET, TMP, MTX, MET + TMP and MET + MTX on HepG2 cells.

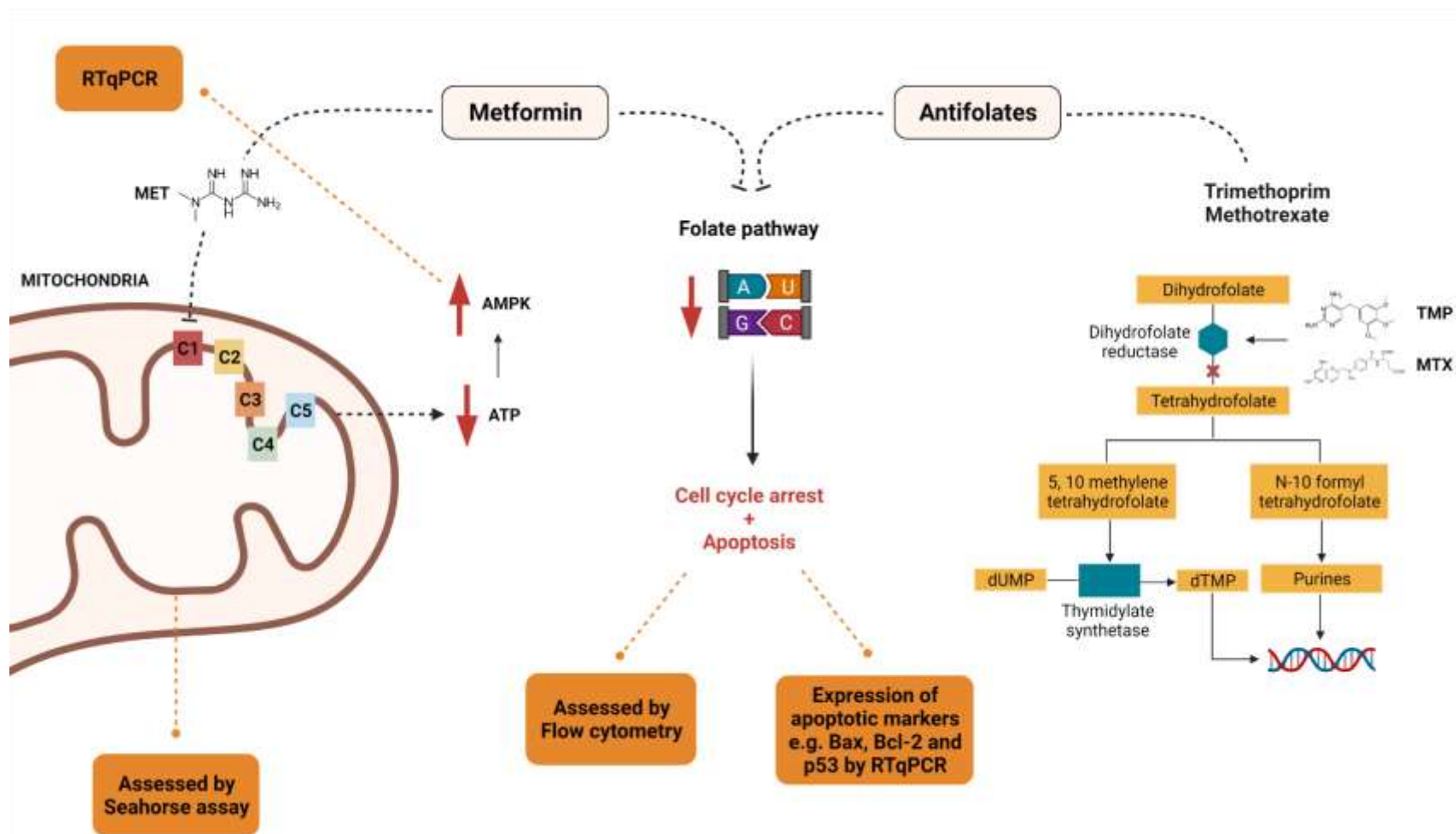


Figure 5.1. Schematic diagram elucidating the proposed mechanism of action of the tested compounds on the mitochondria and folate pathway.

(Figure adapted with modifications from (Hoffman & Williams, 2012; Jara & Lopez-Munoz, 2015))

(Created with [Biorender.com](https://www.biorender.com))

## REFERENCES

- Altekruse, S. F., McGlynn, K. A., & Reichman, M. E. (2009). Hepatocellular carcinoma incidence, mortality, and survival trends in the United States from 1975 to 2005. *Journal of clinical oncology*, 27(9), 1485.
- Amaral, M. E. A., Nery, L. R., Leite, C. E., de Azevedo Junior, W. F., & Campos, M. M. (2018). Pre-clinical effects of metformin and aspirin on the cell lines of different breast cancer subtypes. *Investigational new drugs*, 36(5), 782-796.
- Andrzejewski, S., Gravel, S.-P., Pollak, M., & St-Pierre, J. (2014). Metformin directly acts on mitochondria to alter cellular bioenergetics. *Cancer & metabolism*, 2(1), 1-14.
- Balkwill, F., & Mantovani, A. (2001). Inflammation and cancer: back to Virchow? *The lancet*, 357(9255), 539-545.
- Balogh, J., Victor III, D., Asham, E. H., Burroughs, S. G., Boktour, M., Saharia, A., . . . Monsour Jr, H. P. (2016). Hepatocellular carcinoma: a review. *Journal of hepatocellular carcinoma*, 3, 41.
- Basu, A. K. (2018). DNA damage, mutagenesis and cancer. *International journal of molecular sciences*, 19(4), 970.
- Blakley, R. L., & Benkovic, S. J. (1984). *Folates and pterins: Volume 1, chemistry and biochemistry of folates*: New York: John Wiley & Sons, Inc.
- Bosco, J. L. F., Antonsen, S., Sørensen, H. T., Pedersen, L., & Lash, T. L. (2011). Metformin and incident breast cancer among diabetic women: a population-based case–control study in Denmark. *Cancer Epidemiology and Prevention Biomarkers*, 20(1), 101-111.
- Breckenridge, D. G., & Xue, D. (2004). Regulation of mitochondrial membrane permeabilization by BCL-2 family proteins and caspases. *Current opinion in cell biology*, 16(6), 647-652.
- Buzzai, M., Jones, R. G., Amaravadi, R. K., Lum, J. J., DeBerardinis, R. J., Zhao, F., . . . Thompson, C. B. (2007). Systemic treatment with the antidiabetic drug metformin selectively impairs p53-deficient tumor cell growth. *Cancer research*, 67(14), 6745-6752.
- Cairns, R. A., Harris, I. S., & Mak, T. W. (2011). Regulation of cancer cell metabolism. *Nature Reviews Cancer*, 11(2), 85-95.



- Carmeliet, P. (2000). Mechanisms of angiogenesis and arteriogenesis. *Nature medicine*, 6(4), 389-395.
- Carmeliet, P., & Jain, R. K. (2000). Angiogenesis in cancer and other diseases. *nature*, 407(6801), 249-257.
- Chan, E. S., & Cronstein, B. N. (2010). Methotrexate—how does it really work? *Nature Reviews Rheumatology*, 6(3), 175-178.
- Chance, B., & Williams, G. (1956). The respiratory chain and oxidative phosphorylation. *Adv Enzymol Relat Areas Mol Biol*, 17, 65-134.
- Chen, B., Wei, W., Ma, L., Yang, B., Gill, R. M., Chua, M.-S., . . . So, S. (2017). Computational discovery of niclosamide ethanolamine, a repurposed drug candidate that reduces growth of hepatocellular carcinoma cells in vitro and in mice by inhibiting cell division cycle 37 signaling. *Gastroenterology*, 152(8), 2022-2036.
- Chen, G., Xu, S., Renko, K., & Derwahl, M. (2012). Metformin inhibits growth of thyroid carcinoma cells, suppresses self-renewal of derived cancer stem cells, and potentiates the effect of chemotherapeutic agents. *The Journal of Clinical Endocrinology & Metabolism*, 97(4), E510-E520.
- Chen, L., Ahmad, N., & Liu, X. (2016). Combining p53 stabilizers with metformin induces synergistic apoptosis through regulation of energy metabolism in castration-resistant prostate cancer. *Cell cycle*, 15(6), 840-849.
- Cheng, A.-L., Kang, Y.-K., Chen, Z., Tsao, C.-J., Qin, S., Kim, J. S., . . . Yang, T.-S. (2009). Efficacy and safety of sorafenib in patients in the Asia-Pacific region with advanced hepatocellular carcinoma: a phase III randomised, double-blind, placebo-controlled trial. *The lancet oncology*, 10(1), 25-34.
- Corominas-Faja, B., Quirantes-Pine, R., Oliveras-Ferraros, C., Vazquez-Martin, A., Cufi, S., Martin-Castillo, B., . . . Menendez, J. A. (2012). Metabolomic fingerprint reveals that metformin impairs one-carbon metabolism in a manner similar to the antifolate class of chemotherapy drugs. *Aging (Albany NY)*, 4(7), 480-498. doi: 10.18632/aging.100472
- Corominas-Faja, B., Quirantes-Piné, R., Oliveras-Ferraros, C., Vazquez-Martin, A., Cufí, S., Martin-Castillo, B., . . . Menendez, J. A. (2012). Metabolomic fingerprint reveals that metformin impairs one-carbon metabolism in a manner similar to the antifolate class of chemotherapy drugs. *Aging (Albany NY)*, 4(7), 480.

- Cory, S., & Adams, J. M. (2002). The Bcl2 family: regulators of the cellular life-or-death switch. *Nature Reviews Cancer*, 2(9), 647-656.
- Cronstein, B. N. (2005). Low-dose methotrexate: a mainstay in the treatment of rheumatoid arthritis. *Pharmacological reviews*, 57(2), 163-172.
- Czabotar, P. E., Lessene, G., Strasser, A., & Adams, J. M. (2014). Control of apoptosis by the BCL-2 protein family: implications for physiology and therapy. *Nature reviews Molecular cell biology*, 15(1), 49-63.
- Darrell, J., Garrod, L., & Waterworth, P. M. (1968). Trimethoprim: laboratory and clinical studies. *Journal of Clinical Pathology*, 21(2), 202.
- DeBerardinis, R. J., & Chandel, N. S. (2016). Fundamentals of cancer metabolism. *Science advances*, 2(5), e1600200.
- DeWaal, D., Nogueira, V., Terry, A. R., Patra, K. C., Jeon, S.-M., Guzman, G., . . . Hay, N. (2018). Hexokinase-2 depletion inhibits glycolysis and induces oxidative phosphorylation in hepatocellular carcinoma and sensitizes to metformin. *Nature communications*, 9(1), 1-14.
- Dhanasekaran, R., Limaye, A., & Cabrera, R. (2012). Hepatocellular carcinoma: current trends in worldwide epidemiology, risk factors, diagnosis, and therapeutics. *Hepatic medicine: evidence and research*, 4, 19.
- Dick, F. A., & Rubin, S. M. (2013). Molecular mechanisms underlying RB protein function. *Nature reviews Molecular cell biology*, 14(5), 297-306.
- Divakaruni, A. S., Paradyse, A., Ferrick, D. A., Murphy, A. N., & Jastroch, M. (2014). Analysis and interpretation of microplate-based oxygen consumption and pH data *Methods in enzymology* (Vol. 547, pp. 309-354): Elsevier
- Dowling, R. J., Goodwin, P. J., & Stambolic, V. (2011). Understanding the benefit of metformin use in cancer treatment. *BMC Med*, 9, 33. doi: 10.1186/1741-7015-9-33
- El-Mir, M.-Y., Nogueira, V., Fontaine, E., Avéret, N., Rigoulet, M., & Leverve, X. (2000). Dimethylbiguanide inhibits cell respiration via an indirect effect targeted on the respiratory chain complex I. *Journal of Biological Chemistry*, 275(1), 223-228.
- El-Serag, H. B. (2012). Epidemiology of viral hepatitis and hepatocellular carcinoma. *Gastroenterology*, 142(6), 1264-1273. e1261.

- El-Serag, H. B., Hampel, H., & Javadi, F. (2006). The association between diabetes and hepatocellular carcinoma: a systematic review of epidemiologic evidence. *Clinical Gastroenterology and Hepatology*, 4(3), 369-380.
- Eliopoulos, G. M., & Huovinen, P. (2001). Resistance to Trimethoprim-Sulfamethoxazole. *Clinical Infectious Diseases*, 32(11), 1608-1614. doi: 10.1086/320532
- Evans, J. M., Donnelly, L. A., Emslie-Smith, A. M., Alessi, D. R., & Morris, A. D. (2005). Metformin and reduced risk of cancer in diabetic patients. *Bmj*, 330(7503), 1304-1305.
- Fan, C., Wang, Y., Liu, Z., Sun, Y., Wang, X., Wei, G., & Wei, J. (2015). Metformin exerts anticancer effects through the inhibition of the Sonic hedgehog signaling pathway in breast cancer. *International Journal of Molecular Medicine*, 36(1), 204-214.
- Ferrara, N., Gerber, H.-P., & LeCouter, J. (2003). The biology of VEGF and its receptors. *Nature medicine*, 9(6), 669-676.
- Foretz, M., Guigas, B., Bertrand, L., Pollak, M., & Viollet, B. (2014). Metformin: from mechanisms of action to therapies. *Cell metabolism*, 20(6), 953-966.
- Fraisl, P., Mazzone, M., Schmidt, T., & Carmeliet, P. (2009). Regulation of angiogenesis by oxygen and metabolism. *Developmental cell*, 16(2), 167-179.
- Fujita, H., Hirose, K., Sato, M., Fujioka, I., Fujita, T., Aoki, M., & Takai, Y. (2019). Metformin attenuates hypoxia-induced resistance to cisplatin in the HepG2 cell line. *Oncology letters*, 17(2), 2431-2440.
- Ganapathy-Kanniappan, S., & Geschwind, J.-F. H. (2013). Tumor glycolysis as a target for cancer therapy: progress and prospects. *Molecular cancer*, 12(1), 1-11.
- Gatenby, R. A., & Gillies, R. J. (2004). Why do cancers have high aerobic glycolysis? *Nature reviews cancer*, 4(11), 891-899.
- Gatenby, R. A., & Gillies, R. J. (2007). Glycolysis in cancer: a potential target for therapy. *The international journal of biochemistry & cell biology*, 39(7-8), 1358-1366.
- Gong, J., Robbins, L. A., Lugea, A., Waldron, R. T., Jeon, C. Y., & Pandol, S. J. (2014). Diabetes, pancreatic cancer, and metformin therapy. *Frontiers in physiology*, 5, 426-426. doi: 10.3389/fphys.2014.00426

- González, D. C. F. (2012). Metformin Inhibits Growth of Thyroid Carcinoma Cells, Suppresses Self-Renewal of Derived Cancer Stem Cells, and Potentiates the Effect of Chemotherapeutic Agents. *Revista de Endocrinología y Nutrición*, 20(3), 131-133.
- Green, D. R., & Evan, G. I. (2002). A matter of life and death. *Cancer cell*, 1(1), 19-30.
- Green, D. R., & Kroemer, G. (2004). The pathophysiology of mitochondrial cell death. *Science*, 305(5684), 626-629.
- Greten, T., Papendorf, F., Bleck, J., Kirchhoff, T., Wohlberedt, T., Kubicka, S., . . . Manns, M. (2005). Survival rate in patients with hepatocellular carcinoma: a retrospective analysis of 389 patients. *British journal of cancer*, 92(10), 1862-1868.
- Gu, X., Ma, Y., Liu, Y., & Wan, Q. (2021). Measurement of mitochondrial respiration in adherent cells by Seahorse XF96 Cell Mito Stress Test. *STAR protocols*, 2(1), 100245.
- Guo, Z., Cao, M., You, A., Gao, J., Zhou, H., Li, H., . . . Song, T. (2016). Metformin inhibits the prometastatic effect of sorafenib in hepatocellular carcinoma by upregulating the expression of TIP30. *Cancer science*, 107(4), 507-513.
- Hajarizadeh, B., Grebely, J., & Dore, G. J. (2013). Epidemiology and natural history of HCV infection. *Nature reviews Gastroenterology & hepatology*, 10(9), 553.
- Hanahan, D., & Weinberg, R. A. (2000). The hallmarks of cancer. *cell*, 100(1), 57-70.
- Hanahan, D., & Weinberg, R. A. (2011). Hallmarks of cancer: the next generation. *cell*, 144(5), 646-674.
- Hardie, D. G. (2014). AMP-activated protein kinase: maintaining energy homeostasis at the cellular and whole-body levels. *Annual review of nutrition*, 34, 31-55.
- Hashimoto, T., & Shibasaki, F. (2015). Hypoxia-inducible factor as an angiogenic master switch. *Frontiers in pediatrics*, 3, 33.
- Hassan, M., Watari, H., AbuAlmaaty, A., Ohba, Y., & Sakuragi, N. (2014). Apoptosis and molecular targeting therapy in cancer. *BioMed research international*, 2014.
- Hassan, M. M., Botrus, G., Abdel-Wahab, R., Wolff, R. A., Li, D., Tweardy, D., . . . Lee, J.-S. (2017). Estrogen replacement reduces risk and increases survival times of women with hepatocellular carcinoma. *Clinical Gastroenterology and Hepatology*, 15(11), 1791-1799.
- Hatefi, Y. (1985). The mitochondrial electron transport and oxidative phosphorylation system. *Annual review of biochemistry*, 54(1), 1015-1069.

- Haupt, S., Raghu, D., & Haupt, Y. (2016). Mutant p53 drives cancer by subverting multiple tumor suppression pathways. *Frontiers in oncology*, 6, 12.
- Hay, N. (2016). Reprogramming glucose metabolism in cancer: can it be exploited for cancer therapy? *Nature Reviews Cancer*, 16(10), 635.
- Heinz, S., Freyberger, A., Lawrenz, B., Schladt, L., Schmuck, G., & Ellinger-Ziegelbauer, H. (2017). Mechanistic investigations of the mitochondrial complex I inhibitor rotenone in the context of pharmacological and safety evaluation. *Scientific reports*, 7, 45465.
- Hida, K., Maishi, N., Torii, C., & Hida, Y. (2016). Tumor angiogenesis—characteristics of tumor endothelial cells. *International journal of clinical oncology*, 21(2), 206-212.
- Hirosumi, J., Tuncman, G., Chang, L., Görgün, C. Z., Uysal, K. T., Maeda, K., . . . Hotamisligil, G. S. (2002). A central role for JNK in obesity and insulin resistance. *Nature*, 420(6913), 333-336.
- Hoffman, B. L., & Williams, J. W. (2012). *Williams gynecology*. New York: McGraw-Hill Medical.
- Huang, S. F., Chang, I. C., Hong, C. C., Yen, T. C., Chen, C. L., Wu, C. C., . . . Yu, H. C. (2018). Metabolic risk factors are associated with non-hepatitis B non-hepatitis C hepatocellular carcinoma in Taiwan, an endemic area of chronic hepatitis B. *Hepatology communications*, 2(6), 747-759.
- Hui, L., Zatloukal, K., Scheuch, H., Stepniak, E., & Wagner, E. F. (2008). Proliferation of human HCC cells and chemically induced mouse liver cancers requires JNK1-dependent p21 downregulation. *The Journal of clinical investigation*, 118(12), 3943-3953.
- Huovinen, P. (1987). Trimethoprim resistance. *Antimicrobial agents and chemotherapy*, 31(10), 1451.
- Ibrahim, M. Y., Hashim, N. M., Mohan, S., Abdulla, M. A., Kamalidehghan, B., Ghaderian, M., . . . Yahayu, M. (2014).  $\alpha$ -Mangostin from *Cratoxylum arborescens* demonstrates apoptogenesis in MCF-7 with regulation of NF- $\kappa$ B and Hsp70 protein modulation in vitro, and tumor reduction in vivo. *Drug design, development and therapy*, 8, 1629.
- Indovina, P., Marcelli, E., Casini, N., Rizzo, V., & Giordano, A. (2013). Emerging roles of RB family: new defense mechanisms against tumor progression. *Journal of cellular physiology*, 228(3), 525-535.

- Iyer, J. K., Milhous, W. K., Cortese, J. F., Kublin, J. G., & Plowe, C. V. (2001). Plasmodium falciparum crossresistance between trimethoprim and pyrimethamine. *The Lancet*, 358(9287), 1066-1067.
- Janjetovic, K., Vucicevic, L., Misirkic, M., Vilimanovich, U., Tovilovic, G., Zogovic, N., . . . Trajkovic, V. (2011). Metformin reduces cisplatin-mediated apoptotic death of cancer cells through AMPK-independent activation of Akt. *European journal of pharmacology*, 651(1-3), 41-50.
- Jara, J., & Lopez-Munoz, R. (2015). Metformin and cancer: between the bioenergetic disturbances and the antifolate activity. *Pharmacological research*, 101, 102-108.
- Jewell, J., & Sheron, N. (2010). Trends in European liver death rates: implications for alcohol policy. *Clinical medicine*, 10(3), 259.
- Jones, R. G., Plas, D. R., Kubek, S., Buzzai, M., Mu, J., Xu, Y., . . . Thompson, C. B. (2005). AMP-activated protein kinase induces a p53-dependent metabolic checkpoint. *Molecular cell*, 18(3), 283-293.
- Juin, P., Geneste, O., Gautier, F., Depil, S., & Campone, M. (2013). Decoding and unlocking the BCL-2 dependency of cancer cells. *Nature Reviews Cancer*, 13(7), 455-465.
- Kamat, A. M., & Lamm, D. L. (2004). Antitumor activity of common antibiotics against superficial bladder cancer. *Urology*, 63(3), 457-460.
- Ke, R., Xu, Q., Li, C., Luo, L., & Huang, D. (2018). Mechanisms of AMPK in the maintenance of ATP balance during energy metabolism. *Cell biology international*, 42(4), 384-392.
- Kelland, L. (2007). Targeting the limitless replicative potential of cancer: the telomerase/telomere pathway. *Clinical Cancer Research*, 13(17), 4960-4963.
- Kim, H. G., Hien, T. T., Han, E. H., Hwang, Y. P., Choi, J. H., Kang, K. W., . . . Song, G. Y. (2011). Metformin inhibits P-glycoprotein expression via the NF- $\kappa$ B pathway and CRE transcriptional activity through AMPK activation. *British journal of pharmacology*, 162(5), 1096-1108.
- Kim, M. P., Zhang, Y., & Lozano, G. (2015). Mutant p53: multiple mechanisms define biologic activity in cancer. *Frontiers in oncology*, 5, 249.
- Koopman, G., Reutelingsperger, C., Kuijten, G., Keehnen, R., Pals, S., & Van Oers, M. (1994). Annexin V for flow cytometric detection of phosphatidylserine expression on B cells undergoing apoptosis.

- Kramer, P. A., Ravi, S., Chacko, B., Johnson, M. S., & Darley-USmar, V. M. (2014). A review of the mitochondrial and glycolytic metabolism in human platelets and leukocytes: implications for their use as bioenergetic biomarkers. *Redox biology*, 2, 206-210.
- Kruiswijk, F., Labuschagne, C. F., & Vousden, K. H. (2015). p53 in survival, death and metabolic health: a lifeguard with a licence to kill. *Nature reviews Molecular cell biology*, 16(7), 393-405.
- Kumar, P., Nagarajan, A., & Uchil, P. D. (2018). Analysis of cell viability by the MTT assay. *Cold Spring Harbor Protocols*, 2018(6), pdb. prot095505.
- Lakshmanan, I., & Batra, S. K. (2013). Protocol for apoptosis assay by flow cytometry using annexin V staining method. *Bio-protocol*, 3(6).
- Lardy, H. A., Johnson, D., & McMurray, W. (1958). Antibiotics as tools for metabolic studies. I. A survey of toxic antibiotics in respiratory, phosphorylative and glycolytic systems. *Archives of biochemistry and biophysics*, 78(2), 587-597.
- Lee, M.-S., Hsu, C.-C., Wahlqvist, M. L., Tsai, H.-N., Chang, Y.-H., & Huang, Y.-C. (2011). Type 2 diabetes increases and metformin reduces total, colorectal, liver and pancreatic cancer incidences in Taiwanese: a representative population prospective cohort study of 800,000 individuals. *BMC cancer*, 11(1), 1-10.
- Lei, Y., Yi, Y., Liu, Y., Liu, X., Keller, E. T., Qian, C.-N., . . . Lu, Y. (2017). Metformin targets multiple signaling pathways in cancer. *Chinese journal of cancer*, 36(1), 1-9.
- Leung, D. T., & Chu, S. (2018). Measurement of oxidative stress: mitochondrial function using the seahorse system *Preeclampsia* (pp. 285-293): Springer
- Li, L., Wu, C.-S., Hou, G.-M., Dong, M.-Z., Wang, Z.-B., Hou, Y., . . . Sun, Q.-Y. (2018). Type 2 diabetes increases oocyte mtDNA mutations which are eliminated in the offspring by bottleneck effect. *Reproductive Biology and Endocrinology*, 16(1), 1-8.
- Libby, G., Donnelly, L. A., Donnan, P. T., Alessi, D. R., Morris, A. D., & Evans, J. M. (2009). New users of metformin are at low risk of incident cancer: a cohort study among people with type 2 diabetes. *Diabetes care*, 32(9), 1620-1625.
- Liberti, M. V., & Locasale, J. W. (2016). The Warburg effect: how does it benefit cancer cells? *Trends in biochemical sciences*, 41(3), 211-218.

- Ling, S., Feng, T., Ke, Q., Fan, N., Li, L., Li, Z., . . . Li, Y. (2014). Metformin inhibits proliferation and enhances chemosensitivity of intrahepatic cholangiocarcinoma cell lines. *Oncology reports*, *31*(6), 2611-2618.
- Ling, S., Song, L., Fan, N., Feng, T., Liu, L., Yang, X., . . . Zhao, F. (2017). Combination of metformin and sorafenib suppresses proliferation and induces autophagy of hepatocellular carcinoma via targeting the mTOR pathway. *International journal of oncology*, *50*(1), 297-309.
- Liu, H., Scholz, C., Zang, C., Schefe, J. H., Habbel, P., Regierer, A.-C., . . . Eucker, J. (2012). Metformin and the mTOR inhibitor everolimus (RAD001) sensitize breast cancer cells to the cytotoxic effect of chemotherapeutic drugs in vitro. *Anticancer research*, *32*(5), 1627-1637.
- Liver, E. A. F. T. S. O. T. (2012). EASL–EORTC clinical practice guidelines: management of hepatocellular carcinoma. *Journal of hepatology*, *56*(4), 908-943.
- Llambi, F., & Green, D. R. (2011). Apoptosis and oncogenesis: give and take in the BCL-2 family. *Current opinion in genetics & development*, *21*(1), 12-20.
- Lopez, J., & Tait, S. (2015). Mitochondrial apoptosis: killing cancer using the enemy within. *British journal of cancer*, *112*(6), 957-962.
- Malumbres, M., & Barbacid, M. (2009). Cell cycle, CDKs and cancer: a changing paradigm. *Nature reviews cancer*, *9*(3), 153-166.
- Marchi, S., Giorgi, C., Suski, J. M., Agnoletto, C., Bononi, A., Bonora, M., . . . Poletti, F. (2012). Mitochondria-ros crosstalk in the control of cell death and aging. *Journal of signal transduction*, *2012*.
- Massagué, J., & Obenauf, A. C. (2016). Metastatic colonization by circulating tumour cells. *Nature*, *529*(7586), 298-306.
- Matsushita, H., & Takaki, A. (2019). Alcohol and hepatocellular carcinoma. *BMJ open gastroenterology*, *6*(1).
- Mazurek, M., Litak, J., Kamieniak, P., Kulesza, B., Jonak, K., Baj, J., & Grochowski, C. (2020). Metformin as potential therapy for high-grade glioma. *Cancers*, *12*(1), 210.
- McGuire, J. J. (2003). Anticancer antifolates: current status and future directions. *Current pharmaceutical design*, *9*(31), 2593-2613.



- Morgan, T. R., Mandayam, S., & Jamal, M. M. (2004). Alcohol and hepatocellular carcinoma. *Gastroenterology*, 127(5), S87-S96.
- Morrison, T. B., Weis, J. J., & Wittwer, C. T. (1998). Quantification of low-copy transcripts by continuous SYBR Green I monitoring during amplification. *Biotechniques*, 24(6), 954-958, 960, 962.
- Murphy, M. P. (2009). How mitochondria produce reactive oxygen species. *Biochemical journal*, 417(1), 1-13.
- Nangia-Makker, P., Yu, Y., Vasudevan, A., Farhana, L., Rajendra, S. G., Levi, E., & Majumdar, A. P. (2014). Metformin: a potential therapeutic agent for recurrent colon cancer. *PloS one*, 9(1), e84369.
- Nishida, N., Yano, H., Nishida, T., Kamura, T., & Kojiro, M. (2006). Angiogenesis in Cancer. *Vasc Health Risk Manag*, 2(3), 213-219.
- Nishida, N., Yano, H., Nishida, T., Kamura, T., & Kojiro, M. (2006). Angiogenesis in cancer. *Vascular health and risk management*, 2(3), 213.
- Owen, M. R., Doran, E., & Halestrap, A. P. (2000). Evidence that metformin exerts its anti-diabetic effects through inhibition of complex 1 of the mitochondrial respiratory chain. *Biochemical Journal*, 348(3), 607-614.
- Ozakyol, A. (2017). Global epidemiology of hepatocellular carcinoma (HCC epidemiology). *Journal of gastrointestinal cancer*, 48(3), 238-240.
- Park, J. W., Chen, M., Colombo, M., Roberts, L. R., Schwartz, M., Chen, P. J., . . . Orsini, L. S. (2015). Global patterns of hepatocellular carcinoma management from diagnosis to death: the BRIDGE Study. *Liver International*, 35(9), 2155-2166.
- Pelicano, H., Martin, D., Xu, R., and, & Huang, P. (2006). Glycolysis inhibition for anticancer treatment. *Oncogene*, 25(34), 4633-4646.
- Petrovic, N. (2016). Targeting angiogenesis in cancer treatments: where do we stand? *Journal of Pharmacy & Pharmaceutical Sciences*, 19(2), 226-238.
- Porporato, P. E., Payen, V. L., Baselet, B., & Sonveaux, P. (2016). Metabolic changes associated with tumor metastasis, part 2: mitochondria, lipid and amino acid metabolism. *Cellular and Molecular Life Sciences*, 73(7), 1349-1363.
- Pryor, R., & Cabreiro, F. (2015). Repurposing metformin: an old drug with new tricks in its binding pockets. *Biochemical Journal*, 471(3), 307-322.

- Ramakrishna, G., Rastogi, A., Trehanpati, N., Sen, B., Khosla, R., & Sarin, S. K. (2013). From cirrhosis to hepatocellular carcinoma: new molecular insights on inflammation and cellular senescence. *Liver cancer*, 2(3-4), 367-383.
- Ramteke, P., Deb, A., Shepal, V., & Bhat, M. K. (2019). Hyperglycemia associated metabolic and molecular alterations in cancer risk, progression, treatment, and mortality. *Cancers*, 11(9), 1402.
- Rastegar, M., Marjani, H.-A., Yazdani, Y., Shahbazi, M., Golalipour, M., & Farazmandfar, T. (2018). Investigating effect of rapamycin and metformin on angiogenesis in hepatocellular carcinoma cell line. *Advanced pharmaceutical bulletin*, 8(1), 63.
- Rexer, B. N., Ham, A. L., Rinehart, C., Hill, S., de Matos Granja-Ingram, N., Gonzalez-Angulo, A., . . . Liebler, D. C. (2011). Phosphoproteomic mass spectrometry profiling links Src family kinases to escape from HER2 tyrosine kinase inhibition. *Oncogene*, 30(40), 4163-4174.
- Rezaei, N., Neshasteh-Riz, A., Mazaheri, Z., Koosha, F., & Hoormand, M. (2020). The combination of metformin and disulfiram-Cu for effective radiosensitization on glioblastoma cells. *Cell Journal (Yakhteh)*, 22(3), 263.
- Ribatti, D., Nico, B., & Crivellato, E. (2015). The development of the vascular system: a historical overview. *Vascular Morphogenesis*, 1-14.
- Rich, J. N. (2007). Cancer stem cells in radiation resistance. *Cancer research*, 67(19), 8980-8984.
- Rizos, C. V., & Elisaf, M. S. (2013). Metformin and cancer. *European Journal of Pharmacology*, 705(1-3), 96-108.
- Rocha, G. Z., Dias, M. M., Ropelle, E. R., Osório-Costa, F., Rossato, F. A., Vercesi, A. E., . . . Carvalheira, J. B. (2011). Metformin amplifies chemotherapy-induced AMPK activation and antitumoral growth. *Clinical Cancer Research*, 17(12), 3993-4005.
- Rojas Quintero, J., Chávez, M., Torres, W., Arraiz, N., Cabrera de Bravo, M., & Bermudez, V. (2014). Metformin in Cancer: Chemical Pathways for Tumoral Control Independent of Amp-Dependent Kinase. *Journal of Endocrinology, Diabetes & Obesity*, 2.
- Ruggieri, A., Barbati, C., & Malorni, W. (2010). Cellular and molecular mechanisms involved in hepatocellular carcinoma gender disparity. *International journal of cancer*, 127(3), 499-504.

- Ruiter, R., Visser, L. E., van Herk-Sukel, M. P., Coebergh, J.-W. W., Haak, H. R., Geelhoed-Duijvestijn, P. H., . . . Stricker, B. H. C. (2012). Lower risk of cancer in patients on metformin in comparison with those on sulfonylurea derivatives: results from a large population-based follow-up study. *Diabetes care*, *35*(1), 119-124.
- Sabharwal, S. S., & Schumacker, P. T. (2014). Mitochondrial ROS in cancer: initiators, amplifiers or an Achilles' heel? *Nature Reviews Cancer*, *14*(11), 709-721.
- Sabry, D., Abdelaleem, O. O., Ali, A. M. E. A., Mohammed, R. A., Abdel-Hameed, N. D., Hassouna, A., & Khalifa, W. A. (2019). Anti-proliferative and anti-apoptotic potential effects of epigallocatechin-3-gallate and/or metformin on hepatocellular carcinoma cells: In vitro study. *Molecular biology reports*, *46*(2), 2039-2047.
- Sahra, I. B., Laurent, K., Loubat, A., Giorgetti-Peraldi, S., Colosetti, P., Auberger, P., . . . Bost, F. (2008). The antidiabetic drug metformin exerts an antitumoral effect in vitro and in vivo through a decrease of cyclin D1 level. *Oncogene*, *27*(25), 3576-3586.
- Sakurai, T., & Kudo, M. (2011). Signaling pathways governing tumor angiogenesis. *Oncology*, *81*(Suppl. 1), 24-29.
- Saraei, P., Asadi, I., Kakar, M. A., & Moradi-Kor, N. (2019). The beneficial effects of metformin on cancer prevention and therapy: a comprehensive review of recent advances. *Cancer management and research*, *11*, 3295.
- Sarosiek, K. A., Fraser, C., Muthalagu, N., Bhola, P. D., Chang, W., McBrayer, S. K., . . . Ryan, J. A. (2017). Developmental regulation of mitochondrial apoptosis by c-Myc governs age- and tissue-specific sensitivity to cancer therapeutics. *Cancer cell*, *31*(1), 142-156.
- Scherz-Shouval, R., & Elazar, Z. (2007). ROS, mitochondria and the regulation of autophagy. *Trends in cell biology*, *17*(9), 422-427.
- Schlachterman, A., Craft, W. W., Jr., Hilgenfeldt, E., Mitra, A., & Cabrera, R. (2015). Current and future treatments for hepatocellular carcinoma. *World journal of gastroenterology*, *21*(28), 8478-8491. doi: 10.3748/wjg.v21.i28.8478
- Senior, A. E. (1988). ATP synthesis by oxidative phosphorylation. *Physiological reviews*, *68*(1), 177-231.
- Sliwinska, A., Rogalska, A., Marczak, A., Kasznicki, J., & Drzewoski, J. (2015). Metformin, but not sitagliptin, enhances WP631-induced apoptotic HepG2 cell death. *Toxicology in Vitro*, *29*(5), 1116-1123.

- Smilack, J. D. (1999). *Trimethoprim-sulfamethoxazole*. Paper presented at the Mayo Clinic Proceedings.
- Smolina, N., Bruton, J., Kostareva, A., & Sejersen, T. (2017). Assaying mitochondrial respiration as an indicator of cellular metabolism and fitness *Cell Viability Assays* (pp. 79-87): Springer
- Sporn, M. B. (1996). The war on cancer. *Lancet (London, England)*, 347(9012), 1377-1381.
- Steeg, P. S. (2006). Tumor metastasis: mechanistic insights and clinical challenges. *Nature medicine*, 12(8), 895-904.
- Stracquadanio, G., Wang, X., Wallace, M. D., Grawenda, A. M., Zhang, P., Hewitt, J., . . . Goding, C. R. (2016). The importance of p53 pathway genetics in inherited and somatic cancer genomes. *Nature reviews Cancer*, 16(4), 251.
- Sun, H., Deng, Q., Pan, Y., He, B., Ying, H., Chen, J., . . . Wang, S. (2015). Association between estrogen receptor 1 (ESR1) genetic variations and cancer risk: a meta-analysis. *J BUON*, 20(1), 296-308.
- Sun, R., Zhai, R., Ma, C., & Miao, W. (2020). Combination of aloin and metformin enhances the antitumor effect by inhibiting the growth and invasion and inducing apoptosis and autophagy in hepatocellular carcinoma through PI3K/AKT/mTOR pathway. *Cancer medicine*, 9(3), 1141-1151.
- Tekade, R. K., & Sun, X. (2017). The Warburg effect and glucose-derived cancer theranostics. *Drug Discovery Today*, 22(11), 1637-1653.
- Tian, H., & Cronstein, B. N. (2007). Understanding the mechanisms of action of methotrexate. *Bull NYU Hosp Jt Dis*, 65(3), 168-173.
- Tobinick, E. L. (2009). The value of drug repositioning in the current pharmaceutical market. *Drug News Perspect*, 22(2), 119-125. doi: 10.1358/dnp.2009.22.2.1303818
- Underwood, E., Redell, J. B., Zhao, J., Moore, A. N., & Dash, P. K. (2020). A method for assessing tissue respiration in anatomically defined brain regions. *Scientific reports*, 10(1), 1-14.
- Valastyan, S., & Weinberg, R. A. (2011). Tumor metastasis: molecular insights and evolving paradigms. *Cell*, 147(2), 275-292.

- Waller, L. P., Deshpande, V., & Pysopoulos, N. (2015). Hepatocellular carcinoma: A comprehensive review. *World journal of hepatology*, 7(26), 2648-2663. doi: 10.4254/wjh.v7.i26.2648
- Weinberg, R. A. (1995). The retinoblastoma protein and cell cycle control. *Cell*, 81(3), 323-330.
- Whitburn, J., Edwards, C. M., & Sooriakumaran, P. (2017). Metformin and prostate cancer: a new role for an old drug. *Current urology reports*, 18(6), 46.
- Wishart, D. S., Knox, C., Guo, A. C., Shrivastava, S., Hassanali, M., Stothard, P., . . . Woolsey, J. (2006). DrugBank: a comprehensive resource for in silico drug discovery and exploration. *Nucleic acids research*, 34(suppl\_1), D668-D672.
- Witters, L. A. (2001). The blooming of the French lilac. *The Journal of clinical investigation*, 108(8), 1105-1107.
- World Health Organization. (2012). Prevention and control of viral hepatitis infection: framework for global action: World Health Organization.
- Wu, M., Sirota, M., Butte, A. J., & Chen, B. (2014). *Characteristics of drug combination therapy in oncology by analyzing clinical trial data on ClinicalTrials.gov*. Paper presented at the Pacific Symposium on Biocomputing Co-Chairs.
- Yalcin, A., Telang, S., Clem, B., & Chesney, J. (2009). Regulation of glucose metabolism by 6-phosphofructo-2-kinase/fructose-2, 6-bisphosphatases in cancer. *Experimental and molecular pathology*, 86(3), 174-179.
- Yamaguchi, H., Wyckoff, J., & Condeelis, J. (2005). Cell migration in tumors. *Current opinion in cell biology*, 17(5), 559-564.
- Yang, C.-h., Yang, L.-J., Jaing, T.-H., & Chan, H.-L. (2000). Toxic epidermal necrolysis following combination of methotrexate and trimethoprim–sulfamethoxazole. *International Journal of Dermatology*, 39(8), 621-623. doi: 10.1046/j.1365-4362.2000.00022-3.x
- Yang, J. D., Gyedu, A., Afihene, M. Y., Duduyemi, B. M., Micah, E., Kingham, P. T., . . . Duguru, M. J. (2015). Hepatocellular carcinoma occurs at an earlier age in Africans, particularly in association with chronic hepatitis B. *American Journal of Gastroenterology*, 110(11), 1629-1631.

- Yang, J. D., Mohamed, E. A., Aziz, A. O. A., Shousha, H. I., Hashem, M. B., Nabeel, M. M., . . . Duduyemi, B. M. (2017). Characteristics, management, and outcomes of patients with hepatocellular carcinoma in Africa: a multicountry observational study from the Africa Liver Cancer Consortium. *The lancet Gastroenterology & hepatology*, 2(2), 103-111.
- Yang, J. D., Mohamed, H. A., Cvinar, J. L., Gores, G. J., Roberts, L. R., & Kim, W. R. (2016). Diabetes mellitus heightens the risk of hepatocellular carcinoma except in patients with hepatitis C cirrhosis. *The American journal of gastroenterology*, 111(11), 1573.
- Yang, J. D., & Roberts, L. R. (2010). Hepatocellular carcinoma: a global view. *Nature reviews Gastroenterology & hepatology*, 7(8), 448.
- Yang, X., Sun, D., Tian, Y., Ling, S., & Wang, L. (2015). Metformin sensitizes hepatocellular carcinoma to arsenic trioxide-induced apoptosis by downregulating Bcl2 expression. *Tumor Biology*, 36(4), 2957-2964.
- Yang, Y., Karakhanova, S., Hartwig, W., D'Haese, J. G., Philippov, P. P., Werner, J., & Bazhin, A. V. (2016). Mitochondria and mitochondrial ROS in cancer: novel targets for anticancer therapy. *Journal of cellular physiology*, 231(12), 2570-2581.
- Yang, Y., Sun, M., Wang, L., & Jiao, B. (2013). HIFs, angiogenesis, and cancer. *Journal of cellular biochemistry*, 114(5), 967-974.
- Younossi, Z. M., Otgonsuren, M., Henry, L., Venkatesan, C., Mishra, A., Erario, M., & Hunt, S. (2015). Association of nonalcoholic fatty liver disease (NAFLD) with hepatocellular carcinoma (HCC) in the United States from 2004 to 2009. *Hepatology*, 62(6), 1723-1730.
- Yu, L., Chen, X., Sun, X., Wang, L., & Chen, S. (2017). The glycolytic switch in tumors: how many players are involved? *Journal of Cancer*, 8(17), 3430.
- Zhang, H. H., Zhang, Y., Cheng, Y. N., Gong, F. L., Cao, Z. Q., Yu, L. G., & Guo, X. L. (2018). Metformin in combination with curcumin inhibits the growth, metastasis, and angiogenesis of hepatocellular carcinoma in vitro and in vivo. *Molecular carcinogenesis*, 57(1), 44-56.
- Zhao, Y., & Adjei, A. A. (2015). Targeting angiogenesis in cancer therapy: moving beyond vascular endothelial growth factor. *The oncologist*, 20(6), 660.
- Zhao, Y., Zhang, E., Lv, N., Ma, L., Yao, S., Yan, M., . . . He, J. (2018). Metformin and FTY720 synergistically induce apoptosis in multiple myeloma cells. *Cellular Physiology and Biochemistry*, 48(2), 785-800.

Zi, F., Zi, H., Li, Y., He, J., Shi, Q., & Cai, Z. (2018). Metformin and cancer: An existing drug for cancer prevention and therapy. *Oncology letters*, *15*(1), 683-690. doi: 10.3892/ol.2017.7412

Zong, W.-X., Rabinowitz, J. D., & White, E. (2016). Mitochondria and cancer. *Molecular cell*, *61*(5), 667-676.

# APPENDIX



## Licensing and Usage

	Basic (Free) Account*	Academic Subscription	Industry Subscription
<b>Educational Uses:</b>			
Academic poster	✓	✓	✓
Thesis/dissertation (unpublished)	✓	✓	✓
Internal meetings (lab or team)	✓	✓	✓
Conference presentation	✓	✓	✓
Assignment/exam	✓	✓	✓
Teaching slides	✓	✓	✓
Personal blog/website posts	✓	✓	✓
Personal social media posts	✓	✓	✓
<b>Publishing Uses:</b>			
Journal publication		✓	✓
Textbook publication (< 5 figures)		✓	✓
Published thesis		✓	✓
<b>Commercial Uses:</b>			
Any uses that generate profit			✓
Textbook publication (5+ figures)			✓
Trade show materials (e.g. brochures)			✓
Information packages/user guides			✓

\*Watermark must be included in exported figure  
 \*Free trial on a premium plan recommended for print uses  
 For use cases not listed here, please go to [biorender.com/contact](https://biorender.com/contact)

### Conditions for Publication rights:

1. The figure was exported under a **paid subscription**.
2. Citation of "Created with BioRender.com" appears somewhere in the publication.

All BioRender-made figures must be cited with  
**Created with BioRender**  
**Thanks for using BioRender!**

